THE UNIVERSITY OF QUEENSLAND

AUSTRALIA

Refining Nanocarrier Emulsions for Pharmaceutical Use

Hossam Hatem Tayeb

B. S. Applied Medical Sciences, M. Biotech (advanced)

A thesis submitted for the degree of Doctor of Philosophy at

The University of Queensland in 2018

Australian Institute for Bioengineering and Nanotechnology

Abstract

Nanomaterials with different surface designs and biophysical properties are being developed to improve the efficacy of hydrophobic drugs. To date, these improvements have not overcome the complexity of biological and physical barriers via different delivery routes, however, nanoemulsions (NEs), in particular tailorable nanocarrier emulsions (TNEs), are emerging as promising drug carriers. The novel oil-in-water NEs are stabilised with chemically-engineered biosurfactants (AM1) that allow top-down sequential addition and modification with a chemically-related 4-helix bundle protein, DAMP4, which can be fused to various biomolecules. In this project, the feasibility of using TNEs for diagnostic/therapeutic applications via different delivery routes was investigated. The initially stages of the work were to evaluate the encapsulation and retention capacity of hydrophobic compounds within the oil core of TNEs with varying surface properties. Polyethylene glycol (PEG), an important pharmaceutical tool, was chemically conjugated to DAMP4 and influenced cargo retention within the oil core. In collaboration with Professor Tarl Prow, tuning the TNE surface charge, which was found to be indirectly related to PEG density, allowed TNEs to coat elongated microparticles via electrostatic interactions, creating a promising tool for topical drug delivery. Co-functionalising TNEs with antibody fragments showed receptor-specific targeting in vitro, however, in vivo active targeting was not achieved following intravenous administration. Biodistribution studies suggested rapid clearance via the renal route with some liver involvement, however ex vivo studies involving cytokines, serum and urine analyses demonstrated TNE safety for drug delivery applications. This work suggests that the structure-function relationship of the TNEs interface has a strong influence on their interactions with the surrounding environment, therefore deeper understanding of the structure of TNE interface and how it relates to functional performance was needed. Tuning the amount and type of PEG displayed on TNEs showed that the molecular weight of PEG has considerable impact on the surface charge of the emulsion. Also, targeting moieties presented on TNE surfaces were equally accessible to their receptors even when the PEG layer created differences in interfacial thicknesses determined by X-ray reflectometry that showed a role in reducing non-specific targeting. These findings suggest that precise and controlled bioconjugation of functional moieties to DAMP4 is needed in the design and characterisation of sophisticated interfaces. Genetic engineering of DAMP4 with cysteine residues produced variants with conserved structure, stability, and surface activity that can be specifically conjugated to PEG via maleimide-thiol reaction with nearly 100% yield and showed with molecular precision how interfacial activities of biosurfactants can be affected by the number and mass of their conjugates. Consequently, the ability of DAMP4 variants with multiple PEG conjugates to impart colloidal stability on peptide-stabilised emulsions was reduced. These findings contribute to the design and modification of biosurfactants

increasingly used in industrial processes, nutritional and pharmaceutical formulations. This research investigated the challenges facing the surface design of TNEs and their interactions, helped to better understand the physicochemical properties regarding ligand accessibility and receptor-binding performance; and provided tools to further explore functional interface design and better understand the relationship between genetic and chemical modifications of polypeptides and their function.

Declaration by author

This thesis is composed of my original work, and contains no material previously published or written by another person except where due reference has been made in the text. I have clearly stated the contribution by others to jointly-authored works that I have included in my thesis.

I have clearly stated the contribution of others to my thesis as a whole, including statistical assistance, survey design, data analysis, significant technical procedures, professional editorial advice, financial support and any other original research work used or reported in my thesis. The content of my thesis is the result of work I have carried out since the commencement of my higher degree by research candidature and does not include a substantial part of work that has been submitted to qualify for the award of any other degree or diploma in any university or other tertiary institution. I have clearly stated which parts of my thesis, if any, have been submitted to qualify for another award.

I acknowledge that an electronic copy of my thesis must be lodged with the University Library and, subject to the policy and procedures of The University of Queensland, the thesis be made available for research and study in accordance with the Copyright Act 1968 unless a period of embargo has been approved by the Dean of the Graduate School.

I acknowledge that copyright of all material contained in my thesis resides with the copyright holder(s) of that material. Where appropriate I have obtained copyright permission from the copyright holder to reproduce material in this thesis and have sought permission from co-authors for any jointly authored works included in the thesis.

Publications during candidature

Conference abstracts

Hossam H. Tayeb, Chris B. Howard, Anton P.J. Middelberg and Frank Sainsbury. Directing sophisticated nanoemulsions toward cancer nanomedicine. *The 6th international NanoMedicine Conference 2015*; 2015 6-8 July. *The 6th international NanoMedicine Conference*, Sydney, Australia. Australian Centre for NanoMedicine, The School of Chemical Engineering, The University of New South Wales.

Hossam H. Tayeb, Chris B. Howard, Anton P.J. Middelberg and Frank Sainsbury. Tuneable biophysical properties of peptide-stabilised nanoscale emulsions. *The 8th international Conference on Advanced Materials and Nanotechnology 2017*; 2017 12-16 July. The international Conference on Advanced Materials and Nanotechnology, Queenstown, New Zealand, The MacDiarmid Institute for Advanced Materials and Nanotechnology, Victoria University of Wellington.

Hossam H. Tayeb, Marina. Stienecker, Anton P. J. Middelberg and Frank Sainsbury. Engineering site-specific bioconjugation to a biosurfactant for improved stability in biological applications. The International Conference on Bio-Nano Innovation; 2017; 2017 24-27 September. The International Conference on Bio-Nano Innovation, Brisbane, Australia, The Australian Institute for Bioengineering and Nanotechnology, The University of Queensland.

Peer-reviewed publication

Hossam H. Tayeb, Stefania Piantavigna, Christopher B. Howard, Amanda Nouwens, Stephen M. Mahler, Anton P. J. Middelberg, Lizhong He, Stephen A. Holt and Frank Sainsbury. Insights into the interfacial structure–function of poly(ethylene glycol)-decorated peptide-stabilised nanoscale emulsions. *Soft Matter,* 13 43: 7953-7961. doi:10.1039/c7sm01614j

Publications included in this thesis

Hossam H. Tayeb, Stefania Piantavigna, Christopher B. Howard, Amanda Nouwens, Stephen M. Mahler, Anton P. J. Middelberg, Lizhong He, Stephen A. Holt and Frank Sainsbury. Insights into the interfacial structure–function of poly(ethylene glycol)-decorated peptide-stabilised nanoscale emulsions. *Soft Matter.* 13 43: 7953-7961. doi:10.1039/c7sm01614j

Included as chapter 4

Contributor	Statement of contribution
Hossam Hatem Tayeb (Candidate)	Conception and design (50%) Analysis and interpretation (60%) Drafting and production (60%)
Stefania Piantavigna	Conception and design (5%) Analysis and interpretation (10%) Drafting and production (0%)
Anton P. Middelberg	Conception and design (0%) Analysis and interpretation (0%) Drafting and production (2.5%)
Christopher Howard	Conception and design (5%) Analysis and interpretation (5%) Drafting and production (5%)
Stephen Mahler	Conception and design (0%) Analysis and interpretation (0%) Drafting and production (2.5%)
Amanda Nouwens	Conception and design (0%) Analysis and interpretation (5%) Drafting and production (0%)

Lizhong He	Conception and design (0%) Analysis and interpretation (0%) Drafting and production (2.5%)
Stephen A. Holt	Conception and design (10%) Analysis and interpretation (10%) Drafting and production (7.5%)
Frank Sainsbury	Conception and design (30%) Analysis and interpretation (10%) Drafting and production (20%)

Manuscript included in this thesis

The following manuscript is submitted to Journal of colloids and surfaces B: Biointerfaces;

Hossam H. Tayeb, Marina Stienecker, Anton P. J. Middelberg and Frank Sainsbury. Site-specific bioconjugation with poly(ethylene glycol): impact on the interfacial activity of a protein biosurfactant. *Journal of colloids and surfaces B: Biointerfaces, Elsevier.* The University of Queensland, Australian Institute for Bioengineering and Nanotechnology, St Lucia, QLD 4072, Australia.

Contributor	Statement of contribution
Hossam Hatem Tayeb (Candidate)	Conception and design (50%) Analysis and interpretation (90%) Drafting and production (70%)
Marina Stienecker	Conception and design (5%) Analysis and interpretation (5%) Drafting and production (0%)
Anton P. Middelberg	Conception and design (5%) Analysis and interpretation (0%)

	Drafting and production (0%)
Frank Sainsbury	Conception and design (40%) Analysis and interpretation (5%) Drafting and production (30%)

Contributions by others to the thesis

The thesis was drafted and written by the candidate under the supervision of Dr. Frank Sainsbury, Dr. Christopher Howard and Professor Anton Middelberg.

Frank Sainsbury, main supervisor, contributed to the conception and design of my thesis project, data analysis and interpretation and the critical revision of all written sections. Anton Middelberg also contributed to the conception and design of elements of my thesis project.

Christopher Howard designed and synthesised the scFv-DAMP4 protein fusion in mammalian cells, which were used in sections 3.7, 3.8, 3.9 and 4.6 b and c.

Stefania Piantavigna at the Australian Nuclear Science and Technology Organisation (ANSTO), performed and analysed the experiments presented in Figures 4.3 and 4.5.

Amanda Nouwens at the School of Chemistry and Molecular Biosciences, the University of Queensland (UQ), performed the mass spectrometry analysis presented in Supplementary Figure 4.1.

An internship student at the Australian Institute for Bioengineering and Nanotechnology, UQ, Marina Stienecker, helped in cloning DAMP4 variants, and provided technical assistance in sections 5.1, 5.2 and 5.4.

Statement of parts of the thesis submitted to qualify for the award of another degree

None.

Research Involving Human or Animal subjects

The targeting and biodistribution studies were performed in compliance with the Australian National Health and Medical Research Council guidelines for the care and use of laboratory animals, and with the approval of the EnGeneIC Animal Ethics Committee under ethics application number: AIBN/400/13/ARC/NHMRC.

Acknowledgements

First and foremost, I praise Allah, the almighty, the merciful, the greatest, for granting me the strength to proceed with this great experience and providing me with knowledge and patience. For this thesis to be in this form, the assistance and guidance of many people were required. Therefore, I would like to express my thanks to all of them. Firstly, I would like to express my sincere gratitude and appreciation to my sponsor King Abdul-Aziz University (KAU), Ministry of Higher Education, Saudi Arabia for their generous financial support and giving me the opportunity to study abroad.

A special thanks to my principle supervisor Dr Frank Sainsbury for his mentorship, continuous support and patience throughout my research and the thesis writing process. His attention to details drove me to improve my academic writing as well as my critical thinking. I would also like to extend my gratitude to Professor Anton Middelberg for his valuable advice and for giving me the opportunity to do my PhD research as a part of his group at the Australian Institute of Bioengineering and Nanotechnology (AIBN) at the University of Queensland. I would also like to thank Dr Christopher Howard for his help and advice throughout my PhD program. I would also like to thank my committee members (Professor Michael Monteiro and Dr Barbra Rolf)) for their valuable advice that guided me during my research period. I would like to thank all our collaborators. Professor Tarl Prow, Dr Miko Yamada, Professor Stephen Mahler, Dr Kris Thurecht, Dr Simon Puttick, Dr Nicholas Fletcher, Dr Amanda Nouwens, Dr Lizhong He and Dr Stefania Piantavigna. I would like to thank all my colleagues including; Noor Dashti, Rufika Abidin, Nicolas Pichon, Arjun Seth and Yue Hui for their support and advice that helped me through the challenging times in my research.

I would like to thank my family, my father Hatem Tayeb, my mother Khadija Tayeb, my brothers (especially Nader Tayeb) and sisters for their continuous support. Their prayers for me has kept me going and sustained me this far.

Finally, to my small beautiful family. My wife Nojod Hasaballah, who is always encouraging me to be better and do better. I cannot thank you enough for everything you have done and keep doing for me. To my son Rafel Tayeb, my biggest fan, words cannot describe how thankful I am to have him by my side. Your thoughtful words, your funny jokes and your laughter brought me happiness and always got me through the hardest times.

Financial Support

Hossam Hatem Tayeb acknowledges the financial support including tuition fee and living stipend (Scholarship) from King Abdul Aziz University, Ministry of Higher Education, Kingdom of Saudi Arabia.

Keywords

Nanocarriers, emulsions, biosurfactants, drug delivery, interface, bioconjugation, PEGylation, interfacial activity, surface modification

Australian and New Zealand Standard Research Classifications (ANZSRC)

ANZSRC code: 100402, Medical Biotechnology, 25%

ANZSRC code: 100703, Nanobiotechnology, 50%

ANZSRC code: 100703, Nanomaterials, 25%

Fields of Research (FoR) Classification

FoR code: 1004, Medical Biotechnology, 25%

FoR code: 1007, Nanotechnology, 75%

Table of content

Abstract **2**

Declaration by author **4**

Publications during candidature **5**

Publications included in this thesis **6**

Contributions by others to the thesis **9**

Acknowledgements **10**

Financial Support **11**

Keywords **12**

Table of content **13**

List of Figures **17**

List of Supplementary Figures **19**

List of Tables **20**

List of Supplementary Tables **20**

List of Abbreviations **21**

1 Chapter 1: Project Overview **24**

1.1 Background 24

1.2 Lipid-based drug nanocarriers 28

1.2.1 Liposomes 28

1.2.2 Nanoemulsions as drug delivery systems 28

1.2.2.1 Tailorable nanocarrier emulsions 31

1.3 Bioconjugation 35

1.3.1 PEGylation 37

1.4 Thesis aims 38

1.5 Thesis organisation 39

2 Chapter 2: Literature Review: Nanoemulsion: a Promising Drug Delivery System for Medical Applications **41**

2.1 Introduction 42

2.2 Preparation methods of nanoemulsions 44

2.3 Nanoemulsion-destabilising mechanisms 44

2.4 Nanoemulsion stabilisers 47
2.5 Nanoemulsions in medical applications 48
2.5.1 Topical applications 49
2.5.2 Ingestible nanoemulsions 55
2.5.3 Aerosolised nanoemulsions 56
2.5.4 Injectable nanoemulsions 59
2.5.4.1 Nutrition therapy 59
2.5.4.2 Cancer therapy 60
2.5.4.2.1 Passive targeting 60
2.5.4.2.2 Active targeting 61
2.5.5 Other parenteral applications of nanoemulsions 63
2.5.6 Nanoemulsions in biomedical imaging 63
2.5.7 Emulsions for vaccine applications 64
2.6 The future of nanoemulsions in nanomedicine through top-down assembly 68
2.7 Conclusion and future directions 68
2.8 Acknowledgment 69
3 Chapter 3: Exploring the Use of Nanocarrier Emulsions in Drug Delivery 70
3.1 Introduction 70
3.2 Experimental section 72
3.2.1 DAMP4 expression, purification and quantification 72
3.2.2 Preparation of tailorable nanocarrier emulsions 72
3.2.3 Preparation of targeted and un-targeted TNEs 73
3.2.4 Cargo retention within the TNE oil core 73
3.2.5 Stability of TNEs in different storage conditions 73
3.2.6 Coating efficiency of EMPs by TNEs 74
3.2.7 Release profile of 6-carboxyfluorescein (CFC)-encapsulated TNEs 74
3.2.8 Expression and purification of DAMP4-antibody fusions 74
3.2.9 Epidermal growth factor receptor (EGFR) binding plate assays 75
3.2.10 Solid state EGFR binding assay 75
3.2.11 Flow cytometry 76
3.2.12 *In vivo* targeting and biodistribution studies 76
3.2.12.1 *Ex vivo* biodistribution and cytokine analysis of TNEs 77
3.2.13 DiI retention in simulated plasma fluid 77
3.3 Results 78
3.3.1 Surface properties and cargo retention of the tailorable nanocarrier emulsions 78
3.3.2 Exploring the surface properties of TNEs toward topical (skin) applications 84
3.3.3 Tailorable nanocarrier emulsions toward intravenous applications 88

3.4 Discussion 98

4 Chapter 4: Insights into the Interfacial Structure–Function of Poly(ethylene glycol)-Decorated Peptide-Stabilised Nanoscale Emulsions 101

4.1 Abstract 102

4.2 Introduction 103

4.3 Experimental section 104

4.3.1 DAMP4 expression, purification and quantification 104

4.3.2 DAMP4 PEGylation 104

4.3.3 Matrix-assisted laser desorption/deionisation 105

4.3.4 Interfacial tension analysis 105

4.3.5 Quartz crystal microbalance 105

4.3.6 Preparation of the tailorable nanosized emulsions (TNEs) 106

4.3.7 Interfacial thickness 106

4.3.8 scFv-DAMP4 expression and purification 107

4.3.9 Biolayer interferometry 108

4.3.10 Solid state EGFR binding 108

4.3.11 Flow cytometry 108

4.4 Results and discussion 109

4.4.1 Characterisation of protein co-surfactant PEGylation 109

4.4.2 Interfacial tension of PEGylated DAMP4 111

4.4.3 Sequential addition of DAMP4 conjugates 113

4.4.4 Impact of DAMP4 PEGylation on the size and ζ-potential of TNEs 115

4.4.5 Interfacial thickness of the PEG layer 117

4.4.6 Presentation and accessibility of functional moieties on TNEs 120

4.5 Conclusions 122

4.6 Acknowledgements 124

4.7 Supplementary materials 125

5 Chapter 5: Site-Specific Bioconjugation with Poly(Ethylene Glycol): Impact on the Interfacial Activity of a Protein Biosurfactant 129

5.1 Abstract 130

5.2 Introduction 131

5.3 Materials and methods 133

5.3.1 Molecular cloning 133

5.3.2 Expression and purification of DAMP4 variants 133

5.3.3 PEGylation of DAMP4 variants 133

5.3.4 Interfacial tension analysis 133

5.3.5 Circular dichroism (CD) spectroscopy 134
5.3.6 Differential scanning calorimetry (DSC) 134
5.3.7 Preparation and characterisation of TNEs 134
5.4 Results and discussion 135
5.4.1 DAMP4 variants 135
5.4.2 Structure, stability and activity of cysteine mutants 135
5.4.3 Functional bioconjugation to DAMP4 variants 138
5.4.4 Stability, interfacial activity and bioconjugation to a double cysteine variant 140
5.4.5 Interfacial activity is affected by both the mass and number of conjugates 143
5.5 Conclusion 147
5.6 Acknowledgments 148
5.7 Supplementary materials 149
6 Chapter 6: Conclusion and Future Directions 155
6.1 Exploring the suitability of TNEs in diagnostic and therapeutic applications by employing different routes of administration 156
6.2 Insight into the interfacial structure-function of the polyethylene glycol-decorated peptide-stabilised nanocarrier emulsions 157
6.3 Site-specific bioconjugation with poly(ethylene glycol): impact on the interfacial activity of a protein biosurfactant 158
6.4 Future directions 160
6.5 Concluding remarks 166
6.6 List of References 167
7 Appendix A 194

List of Figures

Figure 1.1. Schematic representation of AM1 peptide. 33

Figure 1.2. Diagrammatic depiction of how TNEs are fabricated. 34

Figure 1.3. List of amino and thiol functional reactive groups. 36

Figure 2.1. Types of emulsion based on the dispersed phase. 43

Figure 2.2. The common techniques used for the formulation of NEs. 45

Figure 2.3. The destabilising mechanisms of the NEs. 46

Figure 2.4. Drug delivery applications of nanoemulsions. 51

Figure 2.5. Targeting strategies of drug delivery systems. 62

Figure 3.1. Size and charge characterisation of TNEs prepared with different PEG densities. 79

Figure 3.2. Effect of PEG density on the DiI retention profile of TNEs. 80

Figure 3.3. Size characterisation and DiI retention within the oil core of TNEs prepared with different PEG densities over time. 82

Figure 3.4. Size of TNEs in different storage conditions 83

Figure 3.5. Coating efficiency of EMPs by TNEs. 86

Figure 3.6. CFC release from the oil core of P20-TNEs 87

Figure 3.7. Functionalisation of peptide-stabilised TNEs with DAMP4 ScFv fusions. 89

Figure 3.8. Binding of TNEs to MDA-MB-468 cells using flow cytometry. 90

Figure 3.9. *In vivo* evaluation of TNEs targeting cancer cells. 92

Figure 3.10. Evaluation of DiI retention in TNEs in simulated serum fluid 93

Figure 3.11. Ex-vivo analysis of TNE biodistribution. 94

Figure 3.12. Biodistribution of TNEs in mouse sera and urine. 95

Figure 3.13. Release of cytokines over time from mice post-TNE injection 97

Figure 4.1. Bioconjugation of NHS-mPEG to DAMP4 110

Figure 4.2. Interfacial tension analysis of the DAMP4:PEG conjugates. 112

Figure 4.3. Typical Δf and ΔD versus time plots of 10K-PEG–DAMP4 interacting with AM1 peptide. 114

Figure 4.4. Dynamic light scattering and ζ-potential measurements of TNEs prepared with DAMP4-PEG conjugates. 116

Figure 4.5. X-Ray reflectivity data and the real space fit to the datasets. 118

Figure 4.6. Functionalising TNEs with a ligand-binding reporter. 121

Figure 4.7. Schematic model of the competing influences on EGFR binding of PEG and an anti-EGFR scFv at the oil-in-water interface of TNEs. 123

Figure 5.1. Sequence design for DAMP4 cysteine variants. 136

Figure 5.2. Thermal stability and interfacial activity of DAMP4 single cysteine variants 137

Figure 5.3. Functionalisation of TNEs by PEGylated DAMP4 variants. 139

Figure 5.4. Thermal stability and interfacial activity of D4C2, a double cysteine variant of DAMP4. 141

Figure 5.5. PEGylation and TNE functionalisation by D4C2 142

Figure 5.6. Interfacial activity of double and single PEGylated DAMP4. 144

Figure 5.7. Stability of TNEs modified with PEGylated DAMP4 variants in the presence of EDTA. 146

Figure 6.1. Accessibility of functional moieties displayed at the TNE interface. 163

List of Supplementary Figures

Supplementary Figure 4.1 125

Supplementary Figure 4.2 126

Supplementary Figure 4.3 127

Supplementary Figure 4.4 128

Supplementary Figure 5.1 149

Supplementary Figure 5.2 150

Supplementary Figure 5.3 151

Supplementary Figure 5.4 154

List of Tables

Table 1.1. Nanomaterials classes, subclasses, properties, products and their applications. 26

Table 1.2. Pharmaceutical NE formulations on the current market (Mansoor and Sandip, 2006, Lovelyn and Attama, 2011). 30

Table 2.1. Examples of NEs in clinical trials for skin applications (Singh et al., 2017). 54

Table 2.2. Examples of the diversity of APIs delivered by aerosolised NEs..... 58

Table 2.3. List squalene O/W emulsions as vaccine adjuvants..... 66

Table 2.4. Examples of squalene O/W emulsion under investigation 67

Table 4.1. Parameters from the fit to the XRR data sets. 119

List of Supplementary Tables

Supplementary Table 5.1. Stability of TNEs formulated with the PEGylated single cysteine variants following dilution in PBS..... 152

Supplementary Table 5.2. Stability of TNEs formulated with the PEGylated single and double cysteine variants following dilution in PBS..... 153

List of Abbreviations

A	Alginate cross-linking
ACN	Acetonitrile
AF	Alginate cross-linking plus freeze-dry coating
AIBN	Australian Institute for Bioengineering and Nanotechnology
APAF	Australian Proteome Analysis Facility
APIs	Active pharmaceutical ingredients
CD	Circular dichroism
CFC	6-Carboxyfluorescein
CHO	Chinese hamster ovary cells
DiI	1,1'-Dioctadecyl-3,3,3'3'-tetramethylindocarbocyanine perchlorate
DLVO	Derjaguin, Landau, Verwey, and Overbeek
DSA	Droplet shape analysis
DSC	Differential scanning calorimetry
EDTA	Ethylenediaminetetraacetic acid
EGFR	Epidermal growth factor receptor
ELISA	Enzyme-linked immunosorbent assay
EMPs	Elongated microparticles
EPR	Enhanced permeability and retention effect
F	Freeze-dry coating
FA	Formic acid
FDA	Food and drug administration
FPF	Fine particle fraction
FRET	Förster resonance energy transfer
GRAS	Generally recognised as safe

HEPES	4-(2-Hydroxyethyl)-1-piperazineethanesulfonic acid
IFN- γ	Interferon gamma
IFT	Interfacial tension
IL2/4/6/10	Interleukin
IV	Intravenous
Log P	Partition coefficient
MALDI-TOF	Matrix assisted laser desorption/ionisation – time of flight
MDR	Multidrug resistance
MRI	Magnetic resonance imaging
NEs	Nanoemulsions
NHS	N-hydroxysuccinimide
NPs	Nanoparticles
O/W	Oil-in-water
O/W/O	Oil-in-water-in-oil
PBS	Phosphate buffered saline
PDI	Polydispersity index
PEG	Poly ethylene glycol
PIT	Phase inversion temperature
QCM	Quartz crystal microbalance
QCM-D	Quartz crystal microbalance with dissipation monitoring
RP-HPLC	Reversed phase – high performance liquid chromatography
RSV	Respiratory syncytial virus
scFv	Single chain variable fragment
SLD	Scattering length density
TCEP	Tris(2-carboxyethyl)phosphine

TNE	Tailorable nanocarrier emulsion
TRI	Translational research institute
VECT	Vectibix®
W	Wet coating
W/O	Water-in-oil
W/O/W	Water-in-oil-in-water
XRR	X-ray reflectometry

1 Chapter 1: Project Overview

1.1 Background

Advances in biotechnology have led to the development of various promising diagnostic and therapeutic small molecules. However, a large number of these molecules are not being exploited successfully due to several disadvantages including toxicity, hydrophobicity and, therefore, insufficient bioavailability levels (De Jong and Borm, 2008). It has been estimated that approximately 40% of newly discovered therapeutic agents are eliminated from the drug development pipeline because of poor aqueous solubility. Also, 90% of the active pharmaceutical ingredients (APIs) in the discovery and development stages feature poor solubility (Loftsson and Brewster, 2010). Various strategies have been developed to overcome the drawbacks of these lipophilic drugs for the treatment of diseases such as cancer. These include the synthesis of different isoforms of APIs to enhance solubility and the development of drug delivery nanocarriers (Devalapally et al., 2007).

Nanotechnology is a rapidly growing multidisciplinary field that has been applied to the formulation of nanoscale pharmaceutical carriers to improve therapeutic outcomes. It is defined by The Royal Society and Royal Academy of Engineering as 'the study of phenomena and manipulation of materials at atomic, molecular, and macromolecular scales, where the properties differ significantly from those at a larger scale; and "nanotechnologies" are the design, characterisation, production, and application of structures, devices, and systems by controlling shape and size at the nanometer scale' (Dowling, 2006). It involves the application, characterisation and engineering of synthetic particles and structures ranging from 1 to 500 nanometres in one or more dimensions (Devalapally et al., 2007). The application of nanotechnology to the medical or pharmaceutical field is known as nanomedicine. The motivating concepts of nanomedicine are to enhance drug safety, solubility, bioavailability and specificity (Jeevanandam et al., 2016); to have a positive impact on clinical diagnosis and treatment of disease (Evers, 2017).

Various nanotechnologies are considered very promising in diagnosis and treatment, particularly for cancer, and some are currently undergoing clinical development. These include nanoparticle (NP) platforms such as polymer-based NPs including dendrimers; inorganic materials-based platforms such as carbon nanotubes and quantum dots; and lipid-based NPs such as liposomes and nanoemulsions (NEs) (Shi et al., 2016) (Table 1.1). Nanotechnology-based drug delivery has the potential to overcome the limitations of traditional chemotherapeutic drugs (Cho et al., 2008). Even though chemotherapy can kill cancer cells, it has several serious disadvantages. These include poor selectivity, the emergence of multi-drug resistance (MDR), limited bioavailability, and the

consequent administration of high drug doses that can lead to cytotoxicity in normal body tissues (Szakacs et al., 2006, Cho et al., 2008). MDR can be developed through different mechanisms including the increase in drug efflux and drug evasion via apoptosis (Gillet and Gottesman, 2010). Because of these disadvantages the development of various NPs for cancer nanomedicine is urgently needed in order to deliver anticancer drugs efficiently, selectively and safely to the diseased tissues. Achieving this goal has become increasingly realistic with the rapidly growing number of nanodiagnostics and nanotherapeutics, both in clinical studies and the pharmaceutical market. Key benefits of such platforms include biocompatibility, prolonging circulation time and improving drug localisation via targeting.

It is believed that the market for nanomedicines will have a growing share in cancer therapeutics over the next few decades (Scheinberg et al., 2010, Peer et al., 2007, Kim et al., 2010). However, the development of nanomedicines is showing slow progress, which is attributed to the complexity of the nanomaterials' structures and, therefore, their specific analytical requirements. Also, it is difficult to control batch-to-batch variability in manufacturing, which is problematic in meeting regulatory requirements (Ragelle et al., 2017). The difficulty of obtaining superior therapeutic benefits over existing approved nanomedicines or API is another major challenge. Recently, it has been estimated that only 0.7% of injected NPs can reach their target site. This almost results in 99% off-target drug delivery, which increases cytotoxicity risks (Wilhelm et al., 2016). The development cost is also high and considered a burden for clinical translation of NPs due to the need for high number of NPs per an injected dose, therefore, cost management of NPs synthesis is also required (Min et al., 2015). In addition, high injected volumes of NPs may cause technical difficulties for patient use (Wilhelm et al., 2016). These issues indicate that patients are not benefiting from the 'magic bullet' idea to date, but this does not mean that these issues cannot be overcome. Therefore, our thinking should be deviated from just targeting, and be focused on exploring new means to accelerate clinical translation of NPs efficiently (Lammers et al., 2016). Also, more fundamental understanding is required into the assembly of NPs and their interactions with biological environments. This includes understanding the target disease, choosing safe and effective materials, exploring methods of surface modifications and routes of administration.

Table 1.1. Nanomaterials classes, subclasses, properties, products and their applications.

Nanomaterial classes and subclasses	Size	Shape	Toxicity	Examples of approved nanomedicines	Product Application	Approval year
Inorganic NPs						
Carbon nanotubes	1-100 (Kaushik et al., 2017)	Cylindrical with open or close ends (Kaushik et al., 2017)	Variable based on geometry and surface chemistry (De Volder et al., 2013)	No approved products	-	-
Silica NPs	<500 (Argyo et al., 2014)	Amorphous (Murugadoss et al., 2017)	Variable based on size and dosage(Kim et al., 2015, Murugadoss et al., 2017)	No approved products	-	-
Gold NPs	10-100 (Yeh et al., 2012)	Spheres, cages and rods (Kaushik et al., 2017)	Low or no toxicity (Connor et al., 2005)	No approved products	-	-
Quantum dots	2-20 (Kaushik et al., 2017)	Spherical or ellipsoid (Kaushik et al., 2017)	Toxicity is a main challenge in drug delivery (Volkov, 2015)	No approved products	-	-
Polymeric NPs						
Dendrimers	1-13 (Cheng et al., 2008b, Müller et al., 2007, Dobrovolskaia et al., 2012)	Highly-branched tree-like structures (Sikwal et al., 2017)	Variable toxicity based on structure (Cheng et al., 2008a)	No approved products	-	-
Micelles	10-100 (Ahmad et al., 2014b, Yokoyama, 2014)	block (Spherical) or random copolymers (Jones and Leroux, 1999)	Low toxicity (Movassaghian et al., 2015)	Estrasorb^{TM} (Novavax) (Simon, 2006)	Menopausal therapy (Simon, 2006)	2003

Magnetic NPs						
Sliver NPs	10-100 (Marin et al., 2015)	spheres, cubes, rods (Helmlinger et al., 2016)	Variable toxicities based on size and synthesis method (Wei et al., 2015)	No approved products	-	-
Iron oxide NPs	1-100 (Laurent et al., 2008)	Spheres (Mahmoudi et al., 2011)	Variable toxicity based on coating	Nanotherm® (MagForce) (Magforce, 2018)	Solid tumours (Bobo et al., 2016, Magforce, 2018)	2010 (Bobo et al., 2016)
Lipid-based NPs						
Liposomes	Nanosize range (Malam et al., 2009)	Sphere (Malam et al., 2009)	Low or no significant toxicity (Bozzuto and Molinari, 2015)	Doxil® (Janssen) (Barenholz, 2012b)	Kaposi's Sarcoma	1995
				DaunoXome® (Galen) (Forssen, 1997)	Kaposi's Sarcoma	1996
				AmBisome® (Gilead Sciences) (Stone et al., 2016)	Fungal or protozoal infections	1997
				Marqibo® (Spectrum pharmaceuticals) (Silverman and Deitcher, 2013)	Acute lymphoblastic leukaemia	2012
Nanoemulsions	20-500 (Gupta et al., 2016)	Sphere (Ganta et al., 2014b)	Low or no toxicity (Borthakur et al., 2016)	Intralipid® (Baxter healthcare) (Hippalgaonkar et al., 2010)	Nutritional therapy	1962
				Diprivan® (AstraZeneca) (Chidambaran et al., 2015)	Anaesthesia	1989
				Restasis® (Allergan) (Ames and Galor, 2015)	Dry eye syndrome	2003
				Durezol® (Alcon pharmaceuticals) (Smith et al., 2010)	Eye inflammation and uveitis	2008

1.2 Lipid-based drug nanocarriers

Lipid-based nanocarriers include liposomes, emulsions and solid lipid NPs, and they have a promising future in meeting the ideal requirements (Lederer and Parascandola, 1998) for a drug delivery system. These requirements include primarily protection of the drug from harsh environments, such as pH (Chanana et al., 2013) and enzymatic degradation (Soenen et al., 2015); increasing the safety profile of these lipophilic drugs in order to reduce their undesirable side effects; and the potential to introduce tissue specificity by cell receptor targeting. In this section, I will discuss only soft lipid carriers, including liposomes and emulsions.

1.2.1 Liposomes

Liposomes are spherical NPs that comprise a lipid bilayer enclosing a central aqueous phase. They have been extensively studied *in vivo* and show remarkable biocompatibility and biodegradability, as well as low immunogenicity (Torchilin, 2005). However, liposomes can be easily removed from the blood circulation by opsonisation. Thus, additional surface coating molecules, such as polyethylene glycol (PEG), are required for the liposomal carriers to extend their serum half-life and enable them to evade the immune system (Hauser-Kawaguchi and Luyt, 2015). Nevertheless, liposomes possess a distinctive feature, the capacity to encapsulate both hydrophobic and hydrophilic drugs in the lipid-bilayers and the aqueous core, respectively (Hauser-Kawaguchi and Luyt, 2015). Currently, several liposomal formulations of different anti-cancer drugs have been approved for human use (Table 1.1). In cancer therapy, Doxil (PEGylated form) (Safra et al., 2000) and Mycoet (non-PEGylated form) (O'Shaughnessy, 2003, Swenson et al., 2001), which are liposomal formulations of the anthracycline doxorubicin, are approved for treating metastatic breast cancer. It was found that Doxil improved the drug accumulation of doxorubicin 10-fold compared to administration of the drug alone (Rosenthal et al., 2002). Currently, numerous liposomal formulations are in preclinical development and are being evaluated in clinical trials.

1.2.2 Nanoemulsions as drug delivery systems

NEs, heterogeneous systems in which one liquid is dispersed as nanosized droplets within another liquid, have evolved as robust carriers for the delivery of a wide range of hydrophobic drugs (Ganta et al., 2014b). NEs are non-equilibrium, kinetically stable systems that feature small droplet sizes typically ranging from 20 to 500 nm (Gupta et al., 2016). NEs are characterised by advantageous features, including ease of production, high loading capacities, long-term stability, increased bioavailability and protection and controlled release of cargos, all of which make them promising carriers for use in nanomedicine (Talegaonkar and Negi, 2015). The presence of commercialised NEs

in various applications (Table 1.2) demonstrates their suitability and their long history of safety in pharmaceutical applications.

Both oil-in-water (O/W) and bicontinuous water-in-oil-in-water (W/O/W) NEs are suitable for the delivery of hydrophobic compounds in aqueous environments. NEs have four main components: the dispersed phase, continuous phase, surfactant and co-surfactant. The selection of the oil type determines the solubility of the encapsulated drug and, therefore, the loading capacity. Surfactants reduce the interfacial tension between liquid phases imparting thermodynamic stability, and they can be anionic, cationic, non-ionic or zwitterionic. In the last few years, NEs have shown promising results as preclinical cancer theranostics (Ganta et al., 2014a). For instance, a recent study has shown a synthesis of a theranostic NE platform that involves the use of vitamin E and D-α-tocopheryl-PEG1000-succinate as an oil core and surfactant, respectively. This platform was applied to co-deliver an imaging probe (sulforhodamine B) and paclitaxel for cancer imaging and therapy (Yang et al., 2014). Another study also showed that NEs hold promise for use as a theranostic platform, where a targeted docetaxel-loaded NE was applied to ovarian cancer using folate as a targeting moiety and gadolinium for magnetic resonance imaging (MRI) (Ganta et al., 2016).

Table 1.2. Pharmaceutical NE formulations on the current market (Mansoor and Sandip, 2006, Lovelyn and Attama, 2011).

Active agent	Indication	Brand name	Company
Propofol	Anaesthetic	Diprivan®	Astra Zeneca
Dexamethasone palmitate	Steroid	Limethason®	Mitsubishi Pharmaceuticals
Palmitate alprostadil	Vasodilator platelet inhibitor	Liple®	Mitsubishi Pharmaceuticals
Flurbiprofen axetil	NSAID	Ropion	Kaken Pharmaceuticals
Vitamins A, D, E or K	Parenteral nutrition	Vitalipid®	Fresenius Kabi

1.2.2.1 Tailorable nanocarrier emulsions

Tailorable nanocarrier emulsions (TNEs) were recently invented by the Middelberg group at the Australian Institute for Bioengineering and Nanotechnology (AIBN) and have shown promising results in the selective delivery of antigens (Zeng et al., 2013). TNEs are easily formulated by the assembly of protein-based surfactants in a bottom-up fashion followed by the top-down sequential addition of reagents. The core of TNEs is made from a pharmaceutical-grade oil, Miglyol 812, which is classed as a generally recognised as safe (GRAS) substance by the US Food and Drug Administration (FDA) (Dexter et al., 2006). It is stabilised by a 21-residue surface active peptide called AM1 (Ac-MKQLADSLHQLARQVSRLEHA-CONH2) (Malcolm et al., 2006) (Figure 1.1).

The design of AM1 was based on an amphipathic peptide Lac21 which adsorbs at fluid-fluid interfaces (Fairman et al., 1995). The difference between AM1 and Lac21 is only in the insertion of two histidines residues at positions 9 and 20. These histidines give AM1 its metal binding properties that allow the cross-linking between AM1 molecules at the oil-water interface, and facilitates the formation of stable foams and emulsions (Dexter et al., 2006). AM1 molecules adsorb at the oil-water interface where the hydrophobic residues (positions 1, 4, 8, 11, 15 and 18) oriented toward the oil phase (Figure 1.1). AM1 has also switchable properties allows easy reversible destabilisation of emulsions through pH change or chelating effects (Dexter et al., 2006, Malcolm et al., 2006). DAMP4, a recently reported protein-based biosurfactant that shows chemical similarity to AM1 (Dwyer et al., 2013) spontaneously integrates into the oil-water interface of TNEs, which have already been stabilised by AM1. Genetic or chemical conjugation of bioactive moieties to DAMP4 for subsequent TNE surface integration enables decoupling of the physical stabilisation and biological functionalities of the TNEs (Sainsbury et al., 2014) (Figure 1.2). That is, it separates emulsification from functionalisation, which is unique among NEs. In this way, DAMP4 allows for the display of a wide range of molecules on the surface and the engineering of sophisticated surfaces at the oil-water interface (Zeng et al., 2013). For example, DAMP4 was chemically conjugated to PEG (Zeng et al., 2013), a non-immunogenic and non-toxic hydrophilic polymer that is widely applied in pharmaceutics for shielding from immune system detection (Harris and Chess, 2003). The importance of PEG for decorating and applying drug delivery systems will be discussed in the next paragraphs. The TNEs were then also functionalised by fusing DAMP4 to a monoclonal antibody (anti-Clec9A), targeting the Clec9A receptor on the dendritic cells (DCs) (Zeng et al., 2013). Functionalising the TNEs with anti-Clec9A antibody enables the specific targeting of the DCs subset in *in vivo* studies. Immunotherapeutic TNEs remain under development for various diseases, including cancer (Sainsbury et al., 2014). However, because of their versatile features, such as ease of production, high

drug loading capacities, cargo protection and cell-selective targeting, they show remarkable potential as carriers for hydrophobic compounds.

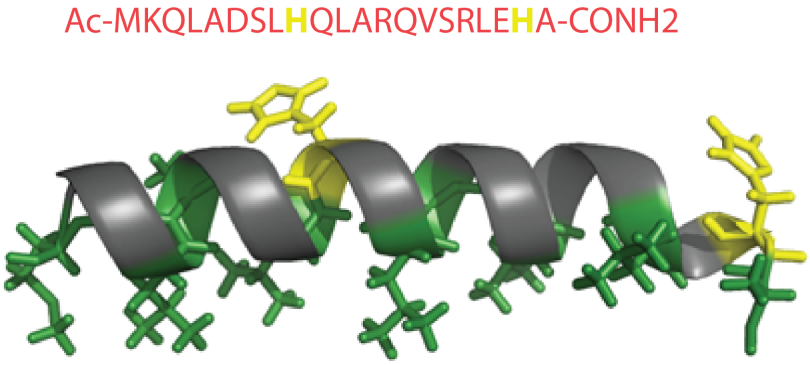

Figure 1.1. Schematic representation of AM1 peptide. The hydrophobic chains of AM1 are presented in green. The metal binding properties of AM1 via histidine molecules are shown in yellow.

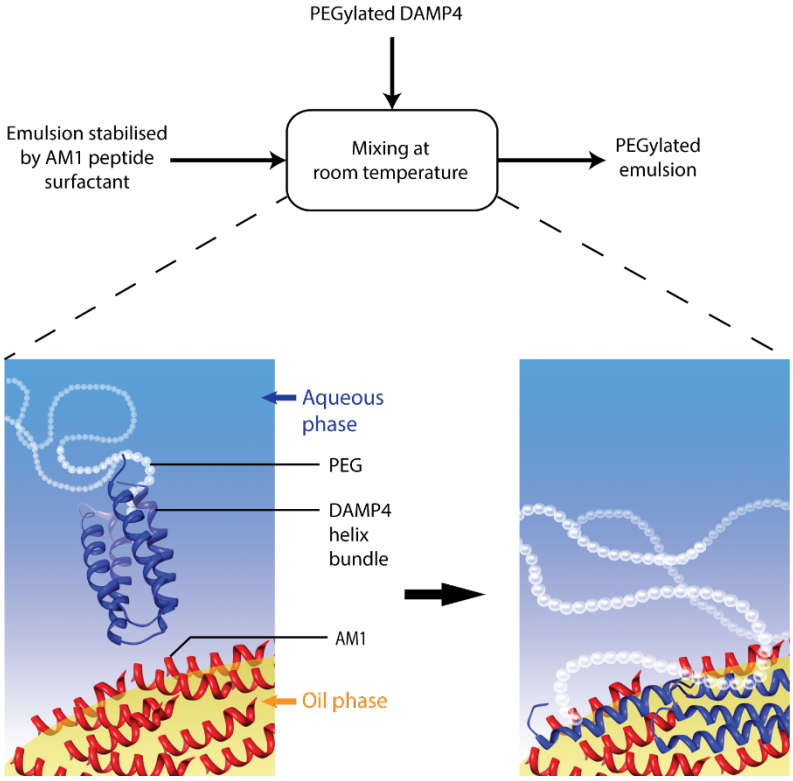

Figure 1.2. Diagrammatic depiction of how TNEs are fabricated. This shows the addition of the PEGylated DAMP4 to the AM1-stabilised TNEs to stabilise the emulsion and impart hydrodynamic stability (Sainsbury et al., 2014). AM1 shown in red, DAMP4 shown in blue and PEG shown in white.

1.3 Bioconjugation

Since the pioneering studies done by Ringsdorf (Ringsdorf, 1975), bioconjugation chemistry has become a central element in pharmaceutical applications as well as fundamental research (Veronese and Morpurgo, 1999). It is defined as 'the covalent derivatisation of biomolecules' (Kalia and Raines, 2010), and it has been the basis of most stabilisation mechanisms against physiological processes, including enzymatic degradation (Fee and Van Alstine, 2006), immunogenicity (Jokerst et al., 2011) and clearance (Monfardini and Veronese, 1998). Therefore, bioconjugation of polymers to biomolecules can improve their properties and, thus, their pharmacokinetic profile (Lu et al., 2002). Bioconjugation is widely used in various applications, including biochemical assays (Newman and Zhang, 2008), discovery of ligands (Rup and O'Hara, 2007) and diagnostics which, in turn, include *in vivo* imaging (Parker, 1990, Wester and Schottelius, 2007), industrial applications (Wong and Whitesides, 1994) and PEGylation (Harris and Chess, 2003, Zalipsky, 1995). Bioconjugates can be attached to their biomolecules either through conjugation to natural amino acids (which will be discussed in this work) or incorporated unnatural amino acids. The most widely used method for protein conjugation is the nucleophile to electrophile attacks where cysteine is the most robust available nucleophile as a natural amino acid, although cysteines are rarely present in most proteins (Veronese and Morpurgo, 1999). The reaction of maleimide to thiol groups of cysteines is a common example for thioether formation (Figure 1.3f). A more commonly applied approach is protein conjugation of the amino groups in lysines by N-hydroxysuccinimides (NHS-chemistry) (Kalia and Raines, 2010). Primary amines of proteins can also react with conjugates having carboxylic groups (Figure 1.3c). The presence of amino groups in most proteins reduces the opportunity for site-specificity conjugations (Veronese and Morpurgo, 1999). Site-specific bioconjugation of proteins can occur through the incorporation of functional groups such as the sulfhydryl group or other reactions such as copper-catalysed azide-alkyne cyclo-addition (Kakwere et al., 2010).

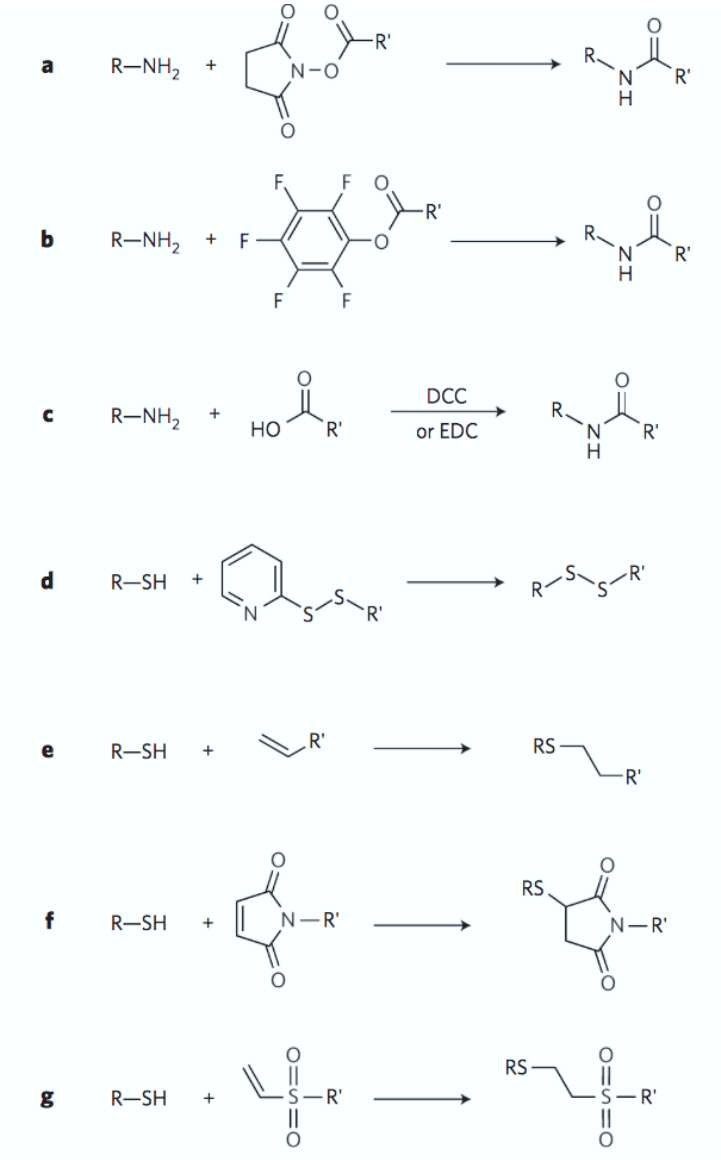

Figure 1.3. List of amino and thiol functional reactive groups.**a.** Reaction of primary amines with N-succinimidyl activated ester leads to amide formation. **b.** Reaction of primary amines with pentafluorophenyl activated ester leads to amide formation. **c.** Reaction of primary amines with carboxylic acid in the presence of N,N'-dicyclohexyl carbodiimide (DCC) or carbodiimide (1-ethyl-3-(-3-dimethylaminopropyl) carbodiimide hydrochloride (EDC) leads to amide formation. **d.** Reaction of pyridyl disulphide with sulfhydryl group (thiol) leads to disulphide formation. **e.** Michael addition of alkene to thiol leads to thioether formation. **f.** Reaction of maleimide to thiol leads to thioether formation. **g.** Michael addition of vinyl sulphone to thiol lead to formation of thioether group (Cobo et al., 2014).

1.3.1 PEGylation

PEG is the most common FDA-approved polymer used for stabilising colloidal nanocarriers in pharmaceutical applications (Gref et al., 2000). It has been reported that PEG can affect the surface charge, size and hydrophilicity of drug delivery systems. Circulation time is considered an important benchmark in the evaluation of drug delivery systems, including emulsions, via the intravenous (IV) route. The half-life of drug delivery systems in blood circulation is usually short due to the rapid clearance by macrophages via the opsonisation mechanism (Juliano, 1988). Hence, coating with hydrophilic polymers, such as PEG and poloxamines, is crucial to extend their half-life in the bloodstream and improve therapeutic efficacy (Allen and Martin, 2004). That is, PEG coating can reduce protein adsorption (opsonisation) (Owens and Peppas, 2006) onto the interface, which prolongs circulation half-life by avoiding phagocytosis. Successful PEG presentation can also minimise aggregation by improving colloidal and steric stability (Moore et al., 2015). In contrast, it has been reported that IV-administered PEG-labelled formulations can induce immune response or opsonisation. The complement system as well can be activated through injected PEG-conjugates or formulations which can result in hypersensitivity reactions (Knop et al., 2010). Even though there are a few concerns surrounding the use of PEG, it is still considered the gold standard polymer for use in drug delivery.

Controlling the surface properties (size, surface charge and hydrophilicity) of an NE system is essential to enable modification and synthesis of a promising drug delivery system for various biological applications (Ganta et al., 2014b). The density of PEG coating is also crucial to any direct drug delivery system for a particular route of delivery. PEG density also relates to targeting efficiency for both passive and active targeting (Xu et al., 2015). PEG also might have a positive or negative impact on the function of conjugated molecules, such as antibodies and surfactants. Therefore, studying the application of PEG molecules on surface-modified emulsions is an important area of research as it provides insight into the future direction for the medical applications of NEs. For example, tuning a biophysical property, such as the surface charge, can affect the interaction of NPs with cells in several ways, including the minimisation of non-specific binding. It can also affect interfacial thickness, stiffness and activity of co-displayed molecules by varying parameters, such as size, PEG length or orientation (D'souza and Shegokar, 2016). Due to the importance of PEG and these possible impacts on the interface of an emulsion system, this research project investigated and characterised the TNEs' interface using the designer biosurfactant, DAMP4, which allows functionalisation with molecules such as PEG. In addition, due to the importance of DAMP4 in imparting stability and functionality to TNEs, the impact of PEG on DAMP4 activity was investigated.

1.4 Thesis aims

The overall aim of this thesis is to further refine the nanocarrier emulsions previously developed by the Middelberg group at the University of Queensland. This aim is addressed by tuning the platform to suit different applications based on the biophysical properties of the oil-water interface. The structural elements of the interface consist of the ensemble of molecules at the surface including AM1, coordinated metal ions and DAMP4 as well as bioconjugated moieties such as PEG and targeting ligands. Together, these determine functional properties of TNEs. Investigation of the structure-function relationship of the interface will be achieved through the following three objectives:

1- To broadly explore the suitability of TNEs in diagnostic and therapeutic applications employing different routes of administration.
2- To gain insight into the interfacial structure-function of the polyethylene glycol-decorated peptide-stabilised Nanocarrier emulsions, and
3- To gain better control over the interface of the TNEs through genetic engineering of DAMP4 for precise bioconjugation of DAMP4 and interfacial activities.

To achieve the first aim of this project, I evaluated the feasibility of using TNEs for diagnostic/therapeutic applications via the IV and topical (skin) routes. This includes the encapsulation and retention capacity of hydrophobic compounds within the oil core of TNEs based on variable DAMP4-PEG densities on TNE interfaces. Control over the surface charge of TNEs was harnessed for electrostatic interactions to form a hybrid system with a promising technology called silica elongated microparticles (EMPs) developed by Professor Tarl Prow at the Translational Research Institute (TRI).

The application of TNEs as a targeted drug delivery system was also evaluated by developing a DAMP4-scFv fusion protein. The integration of this fusion into the TNE interface was evaluated, and the scFv-labelled TNEs were applied to cancer cells for *in vitro* targeting studies. Targeted and un-targeted TNEs were tested for *in vivo* studies in tumour mouse models.

The second aim was addressed by exploring the interfacial structure-function relationship of the polyethylene glycol-decorated peptide-stabilised nanocarrier emulsions, which have profound influence on biodistribution, stability and efficiency of functional surface properties such as active targeting. Surface modification of drug delivery systems is commonly applied to improve their stability and further biological applications. PEG is an FDA-approved hydrophilic polymer widely applied to fabricate nanomaterial surfaces to achieve better pharmacokinetics. Therefore,

understanding the molecular characteristics of the PEG layer offers insight into the structure-function relationship for the development of soft nanomaterials more broadly.

The third aim involved studying the impact of covalent modification on genetically engineered DAMP4 variants. DAMP4 variants were evaluated for structural and functional alterations following the introduction of cysteine residues. The variants allow for more accurate design and analyses of the TNE interface. They provide more precise information on the structure of biosurfactants following the covalent attachment of PEG, and how this can affect their functional properties including interfacial activity, stabilisation of emulsions and presentation of biomolecules.

1.5 Thesis organisation

Chapter 2 - Comprises a literature review (publication manuscript) under the title of 'Nanoemulsions: promising drug delivery systems for medical applications'. The review addresses the basic science of NE formulations as it relates to the medical application and route of administration. It summarizes the dispersion and stabilisation of O/W emulsions and discusses their physical properties in terms of pharmacological performance. Then, it critically examines the uses of NEs in the treatment and prevention of disease by route of administration. Finally, we comment on the potential for the functionalisation of NEs by both bottom-up and top-down self-assembly mechanisms to formulate sophisticated NEs for specific applications.

Chapter 3 - Investigates the use of TNEs as a drug delivery and imaging tool for topical and IV route applications. This work was to elucidate the possible biological challenges that might be faced during topical and IV administration. A hydrophobic fluorescent dye, 1,1′-dioctadecyl-3,3,3′3′-tetramethylindocarbocyanine perchlorate (DiI) used to evaluate the interfacial properties of TNEs including the capacity of cargo retention and physical and colloidal stability. These tuneable properties were explored for coating a promising EMPs for human skin applications and stabilising TNEs for IV delivery.

Chapter 4 - Presents a fundamental insight into the interfacial structure-function of the polyethylene glycol-decorated TNEs. This chapter relates physio-chemical properties of TNEs as a tuneable model interface to ligand accessibility and receptor-binding performance. PEG-mediated surface shielding is commonly used to impart anti-fouling and immune-evading characteristics on interfaces and NPs. This chapter uses the precise control over the surface decoration of TNEs to study the interfacial properties of a PEG-modified oil-water interface, and examines how the physical properties of different PEG layers influence the accessibility of a co-decorated single-chain fragment antibody.

Chapter 5 - Reports the development of a second generation of the protein biosurfactant, DAMP4, to enable precise and efficient bioconjugation of PEG and, therefore, more controlled investigation of the impact of DAMP4 adsorption on interfacial activity. The second-generation biosurfactants (cysteine variants of DAMP4) were engineered using rational amino acid substitution, and their structure, stability and interfacial activity were studied and compared to the parent molecule. The mass and number of bioconjugated PEG molecules to the cysteine variants were evaluated for their impact on the interfacial activity of DAMP4 and the overall stability of the TNEs interface.

Chapter 6 - Provides a summary of all the thesis findings and relates these to the future directions of research.

2 Chapter 2: Literature Review: Nanoemulsion: a Promising Drug Delivery System for Medical Applications

The following literature review manuscript will be submitted to the *Journal of Nanomedicine, Future medicine:*

Hossam. H Tayeb[1, 2], Frank Sainsbury[1]*

1 The University of Queensland, Australian Institute for Bioengineering and Nanotechnology, St Lucia, QLD 4072, Australia.

2 King Abdul Abdul-Aziz University, Faculty of Applied Medical Sciences, Jeddah, Kingdom of Saudi Arabia.

Abstract

Emulsions are heterogeneous systems of two immiscible liquids stabilised by emulsifiers or surfactants. Nanoscale oil-in-water emulsions (NEs) show great potential in a broad range of medical applications because of their attractive characteristics for drug delivery. These include enhanced drug solubility, the use of generally recognised as safe ingredients (GRAS), ease of production and high loading capacity. NEs have been explored as therapeutic delivery vehicles for hydrophobic compounds via various routes of administration including via the skin, ocular, nasal cavity, respiratory tract, and ingestion and via injections. In some cases, NEs provide opportunities to improve drug delivery via alternative administration routes. However, deep understanding of the fundamental processes of NE manufacturing and functionalisation, and how they relate to the choice of administration route and pharmacological profile is still limited. These challenges remain to be overcome to ease the transition of NEs from laboratories to patients use. Here we review the diversity of medical applications for NEs and how that governs their formulation, route of administration, and the emergence of increasing sophistication in NE design for specific applications.

2.1 Introduction

NEs, also known in the literature as ultrafine emulsions, mini-emulsions and submicron emulsions, are heterogeneous systems in which one liquid (dispersed phase) is dispersed as nanosized droplets in another liquid (continuous phase) (Solans and Solé, 2012, Ganta et al., 2014b, McClements, 2011, Lu et al., 2012). The droplet size range of NEs is between 20-500 nm (Gupta et al., 2016). NE types are based on the class of the dispersed and continuous phases, for example, oil-in-water (O/W), water-in-oil (W/O) and double emulsions (W/O/W or O/W/O) (Figure 2.1). NEs can be relatively easily fabricated with biocompatible and biodegradable ingredients involving FDA-approved oils. They are non-equilibrium (thermodynamically unstable) and kinetically stable systems (Solans et al., 2005, McClements and Jafari, 2018). Therefore, they require energy input (high or low energy methods) for their formation (Tadros et al., 2004) and surfactants or emulsifiers to impart colloidal stability. Surfactants and co-surfactants used to stabilise NEs can be lipid-based molecules (Gianella et al., 2013) or peptides/proteins (Malcolm et al., 2006, Dwyer et al., 2013) both of which show a degree of compatibility for human use. Surfactants reduce the interfacial tension (IFT), surface energy (δA) per unit area (A), between the dispersed and continuous phases, providing thermodynamic instability which leads to an increase in the shelf-life stability (Mason, 1999). Surfactants can also act to stabilise NEs through repulsive electrostatic forces (Mason et al., 2006)

Our review addresses the basic science of NEs formulation as it relates to the medical application and route of administration. We summarize the dispersion and stabilisation of O/W emulsions and discuss their physical properties in terms of pharmacological performance. We then critically examine the uses of NEs in the treatment and prevention of disease by route of administration. Finally, we comment on the potential for the functionalisation of NEs by both bottom-up and top-down self-assembly mechanisms to formulate sophisticated NEs for specific applications.

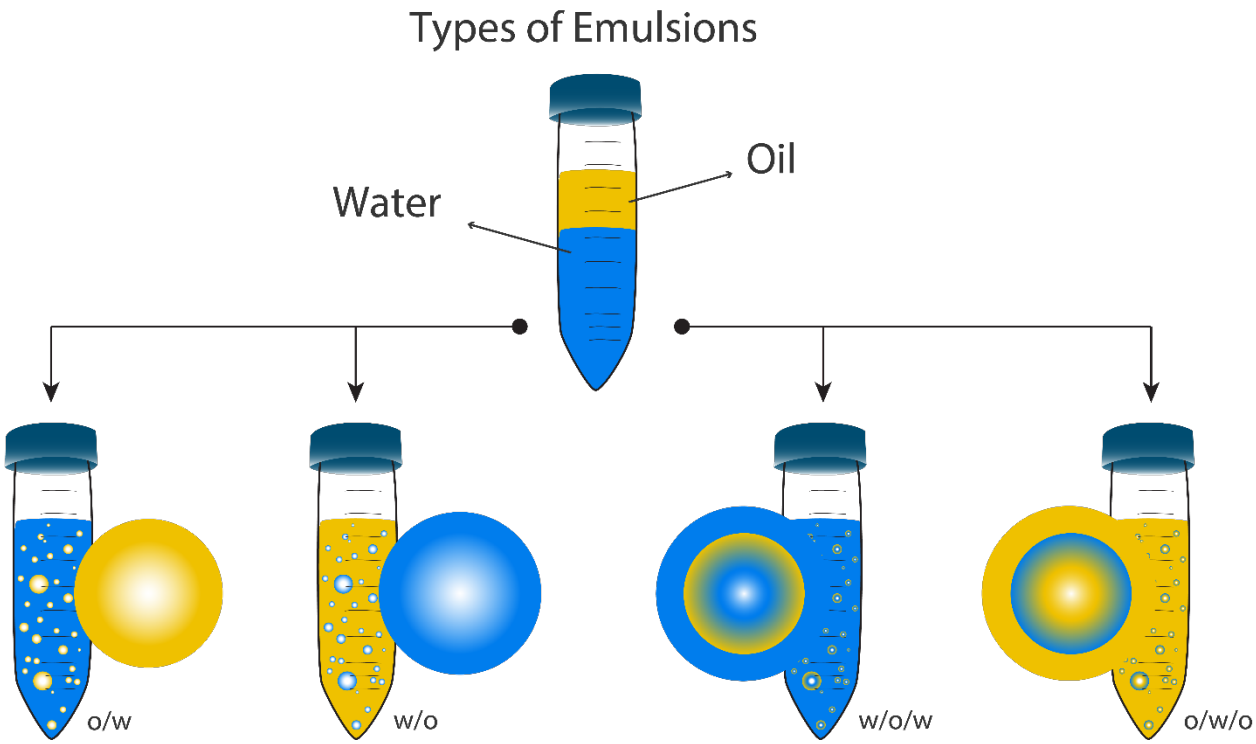

Figure 2.1. Types of emulsion based on the dispersed phase.

2.2 Preparation methods of nanoemulsions

NEs are synthesised by various techniques that fall under one of two energy input paradigms; high-shear forces (e.g. ultrasonication) and low-shear forces (e.g. phase inversion temperature (PIT) (Fryd and Mason, 2012, Talegaonkar and Negi, 2015, Gupta et al., 2016). The high energy methods involve the use of mechanical devices to exert shearing forces to split the dispersed phase into fine droplets (Musa et al., 2013). Sonication devices are mostly used in research laboratories; however, rotator-stator and high-pressure devices are usually used in industry (Solans et al., 2005, Kentish et al., 2008). The low energy methods leverage the internal chemical potential of the system to formulate NEs (Komaiko and McClements, 2016). The production of NEs using high-energy approaches is determined by the formulation composition and the required energy input. There are two major mechanical-shearing methods using high energy, ultrasonication and homogenisation (Figure 2.2). The ultrasonication method applies high-frequency sound waves to two immiscible liquids. These generated shearing forces break up the dispersed phase into small droplets in the presence of a surfactant that prevents droplet coalescence or flocculation by reducing the IFT (Maa and Hsu, 1999). Homogenisation involves the application of very high pressures on the formulation mixture which is then pumped via a restrictive valve. This generates high shearing force resulting in the formation of small droplets of the dispersed phase (Tadros et al., 2004, Quintanilla-Carvajal et al., 2010, Håkansson and Rayner, 2018).

The low energy methods utilise the chemical potential of the system internal components to formulate dispersions. Low energy emulsification and condensation methods use the phase transitions that take place in response to temperature and composition changes (Gupta et al., 2016, Usón et al., 2004). The phase inversion temperature (PIT) method, first reported by Shinoda and Saito (Shinoda and Saito, 1968), is one of these methods widely applied in industry.

2.3 Nanoemulsion-destabilising mechanisms

In the absence of the following mechanisms: flocculation, creaming, cracking and Ostwald ripening, NEs are generally known as a stable platform. The most common destabilisation mechanism is Ostwald ripening (Delmas et al., 2011, Kabalnov, 2001). It is defined as the growth of the dispersed phase larger droplets at the expense of the smaller droplet (Figure 2.3). In other words, Ostwald ripening is the process by which smaller droplets of the dispersed phase (higher Laplace pressure) migrate via the continuous phase into large droplets that have lower Laplace pressure (Mason et al., 2006).

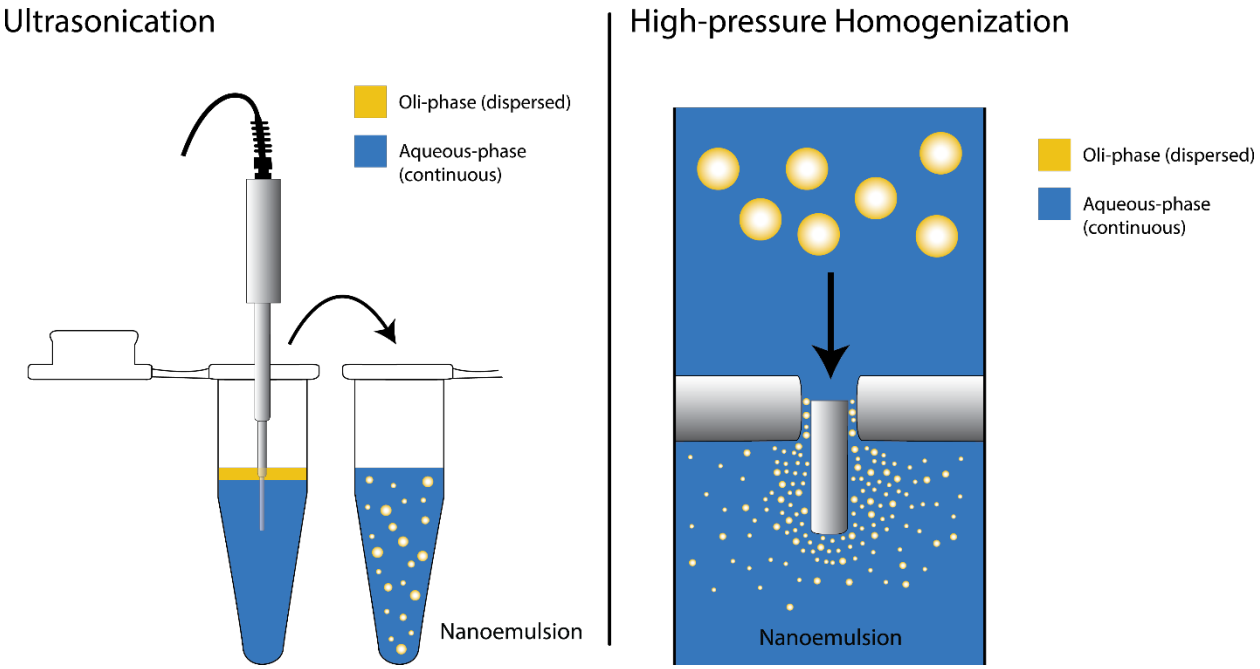

Figure 2.2. The common techniques used for the formulation of NEs.

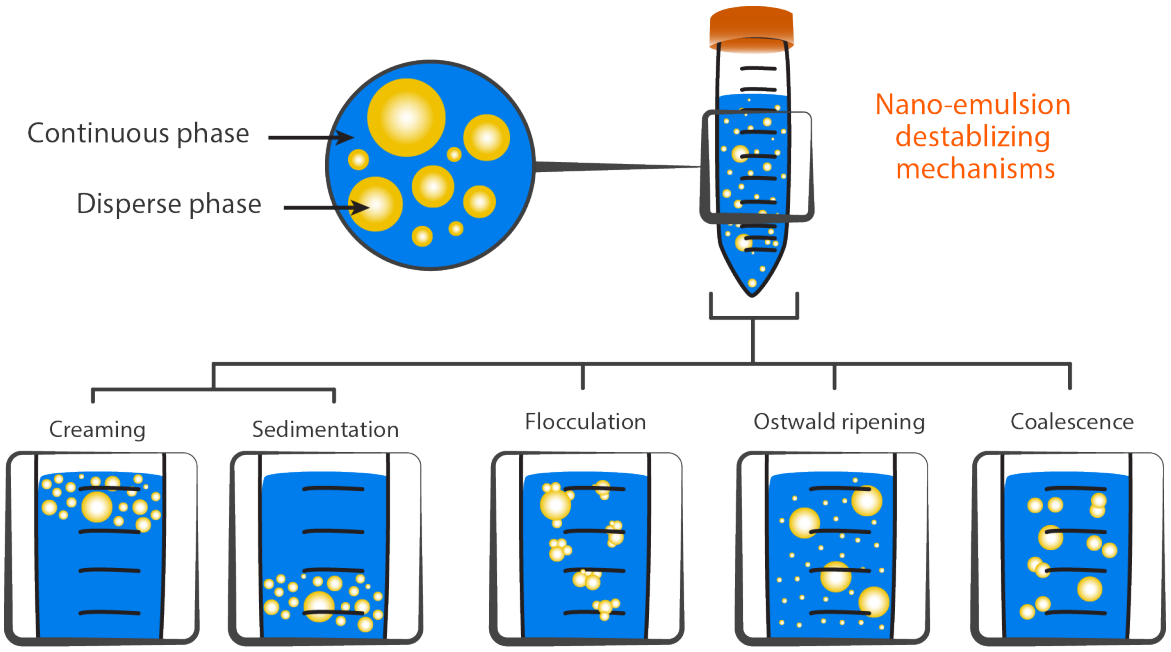

Figure 2.3. The destabilising mechanisms of the NEs. The continuous phase and the dispersed phase are in (blue) and (yellow) respectively.

Laplace pressure differential allows for mass transfer from smaller to larger droplets. The solubility of the dispersed phase (e.g. oil) in the continuous phase plays a major role in the ostwald ripening phenomena (Rahn-Chique et al., 2012, Lifshitz and Slyozov, 1961), which can be suppressed by selecting two phases that are highly immiscible where the dispersed-phase droplets have very low solubility in the continuous phase.

Flocculation or coagulation occur when two or more droplets join and form dispersed larger clumps or floccules due to attractive forces. These floccules move in the solution as a single object (Figure 2.3). The DLVO theory suggests that when the repulsive minimum between two droplets is low, these droplets tend to form floccules or clumps (Rahn-Chique et al., 2012). Floating of these clumps is known as creaming; therefore, flocculation might lead to creaming (Jaiswal et al., 2014, Rahn-Chique et al., 2012). This floating (buoyancy) occurs because of an upward exerted force by the fluid because the pressure under the floating droplet is greater than the pressure on the top of the droplet. This buoyant force controls the degree of freedom of a particular system when it dominates thermal fluctuations and Brownian motion. In the case where the dispersed phase is less dense than the continuous phase, it leads to floating of the droplets (creaming) (Mewis and Wagner, 2012). In the case where the dispersed phase is denser than the continuous phase, it leads to sedimentation (Figure 2.3). These floating droplets form a thick (concentrated) layer of the dispersed phase. A cracked NE is characterised by the separation of the dispersed phase from the continuous phase where the NE cannot be reverted to its normal condition. However, creamed NE can be reconstituted by mixing (Jaiswal et al., 2014).

2.4 Nanoemulsion stabilisers

Long shelf-life and stability in various environments are important requirements for the use of NEs in medical applications (McClements and Gumus, 2016). Surfactants or emulsifiers are surface-active molecules that can maintain the kinetic stability of NEs by reducing IFT between the dispersed and continuous phases. Stabilisers can be ionic, non-ionic surfactants, polymers or solids. Polymers and non-ionic surfactants can help to prevent destabilisation of NE through steric hindrance. Ionic surfactants (charged surfactants) can also prevent instability of NEs via electrostatic repulsion (Otto and du Plessis, 2015). Currently used stabilisers are either chemically-synthesised (Spans, Tweens or Cremophors) (Kralova and Sjöblom, 2009, Kaur et al., 2016) or bio-sourced (egg lecithin, whey protein, caseinate and microbial) (Dickinson, 1986, Dickinson, 1994, Rodrigues et al., 2006). Some of these surfactants are associated with toxicity concerns, therefore considering selection criteria that include surfactant source, concentration and safety profile is important for the formulation of stable NEs. For example, the stabilisation of NE systems usually requires high concentration of surfactants

and co-surfactants, and this may cause irritation and toxicity in oral and topical drug delivery applications. The selection of surfactants based on chemical properties is also another important aspect in the formulation of NEs for drug delivery. For instance, it has been reported that non-ionic synthetic surfactants show less toxicity when compared to ionic surfactants, which can damage biological membranes (Azeem et al., 2009). In addition, non-ionic surfactants tend to have better in vivo stability in comparison with their ionic counterparts (Kawakami et al., 2002). Although non-ionic surfactants such as Cremophor have been marketed as part of paclitaxel formulation (Taxol), this formulation still have a considerable level of toxicity (Kaur et al., 2016). In addition to toxicity, chemically synthesised surfactants are not biodegradable and non-renewable, whereas biosurfactants are gaining interest as stabilisers in food and medical applications due to their biocompatibility, biodegradability and sustainability. Even though biosurfactants are less toxic than chemically-synthesised surfactants, some of these can still provoke adverse reactions such as egg lecithin. Biosurfactants can be classified as low molecular weight (peptides, proteins and glycolipids) or high molecular weight (proteins, lipoproteins and polysaccharides) compounds (Marchant and Banat, 2012, Rodrigues et al., 2006). Lipid-based surfactants have been used to stabilise multifunctional NE in drug delivery applications (Gianella et al., 2013). Glycolipids extracted from microorganisms were studied extensively as surfactants with antimicrobial activity (Gerard et al., 1997). They were also applied for stabilising NE for drug delivery applications such as analgesia (Ahmad et al., 2014a). Proteins have a safety profile history in both food and pharmaceutical applications. Peptide and polypeptide surfactants are promising amphiphilic molecules for stimuli-responsive and self-assembly systems (Dexter et al., 2006, Malcolm et al., 2009). They can be conjugated to a wide range of molecules to stabilise and functionalise NEs for a particular application (Zeng et al., 2013, Sainsbury et al., 2014). These conjugates include polymers such as PEG that is commonly used in drug delivery to achieve immune shielding and *in vivo* stability through steric hindrance. Thus protein-based surfactants can potentially be utilised to functionalise NEs for a wide range of medical applications.

2.5 Nanoemulsions in medical applications

The emergence of high-throughput screening methods and combinatorial chemistry has facilitated the design of potent therapeutics. However, most of these promising therapeutic agents show poor aqueous solubility. It is estimated that approximately 40% of newly discovered therapeutic agents are eliminated from the drug development pipeline because of poor aqueous solubility (Ganta et al., 2014b). NEs have evolved as a robust carrier for the delivery of a wide range of hydrophobic drugs. Their attractive features, including ease of production, enhanced loading capacities, long-term

stability, increased bioavailability and protection and controlled release of cargos, make them promising carriers for use in nanomedicine (Fryd and Mason, 2012). NEs have been broadly applied to a broad range of applications including food industry (Silva et al., 2012, McClements and Rao, 2011), cosmetics (Sonneville-Aubrun et al., 2004) and medicine(Jaiswal et al., 2014, Singh et al., 2017). They have been applied via different administration routes and they are applied as dried (powdered) formulations, aerosols, ingestible and injections (Figure 2.4). NEs have been widely applied to improve pharmacokinetics and bioavailability of water-insoluble drugs.

Our review addresses the fundamentals of O/W NE formulation as it relates to drug delivery applications. The physiochemical properties of NE formulations including charge, size and the type of oil or surfactants are important for successful medical application. Therefore, studying and relating the physiology of both application and indication is essential for integrating desired properties into bespoke NE formulations.

2.5.1 Topical applications

Skin provides a layer of protection for the human body against the surrounding environment. However, it is also considered as an administration route for topical drug delivery. The skin is a multi-layered organ (Cosco et al., 2008). The stratum corneum (SC), the outer layer, is composed of the epidermis, dermis and subcutaneous tissues. The lipid matrix of the SC comprises keratinocytes, cholesterol, fatty acids and ceramides (Morrow et al., 2007). This lipid matrix provides a barrier against environmental factors such as radiation.

Drug application to the skin offers various advantages including the non-invasive administration of medicines either locally or systemically (Barry, 2004). However, this requires diffusion of a drug to the dermis layer, which presents a challenge in topical drug delivery due to the presence of a protection layer, the epidermis. The inherent properties of O/W emulsions can enhance the absorption of lipophilic drugs when applied topically to the skin. Firstly, the encapsulation of lipophilic drugs within the NEs oil core can improve their bioavailability. Also, the use components (surfactants and co-stabilisers) within the interface can enhance penetration activity of the SC layer (Rhee et al., 2001). The small size and the low-surface tension of NEs might also improve the permeation rate of the encapsulated drug (Talegaonkar and Negi, 2015). A large number of studies have been published on NEs for topical skin drug delivery (Mou et al., 2008, Salim et al., 2016) and various NE candidates have entered clinical trials (Table 2.1). NE have shown improved bioavailability and pharmacological effect of various water-insoluble compounds. For example, Quercetin is a flavonoid that has potential chemo-protective effects including antioxidation and wound healing. However, it has also low bioavailability because of poor aqueous solubility and low skin absorption and penetration (Galho et

al., 2016). The enhancement of quercetin permeation through the skin was demonstrated when loaded into the lipid core of positively-charged NEs formulated using spontaneous emulsification (Fasolo et al., 2009).

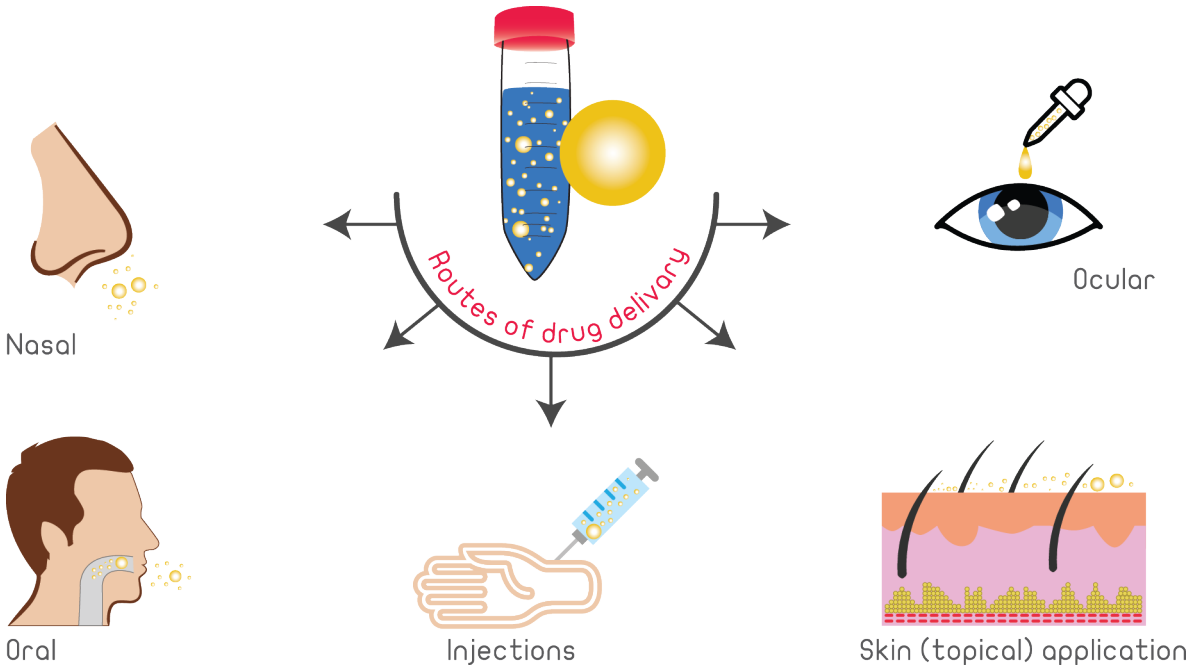

Figure 2.4. Drug delivery applications of nanoemulsions. It illustrates the medical application of NEs based on the routes of administration. These include the nasal, ocular and oral cavities, injections and topical applications.

This indicates the importance of tuning the biophysical properties to improve drug permeation where the positively charged interface of NEs enhance the interaction with the negatively-charged epithelial cells. However, the composition of these NEs include the use egg-lecithin as emulsifier (Fasolo et al., 2009). Egg lecithin is not approved by FDA for medicinal use because of safety concerns, and therefore, biocompatible, FDA-approved, or generally recognised as safe (GRAS) surfactants should be considered to enhance the translation of NE formulations to the clinic.

Skin layers can be targeted through various drug delivery approaches. For example, the treatment of psoriasis requires drug delivery to keratinocytes (epidermis) and deeper layers involving angiogenesis. Formulations for the treatment of psoriasis showed higher bioavailability of paclitaxel at the respective skin layers with minimal leakage to the blood stream when they loaded paclitaxel into NE formulation (Khandavilli and Panchagnula, 2007). The surfactant, labrasol (Hu et al., 2001), known as skin penetration enhancer, was used to improve drug permeation to the required site of action (Khandavilli and Panchagnula, 2007). NE formulations have been developed for poorly soluble compounds with a range of therapeutic effects including anti-proliferative (Pham et al., 2016), anti-microbial (Savi et al., 2005, Kelmann et al., 2016), and antioxidation (Kuo et al., 2008).

Skin drug delivery also offers great opportunities for water-insoluble drugs that show low availability when taken via other routes of administration. To avoid systemic delivery and its side effects for breast cancer therapy, local or intraductal drug delivery to mammary tissues using topical application of cationic NEs loaded with C6 ceramide was recently reported. This study showed that NEs can prolong the drug localisation within the mammary tissues compared to IV delivery of the API in solution (Migotto et al., 2018). Also, it provides convenient non-invasive systemic drug delivery via systemic escape. Allowing systematic escape of encapsulated drugs through dermal layers without accumulation in these layers is known as transdermal delivery. NE properties can be harnessed to disrupt the stratum corneum (barrier), increase thermodynamic activity against skin or flux using penetration enhancers as alternative promising approaches to systemic delivery of hydrophobic drugs (Aqil et al., 2016). For example, the transdermal delivery of indomethacin, an anti-inflammatory drug, using NE facilitated skin permeation via surfactants and co-surfactants that penetration enhancing capabilities (Williams and Barry, 2004). This suggests that the transdermal route can be an alternative non-invasive IV route. Here we suggest the use of biocompatible surfactants to ease the formulation and fabrication of NEs for topical delivery, and also to facilitate the approval of NEs candidates for patient use. Understanding of drug absorption mechanisms through the skin layers in accordance with the composition, formulation, fabrication and the biophysical properties of NEs is crucial to accelerate the progress in topical therapy.

Ocular drug delivery via the cornea is a type of topical applications of NEs, for which there are particular formulation considerations. These include the refractive index, transparency and viscosity. To control these elements, the type and concentration of the dispersed phase (oil) should be chosen carefully. O/W cationic NEs carrying antisense oligonucleotides have been developed to prevent neovascularisation and treat retinopathy (Hagigit et al., 2012). The benefit of using NE in this context was to prevent degradation of the antisense oligonucleotides and improve their ability to cross the cellular membranes. The delivered oligonucleotides targeted the tyrosine kinase vascular endothelial growth factor receptor-2, which is responsible for angiogenesis (Hagigit et al., 2012). In addition, NEs have also been used to improve the delivery efficiency of other APIs for ophthalmic diseases including lutein (Lim et al., 2016) and loteprednol etabonate (Patel et al., 2016).

Table 2.1. Examples of NEs in clinical trials for skin applications (Singh et al., 2017).

Disease (application)	Encapsulated API*	Clinical trial stage	Formulation	Sponsor	Clinical trials, gov identifier
Osteoarthritis	Diclofenac	II (completed)	3%-Diclofenac-NE Cream	Pharmos	NCT00484120
Women (menopause) libido	Testosterone	II (not complete)	Testosterone NE (Biolipid/B2)	University Potiguar	NCT02445716
Multiple actinic keratosis	Aminolevulinic acid	VI (completed)	BF-200 ALA cream	Joint Authority for Päijät-Häme Social and Health Care	NCT01966120
Lentigo maligna	5-aminolevulinic acid	VI (not complete)	NE as light sensitising cream	Joint Authority for Päijät-Häme Social and Health Care	NCT02685592
Basal cell carcinoma	Aminolevulinic Acid	II (not complete)	BF-200 ALA NE	Joint Authority for Päijät-Häme Social and Health Care	NCT02367547

* Active pharmaceutical ingredient

2.5.2 Ingestible nanoemulsions

The oral route is considered a viable and promising option for the delivery of hydrophobic drugs (Strickley, 2004). This is because orally-administered drugs can be conveniently self-administered and do not require intervention by healthcare professionals (Sastry et al., 2000). In contrast, the drug administration via the oral route faces many obstacles, including the pH changes and the presence of digestive enzymes within the gastrointestinal route that can degrade ingested drugs. Other contents of the gastrointestinal tract such as fat and proteins released from food can also interact with orally-administered drugs (Kong and Singh, 2008). Therefore, protecting the ingested drugs from endogenous factors as well as minimising their side effects are primary concerns for orally administered therapeutics.

In addition to improving solubility, NE formulations can also increase absorption and efficacy of orally-administered drugs by prolonging residence in the gastrointestinal tract (Rubinstein et al., 1991) and initiation of the intestinal lymphatic transport pathway (Kotta et al., 2012). The intestinal lymphatic pathway can be stimulated via increasing the association of lipophilic drugs to chylomicrons (Subramanian and Ghosal, 2004, Dahan and Hoffman, 2005), resulting in avoidance of the first-path metabolism by the liver. Furthermore, NE formulation can also improve reproducibility of systemic drug delivery via the oral route (Tirnaksiz et al., 2010). NEs are proven to protect hydrophobic compounds when encapsulated in the oil phase from hydrolysis and degradation (Khani et al., 2016, Sun et al., 2012). In contrast, utilising the high surface area of NEs, in comparison to coarse emulsions and suspensions, can enhance drug absorption by increasing lipid digestion and drug release (Nicolaos et al., 2003).

Improving the efficacy of administered drugs is one of the major aims of drug delivery. An example of that was shown in an *in vivo* study of orally-administered curcumin-loaded NEs that showed an improved anti-inflammatory effect of curcumin when compared to curcumin in a surfactant solution (Young et al., 2014, Wang et al., 2008). Another example is the Primaquine-loaded NEs, which showed better antimalarial activity when administered orally using 25% lower dose when compared to free primaquine (Singh and Vingkar, 2008). Orally-administered NEs have been intensively investigated as well for systemic delivery via the oral route in various medical applications (Tiwari et al., 2006, Tang et al., 2012, Borhade et al., 2012). However, as discussed, there are many considerations to improve drug delivery via the digestive system that need to be overcome for clinical success via this route.

2.5.3 Aerosolised nanoemulsions

Aerosolised therapeutics and diagnostics using colloidal nanocarriers for respiratory diseases are a promising alternative for non-invasive drug delivery (Courrier et al., 2002, Azarmi et al., 2008). The pulmonary delivery route provides a large surface area for drug absorption, low enzymatic activity, thin epithelial barrier, accessible vasculature and avoidance of the first-path metabolism (Azarmi et al., 2008, Patton and Byron, 2007, Gaspar et al., 2008). During last 20 years, many nanocarriers have been developed for different respiratory diseases including liposomes, solid NPs and emulsions, and some have obtained clinical approval to reach the pharmaceutical market. Showing the potential of lipid-based NPs to act as surfactants in the lung, the liposomal formulation, Alveofact®, was approved in 1980 as a synthetic lung surfactant. It is mainly used to prevent or treat respiratory distress syndrome in premature babies who were born with immature lungs (Beija et al., 2012).

The type and characteristics of a pulmonary drug delivery device are important elements for the delivery and, therefore, NE formulations for this route of administration. Examples of these are active breath inhalers (dry powder inhalers) (Islam and Gladki, 2008) or passive breath nebulisers (Groneberg et al., 2003). Active breath inhalers depend on patient inspiratory force (Virchow, 2004) and the internal turbulence of the device (Kruger et al., 2014). Nebulisers are based on the breakdown mechanism of any pre-filled formulation such as the air-blast atomisation (Martin and Finlay, 2015). All these devices are selected for compatibility with particle drug formulations based on a number of factors including their pore size. The optimal pore size is defined by the biophysical characteristics, particle/droplet size, of any given formulation (Groneberg et al., 2003).

There are relatively few published studies demonstrating NEs for drug delivery via the pulmonary route (Table 2.2). Because NEs act as solutions with a large fine particle fraction (FPF), they show high aerosolisation performance after nebulisation when compared to suspensions (Amani et al., 2010). For example, the emulsification of budesonide NE showed a significant improvement in the aerosolisation capacity when compared with the commercially available suspension-based budesonide, PulmecortRespules® (Amani et al., 2010).

Amphotericin B (AmB) is an antifungal antibiotic applied for both local and systemic fungal infections such as Aspergillosis, a life-threatening infection (Tomee and van der Werf, 2001, Soubani and Chandrasekar, 2002) caused by the inhalation of Aspergillus conidia. However, AmB possesses poor aqueous solubility which limits its therapeutic window (Brajtburg et al., 1990). Two AmB NE formulations, intralipid® and clinoleic®, are commercially available products for the treatment of aspergillosis. Both intralipid® and clinoleic® have high encapsulation efficiencies, however, the clinoleic® formulation was shown to have higher drug deposition (over 80%) when compared to

Intralipid (57%). This is due to the fact that clinoleic® NEs have higher FPF than the Intralipid® NEs (Nasr et al., 2012).

Ibuprofen O/W NE mists have also been synthesised as an inhalable formulation for asthma and other inflammatory diseases (Nesamony et al., 2014). NEs were also prepared as a carrier for oligonucleotides through electrostatic interactions. These carriers were used to protect against *Mycobacterium tuberculosis* (pulmonary immunisation). The pulmonary immunisation was achieved via the delivery of DNA to the lungs using cationic submicron emulsions (Bivas-Benita et al., 2004).

Cyclosporine A (CsA)-loaded NEs were also prepared as dry formulation (lipid-based powder) using the spray-drying technique. These emulsions can be rehydrated to form the original O/W emulsion formulation (Onoue et al., 2012). CsA plays a role as an anti-inflammatory (asthma and other respiratory inflammations), anti-fungal and anti-parasitic drug. It is not commonly used in clinics because of its poor solubility and limited oral bioavailability (Beauchesne et al., 2007). However, CsA dry emulsions combined with a lactose carrier and obtained a remarkable 4,500-fold improvement in the dissolution behaviour of CsA resulting in a dispersion suitable for inhalation therapy (Onoue et al., 2012).

Drug delivery via the intranasal route is also considered desirable because it is painless and non-invasive, and can be used to administer drugs either locally (paranasal sinuses) or systemically. This route provides an opportunity for NE formulations that have excellent aerosolisation capacity. The nasal route is mainly utilised for the local treatment of nasal aliments and paranasal sinuses, including the sinusitis, nasal congestion and infections (Pardeshi and Belgamwar, 2013). However, to date, there are no approved NEs for local delivery of drugs such as corticosteroids or antihistamines to treat these indications. There are some examples of intranasal NE for local delivery including vaccination by the delivery of an influenza vaccine to mucosal immune cells (Das et al., 2012), and small molecule delivery for psychological and neurological disorders (Boche and Pokharkar, 2017, Kumar and Jain, 2017, Mahajan et al., 2014, Pandey et al., 2015).

Table 2.2. Examples of the diversity of APIs delivered by aerosolised NEs.

Encapsulated API	Encapsulated API	Finding	Reference
Fungal infections	Amphotericin B	Nebulisation (Higher drug efficacy than chitosan-coated AmB liposomes	(Nasr et al., 2012)
Inflammatory diseases and asthma	Budesonide	Nebulisation (better aerosol outputs and FPF values compared to suspensions	(Amani et al., 2010)
	Ibuprofen	Nebulisation (biocompatible and sterile Ibuprofen pulmonary delivery.	(Nesamony et al., 2014)
Transplantation	Cyclosporine A	Dry-powdered inhaler (lower systemic exposure compared to drug only)	(Onoue et al., 2012)
Gene delivery	DNA	Nebulisation (Not toxic to cells and protect DNA)	(Bivas-Benita et al., 2004)

On the other hand, there are a number of formulations developed for systemic delivery via the nose. For example, aerosolised NE formulations have been developed for the treatment of migraine (Zolmitriptan) (Abdou et al., 2017) and immunisation (inactivated respiratory syncytial virus) (O'Konek et al., 2015).

Nasal systemic delivery offers many advantages including rapid absorption and the avoidance of the first-path metabolism. NEs can improve the delivery of hydrophobic drugs via the nasal mucosa, improving their bioavailability when compared with drug solutions or suspensions. Nasally-administered drugs have shown an improved systemic bioavailability (Comfort et al., 2015). For example, nitrendipine, a highly lipophilic calcium channel blocker used for hypertension treatment, bioavailability was improved in a NE formulation and delivered through the nasal cavity (Jain and Patravale, 2009). Avoiding the blood brain barrier and the first-path metabolism through the nasal route is another alternative strategy for the treatment of central nervous system disorders (Kumar et al., 2008), to minimise invasiveness, bioavailability issues and undesired side effects. Therefore, NE use in the systemic delivery of hydrophobic drugs through the nasal route can be a promising way of overcoming some of the hurdles of IV injections.

2.5.4 Injectable nanoemulsions

2.5.4.1 Nutrition therapy

By the 17th century, the first trial of IV administration of olive oil to a dog at 1 g olive oil/kg as a nutritional supply was conducted by William Courten and resulted in embolism and death because injecting a pure oil into the circulation is fatal. In 1962, the first safe lipid-based IV nutritional NE, Intralipid®, was approved in Europe (Hippalgaonkar et al., 2010). Intralipid® is still marketed and used for calories, and essential fatty acids supply for nutrition-deficient and ill patients. It is composed of made up of 20% soybean oil, 1.2% egg yolk phospholipids, 2.25% glycerine, and water for Injection. Even though Intralipid® was approved and marketed for clinical use, hypersensitivity has been observed in a small number of patients, who are allergic to egg yolk, egg whites and soybean protein (Rotenberg et al., 1991).

NEs have since been investigated for use in various parenteral applications. Cancer diagnosis and therapy are major targets for the use of drug delivery systems in general and the improved parenteral administration of lipophilic materials.

2.5.4.2 Cancer therapy

The tumour microenvironment contains a diversity of biochemical conditions and cell types. Tumour progression into malignancy is promoted by the components of its particular microenvironment. There are critical differences between the growth of tumours and normal tissues, depending on various parameters, such as vascular abnormalities and angiogenesis, oxygenation and perfusion, which can potentially be harnessed for the development of drug delivery systems (Jaiswal et al., 2014). Drug delivery to tumours can be either through passive or active targeting (Figure 2.5) which will be discussed in the coming sections.

2.5.4.2.1 Passive targeting

Targeting cancer cells can be achieved by passive targeting via the enhanced permeability and retention (EPR) effect, where the size of the delivery system is crucial (Kumar Bishwajit and Md. Lutful, 2014). Conditions with EPR effect occur due to unrestricted angiogenesis that leads to the development of poor tumour vasculature, deficiency of pericytes and abnormal basement membranes, thus increasing vascular permeability (Maeda et al., 2000) (Figure 2.5). Drug delivery systems should be between 10 and 100 nm to achieve optimum levels of the accumulation of the therapeutic agent at the tumour mass (Danhier et al., 2010).

Particles sizes less than 10 nm can be cleared by the reticuloendothelial system (RES), whereas particles larger than 100 nm can be engulfed by immune cells (Caron et al., 2013). Engineering of colloidal carriers with neutral or negative charges can help to evade the immune system (Ganta et al., 2014b). Coating NEs with hydrophilic polymers, such as PEG (Ikeda and Nagasaki, 2012, Harris and Chess, 2003) and poloxamines, modifies their surface properties (charge and size), extends their serum half-life and can improve their therapeutic efficacy (Allen and Martin, 2004). Thus, the size, surface charge and hydrophilicity of NEs are important parameters that can be modified to tune the effectiveness of drug delivery to cancer cells by passive targeting (Ganta et al., 2014b).

There are a number of reports of NEs for passively targeting cancer (Ragelle et al., 2012, Venkateshwarlu et al., 2010, Desai et al., 2008). Ganta et al. studied the delivery of chlorambucil using NEs for adenocarcinoma where the effect of PEGylation on circulation was investigated. The PEGylated NEs in this study showed longer circulation and higher accumulation of the drug in the colon-38 adenocarcinoma tumours (Ganta et al., 2010). TOCOSOL™ is an example of the use of NEs to achieve better accumulation and efficacy of a chemotherapeutic at the tumour site that reached the clinic.

The tumour suppression of colon adenocarcinoma was higher using this NE formulation, however, this formulation was discontinued because it did not meet phase 3 efficacy targets (Insight, 2017). Controlling the interface of the NE systems is crucial to obtain the optimum stability against the surrounding biological environment and determine biodistribution. Ideally, PEG density, and other surface biophysical properties can be precisely tuned.

2.5.4.2.2 Active targeting

Active targeting of NEs can be achieved by surface modification with targeting ligands, such as antibodies (Ansell et al., 2000), aptamers (Wu et al., 2015, Aaldering et al., 2015) and small molecules (Kue et al., 2016) specific to cell surface receptors in cancer tissues. Distinct from passive targeting, therapeutics can theoretically be delivered to their target with high specificity, thereby minimising interaction with healthy tissues.

Moreover, internalisation and endocytosis can be facilitated by active targeting in cases where endocytic receptors are targeted, delivering payloads intracellularly where their cytotoxic effects are executed. For optimum selectivity of the tumour-related receptors, it is crucial to select receptors that are overexpressed in cancer cell lines but not in normal tissue. For example, folate, transferrin and the epidermal growth factor receptor (EGFR) are overexpressed in several types of cancers, such as ovarian and breast cancers (Milane et al., 2010). Targeting moieties that can be conjugated to NEs to target a specific antigenic site include vitamins, aptamers, sugars, peptides, antibodies and synthetic polymers, (Zeng et al., 2013, Tayeb et al., 2017, Talekar et al., 2012, Mulik et al., 2010). Monoclonal antibodies and their derived fragments are commonly used for active tumour targeting due to their exquisite specificity, high affinity and, in the case of Fab fragments and scFv antibodies, their small size (Ahmad et al., 2012).

Many studies of NEs have been published on the active targeting of cancer to deliver a broad range of water-insoluble drugs, including the exploration of this concept as a way of overcoming multidrug resistance (Meng et al., 2016). For example, NEs loaded with aclacinomycin A and externally functionalised with folate for targeting human nasopharyngeal tumour cells showed better efficacy of the loaded drug compared to an untargeted formulation (Ohguchi et al., 2008).

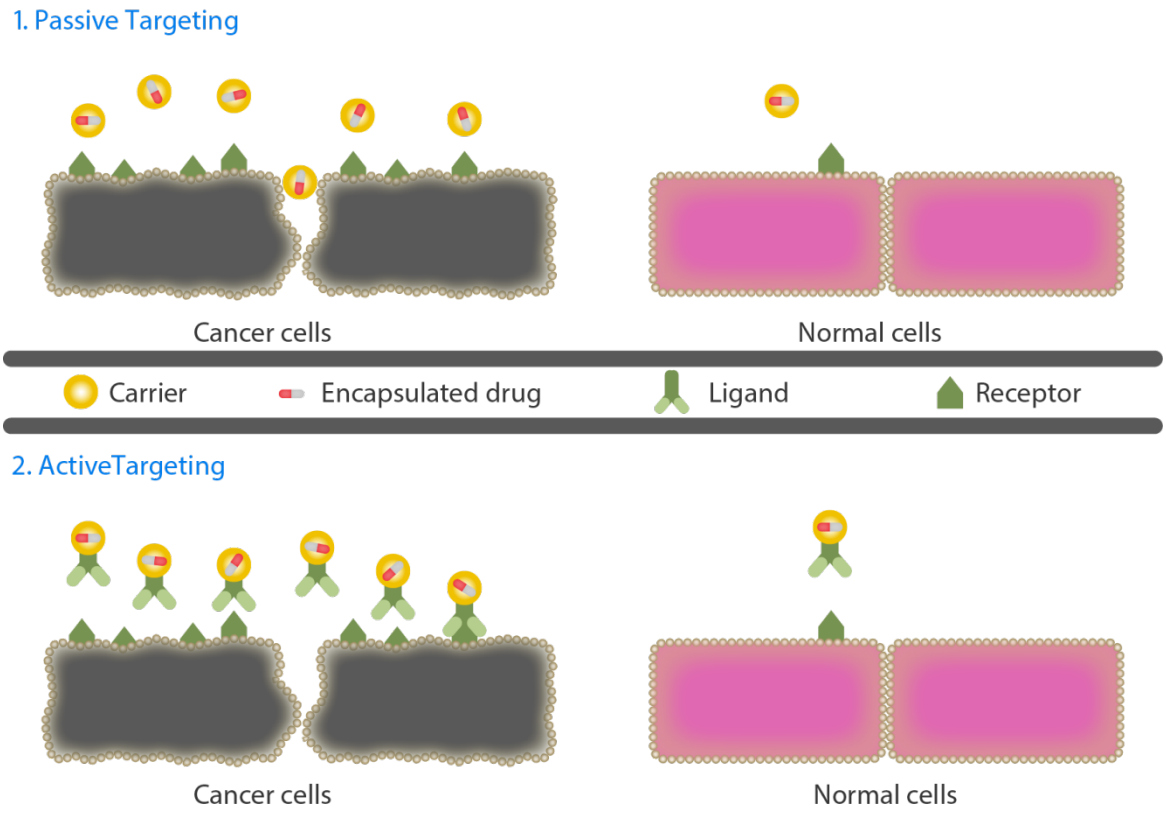

Figure 2.5. Targeting strategies of drug delivery systems.

2.5.5 Other parenteral applications of nanoemulsions

NE can be applied to overcome challenges of a particular route or delivery through alternative routes. Parenteral delivery of NEs has been developed to treat health problems including sepsis (curcumin) (Shukla et al., 2014), hypertension (Clevidipine, Cleviprex®) (Cleviprex, 2018) and erectile dysfunction (Alprostadil, Liple®) (Ganta et al., 2014b, Hörmann and Zimmer, 2016) to protect API from degradation, and minimise their side effects. IV-administered NEs have also been applied and improved the bioavailability of an anti-convulsing (anti-epileptic) agent, Carbamazepine (CBZ), when compared to oral administration (Kelmann et al., 2007). In addition, NEs have been utilised to facilitate the IV administration of drugs for patients having upper gastrointestinal tract complications (such as ulcers) and difficulties in taking oral therapies (Araújo et al., 2011).

2.5.6 Nanoemulsions in biomedical imaging

Non-invasive diagnostic imaging is one of the important future applications of nanomedicine. In 2002, the word "theranostic" first appeared in the literature by Funkhouser, and it is defined as the integration of diagnostics and therapeutics in a particular delivery system (Chen and Wong, 2014). Before the initiation of any treatment plan for complex pathologies such as cancer or cardiovascular disease, it is beneficial to conduct diagnostic imaging to reveal the location, cellular phenotype and the heterogeneity of the affected tissue (McCarthy, 2009, Sumer and Gao, 2008, Warenius, 2009). Thus, rather than the development of two individual systems for each process, theranostics can offer both diagnostic and therapeutic tools in one package that have the potential to overcome the biodistribution and selectivity issues of traditional imaging modalities and cancer therapies. NEs have the potential to be harnessed for localising imaging and drug delivery to the site of action that will eliminate the unwanted side effects of some hydrophobic drugs.

In MRI imaging, perfluorocarbons (PFCs) are considered highly promising intracellular MRI tracers, however, they are highly hydrophobic (Krafft and Riess, 2007). NEs developed to improve the delivery of PFCs to allow for monitoring and imaging of specific cell types or pathologies of diseases such as cancer and atherosclerosis (Balducci et al., 2013, Kislukhin et al., 2016, Lanza et al., 2010). They have also been developed as targeted imaging tools using metallic MRI contrast agents. For example, ScFv-functionalised NEs loaded with iron oxide particles have been used to image atherosclerosis (Prévot et al., 2017). Theranostic NEs with folate-targeting have been developed to deliver docetaxel to ovarian cancer cells (Ganta et al., 2015). The surface of these NEs was functionalised with gadolinium as an imaging agent, and their diagnostic efficiencies were compared favourably to a clinically-relevant MRI contrast agent, Magnevist® (Ganta et al., 2015), This showed

that the NEs formulation was less toxic than cisplatin in the treatment of ovarian cancer model in mice.

NEs have also been used as platforms for fluorescence-based imaging. Vascular inflammation was targeted, treated and visualised using a P-selectin-targeted NE loaded with dexamethasone to treat inflammation, and rhodamine as a molecular imaging agent (Simion et al., 2016). This approach has also been used for the simultaneous monitoring and treatment of inflammation by celecoxib delivery (Patel et al., 2015), and for cancer theragnosis by paclitaxel delivery (Yang et al., 2014). Furthermore, careful NE design has allowed the combination of imaging modalities within a single particle, for example, integrin-targeted paramagnetic and fluorescent NEs designed to target human umbilical vein endothelial cells (HUVEC) cells (Hak et al., 2012).

2.5.7 Emulsions for vaccine applications

Historically, emulsions have been used as effective adjuvants for vaccine formulations in both human and animals (Table 2.3). Paraffin W/O emulsions including inactivated mycobacterial cells is known as Freund's complete adjuvant (FCA) and a non-bacterial form of these emulsions, Freund's adjuvant (FIA), have been used as immunopotentiators in animals (Hilleman, 1966) and human vaccines (Salk et al., 1951, Edelman, 1980). However, the w/o formulation is generally reactogenic due to the presence of high content of oil (Allison and Byars, 1986). W/O emulsions have also been applied as adjuvants for human immunodeficiency virus and malaria, but they also showed undesired local reactions (Aucouturier et al., 2002). In the 1980s, Syntax Adjuvant Formulation (SAF), was used as the first squalane O/W emulsion with an antigen (Allison, 1999). As a less toxic replacement for mineral oils, SAF is also able to induce a robust cell-mediated response (Lidgate and Byars, 1995), however, SAF is associated with muramyl dipeptide (MPL) analogue and discontinued because it had evoked reactogenicity (Allison, 1999) as well as muscular irritation (Lidgate and Byars, 1995). Squalene/squalane emulsions are considered non-toxic adjuvants of growing interest (Allison, 1999). One of the most widely used squalane emulsion adjuvants is the MF59®, which shows higher potency in triggering the cell-mediate immune response when it is compared to aluminum-based adjuvants. MF59 was first licensed as Fluad® in 1997 and is currently approved in US, Canada and various European countries for human use. It is an O/W emulsion that is prepared with 5% v/v squalene in citrate buffer (Ott et al., 1995, O'Hagan and Podda, 2008). MF59 is considered safe and contributes to a potent trivalent (2 subtype A and one B) vaccine against influenza mainly for over 65 years-old patients (O'Hagan and Podda, 2008).

Squalene emulsions and those of its hydrogenated form, squalane, have also been developed as immunotherapeutic and immunostimulant adjuvant. The DETOX® formulation is composed of a bacterial cell wall and monophosphoryl lipid A (MPL) dissolved in squalane and Tween 8 (Baldridge and Ward, 1997). It showed potent adjuvanting activity against melanoma cell lines as a cancer immunotherapy, however, reactogenicity and granulomas have also been observed at the injection site (Ott and Van Nest, 2007). Despite that, DETOX® was licensed for the treatment of melanoma as Melacine®.

Other examples of squalene-based emulsions as adjuvants include the Ribi adjuvant system (RAS) (Table 2.4) (Gomez et al., 1998) and the so-called stable emulsion (SE) (Leesman, 2003). The addition of MPL to SE resulted in a potent vaccine adjuvant for the prevention of leishmaniasis (Reed et al., 2009). Other prominent examples are the SB62 and its two-fold diluted form, AS03. AS03 was approved as a constituent of prepandrix®, the pandemic flu vaccine (Reed et al., 2009). AS03 was also a component of other vaccines including the Arepanrix® for the prevention of influenza caused by H1N1, and H5N1 pre-pandemic vaccines. AS02 is formulated by adding immune-stimulatory agents such as MPL and triterpenoid saponin molecules (QS21) to AS03 (Fox, 2009) and has been tested as an effective adjuvant for vaccines against malaria (Cohen and Druilhe, 2002), HIV, hepatitis B and tuberculosis (Reed et al., 2009). However, the development of AS02 vaccines was discontinued due to the presence of undesirable reactogenicity at the injection site (Table 2.3) (Roestenberg et al., 2008, Garçon and Di Pasquale, 2017). Using emulsions as adjuvant systems are of growing interest for various prophylactic and therapeutic vaccines. Balancing the immunogenic benefits with the safety profile of any formulation is a major concern in vaccine development. Selecting the right antigen or adjuvant and the emulsion composition directly affects the benefit-risk scale. Therefore, rational selection of the oil composition, the adjuvants, surfactants, particles size for a particular disease could provide more efficient vaccines against pandemic diseases such as influenza.

Table 2.3. List squalene O/W emulsions as vaccine adjuvants.

Adjuvant name	Application (disease)	References
MF59® (Novartis)	Influenza	(Ott et al., 1995, O'Hagan and Podda, 2008, Mosca et al., 2008, Pellegrini et al., 2009)
AS03 (GSK)	H5N1 (pre-pandemic) and H1N1 (pandemic) influenza	(Fox, 2009, Garçon et al., 2012, Schwarz et al., 2009)
AS02 (GSK)	Malaria, HIV and tuberculosis (discontinued)	(Roestenberg et al., 2008, Garçon and Di Pasquale, 2017)
MPL® SE (Monophosphoryl lipid A-Stable emulsion) (Infectious Disease Research Institute, IDRI)	Leishmaniasis	(Leesman, 2003, Fox et al., 2008)
AF03 (Sanofi)	Pandemic H1N1 influenza	(Klucker et al., 2012)
DETOX® (MPL in squalane) (Corixa corporation)	Melanoma (Melacine®)	(Sosman and Sondak, 2003)

Table 2.4. Examples of squalene O/W emulsion under investigation

Adjuvant name	Application (disease)	References
Thermo-reversible O/W emulsions (E6020 in AF03)	Immunostimulants	(Klucker et al., 2007, Haensler et al., 2015)
RAS (Synthetic trehalose dicorynomycolate, bacterial cell wall skeleton, and MPL)	Immunostimulants (Sigma-Aldrich) for research	(Gomez et al., 1998, Sjolander et al., 1996)
ESA **Abil®-Care (polysiloxan polymer dimethicone copolyol)**	Veterinary vaccine	(Suli et al., 2004, Beníšek et al., 2004)
Baldridge (Monophosphoryl lipid A)	Immunostimulants	(Baldridge and Crane, 1999)
Hjorth1 and Hjorth2	Veterinary vaccine	(Allison, 1999)

2.6 The future of nanoemulsions in nanomedicine through top-down assembly

Nanosized formulations can be fabricated using bottom-up, top-down or both approaches (McClements, 2015). Bottom-up assembly is characteristic of most approaches to add functionality to NE interfaces, where functional moieties are covalently linked to one or more emulsifiers. However, this restricts the tuneability of NE interfaces due to the need to maintain compatibility with stable emulsification (Sainsbury et al., 2014). In contrast, top-down approaches to modifying NEs has traditionally relied on the rather unspecific adsorption of functional layers by electrostatic deposition. While this approach separates functionality from the need to impart stability during emulsification, it does not result in controlled deposition or the rational presentation of functional groups (Sainsbury et al., 2014). Recently, a novel peptide-stabilised NE system has been developed that decouples emulsification from controlled surface modification. Characterised by the spontaneous and step-wise addition of functional moieties linked to a designer protein biosurfactant (Zeng et al., 2013), this platform allows the rational generation of sophisticated interfaces (Tayeb et al., 2017). Such interfaces will provide valuable insight into the interaction of NEs with their environment, and will aid in the functional design of NEs tailored to specific applications and routes of administration.

2.7 Conclusion and future directions

The continued progress in NE development shows great promise in nanomedicine and is expected to attract greater attention as a versatile platform for drug delivery, molecular imaging and vaccine formulation. Oral delivery was the inspiration for the development of therapeutic emulsions, however, they were first clinically applied as injectable formulations. NE have enjoyed most success as vehicles for delivery of APIs to various epithelial or mucosal surfaces. With the use of clinically approved ingredients and the success of injectable formulations such as vaccine adjuvants, the potential of NEs to improve solubility, bioavailability and pharmacokinetics of hydrophobic compounds they have a bright future in IV applications. In addition, NE formulations can improve the therapeutic efficacy of APIs via alternative routes of administration in many situations, as highlighted in this review. Amenable to the incorporation of multiple functionalities, either loaded in the oil core or presented on the surface, they have also demonstrated great potential in molecular imaging and theranostics. The further development of NE technologies will require a deep understanding of the relationship between NE formulation science and the various physical, chemical and physiological challenges associated with various pathologies and routes of administration. To facilitate the translation of candidate NEs from research laboratories to the pharmaceutical market, numerous considerations must be met. These include careful selection of components, including the oil phase and emulsifiers with regards to safety concerns including hypersensitivity (Galho et al., 2016, Khandavilli and

Panchagnula, 2007). Therefore, formulating NEs with biocompatible surfactants and FDA-approved excipients is a pre-requisite for any future pharmaceutical application. In addition, formulation challenges including ease of synthesis at large scale, storage and stability must be addressed with the application in mind. The continued research on approaches to create ever more sophisticated NEs with controlled interfacial structure will lead to increasing opportunity for clinical translation of NEs for a wide range of indications.

2.8 Acknowledgment

H.H.T. acknowledges the financial support (Scholarship) from King Abdul Aziz University, Ministry of Higher Education, Saudi Arabia. The preparation of this manuscript did not involve any writing assistance.

3 Chapter 3: Exploring the Use of Nanocarrier Emulsions in Drug Delivery

3.1 Introduction

Nanoscience in medical research focuses on the potential role of drug nanocarriers to improve the therapeutic outcomes of hydrophobic drugs. The application of nanotechnology that involves multidisciplinary sciences including physics, chemistry and biology in medicine is known as nanomedicine (Webster, 2006). According to the European Science Foundation, nanomedicine aims at "ensuring the comprehensive monitoring, control, construction, repair, defence and improvement of all human biological systems, working from the molecular level using engineered devices and nanostructures, ultimately to achieve medical benefit."(Anderson, 2005).

Nanocarriers, such as liposomes, have evolved as successful vehicles for solubilising hydrophobic drugs whilst also prolonging their circulation time and accumulation at target sites due to the EPR effect (Torchilin, 2005, Northfelt et al., 1998, Safra et al., 2000). Doxil® was the first successful liposomal formulation approved by FDA for the treatment of Kaposi's sarcoma (Barenholz, 2012a). Nanocarriers have also been applied to a broad range of diseases including fungal infections, multiple sclerosis and late-stage renal conditions (Zhang et al., 2008). Most of these applications have led to improvements in patient safety and have possibly contributed to lower morbidity rates (Gradishar et al., 2005), however these improvements are still considered minor when compared to the benefits of traditional formulations (O'Brien et al., 2004).

Nanocarriers face many biological barriers including opsonisation, phagocytosis (Gustafson et al., 2015) and off-target delivery (Wilhelm et al., 2016) that limits optimum bioavailability and functionality. The complexity of these barriers varies with different routes of administration (IV, oral, skin, etc.), disease type (cancer, infections) and condition (stage of disease) (Blanco et al., 2015). Nanocarriers designed with targeting (Wang and Thanou, 2010, Lammers et al., 2016), stimuli-responsive (Lopes et al., 2013) or controlled release functionalities (Mura et al., 2013) fail to overcome most of these barriers resulting in minimal therapeutic impact. The clinical translation of nanocarriers could be improved by addressing and overcoming these biological barriers through the rational and informed design of a particular drug delivery system (Blanco et al., 2015).

Nanocarriers offer a variety of possible advantages when compared to free drugs such as drug protection, enhanced drug solubility and cellular targeting (De Jong and Borm, 2008). However, ensuring biocompatibility in their design is probably going to be the key to transforming nanocarriers into nanomedicine platforms (Farokhzad and Langer, 2009). Well-defined characteristics, simple

surface functionalisation, specific cellular uptake, aqueous solubility and colloidal stability are other important considerations in the design of effective nanocarriers. Developing sophisticated nanocarrier design is challenging and may not be compatible with a specific route of administration and disease. This design challenge may be addressed through the development of nanocarrier screening techniques for specific applications or by exploring different routes of administration (Peer et al., 2007).

The aim of this chapter is to explore TNEs as a carrier of lipophilic compounds via topical (skin) and IV routes to elucidate the possible biological challenges that might be faced during topical and IV administration. A lipophilic fluorescent dye, DiI (Li et al., 2008) was used as a model drug to evaluate the properties of TNEs including the capacity of cargo retention and physical and colloidal stability. Encapsulation of DiI within the oil core (miglyol 812), which is a material generally recognised as safe (GRAS) by FDA, was investigated after varying the density of PEGylated DAMP4 integrated on the interface of AM1-stabilised TNEs. DAMP4 (Middelberg and Dimitrijev-Dwyer, 2011), was chemically-conjugated to PEG and integrated onto the TNE interface to impart colloidal and functional stability.

TNEs were assembled in a bottom-up fashion via the top-down sequential addition of reagents. The bottom-up approach starts with the individual components leading to the formulation of TNEs. These components include the surfactant (AM1), coordinated metal ions, and the oil and water phases. In contrast, the top-down modification comprises the sequential addition of functional moieties, such as PEG, bioconjugated to DAMP4, which promotes self-assembly at the oil-water interface. Varying the PEG density onto the TNE interface using spontaneous integration of DAMP4 facilitated control over TNE surface properties like surface charge. This surface optimisation enabled TNEs to be combined with a EMPs (Raphael et al., 2013) technology via electrostatic interactions subsequently translating TNEs into a promising drug delivery system for topical applications. The EMPs facilitated physical targeting, allowed penetration through the dermal-epidermal junction and maximised the bioavailability of payloads into the epidermis (Raphael et al., 2014). The coating efficiency of EMPs with TNEs was also studied with respect to the density of the PEG layer, electrostatic interactions and the method of coating. To investigate the release profile *in vivo*, a human-safe dye, 6-carboxyfluorescein (CFC), was loaded into the TNE oil core before being applied to human skin.

To explore TNEs in IV applications, a DAMP4-single chain variable fragment (scFv) fusion protein was genetically engineered and expressed in mammalian cells to impart surface targeting functionalities. Receptor and cell-based studies evaluated the potential use of emulsions in parenteral drug delivery systems encapsulating DiI as a model drug. As a pilot study to test the feasibility of *in vivo* targeting, scFv-functionalised and DiI-labelled TNEs were administered intravenously in a

breast cancer animal model. Rapid clearance of TNEs prompted an investigation of biodistribution through the analysis of urine, serum and cytokines immediately post-injection and at short time intervals thereafter. These studies provided important information regarding biocompatibility and safety, targeting and the possibility of using TNEs as an IV formulation. This information directed further studies towards understanding the fundamentals of the TNE interface that impact the structure-function relationship of TNEs. These studies are discussed in chapter 4.

3.2 Experimental section

3.2.1 DAMP4 expression, purification and quantification

DAMP4, a protein biosurfactant, sequence (MD(PSMKQLADSLHQLARQ VSRLEHAD)4) was expressed in *E-coli*, and purified as previously published (Middelberg and Dimitrijev-Dwyer, 2011). DAMP4 purified using chromatography in three steps; immobilised metal affinity chromatography harnessing the presence of eight histidine molecules, ion exchange chromatography taking advantage of the neutral charge of DAMP4 at pH 7.0 and reversed phase (RP) HPLC. These combined techniques were sufficient for the removal of endotoxins from the expressed protein samples. Endotoxin levels of DAMP4 were evaluated using the LAL-based endosafe PTS™ (www.criver.com). The collected RP-HPLC fractions of DAMP4 were lyophilised, quantified using analytical HPLC and stored at - 80°C.

3.2.2 Preparation of tailorable nanocarrier emulsions

The custom synthesis of AM1 (Ac-MKQLADSLHQLARQVSRLEHA-CONH2) peptide, with a molar mass of 2473 Da and ≥ 95% purity, was performed by Genscript (www.genscript.com). Lyophilised AM1 was dissolved using 25 mM 4-(2-Hydroxyethyl)-1-piperazineethanesulfonic acid (HEPES) containing 800 µM $ZnCl_2$, to a final concentration of 400 µM. DiI, 1,1′-dioctadecyl-3,3,3′3′-tetramethylindocarbocyanine perchlorate (www.thermofisher.com), stock was prepared by dissolving DiI powder in 100% ethanol at a final concentration of 10 mg/ml. This stock was diluted in Miglyol 812, the oil core of TNEs (AXO Industry SA, www.axoindustry.com) to a final concentration of 1 mg/ml. Miglyol 812, also known as caprylic/capric triglyceride, is a neutral and clear medium chain triglyceride excipient. Miglyol 812 is a derivative of saturated coconut oil and comprises 6 to 12 carbon (C) chain fatty acids (Sellers et al., 2005). Miglyol 812 is composed of 50-65% caprylic acid (C8) and 30-45% capric acid (C10) (Cremer, March 2013). DiI-labelled Miglyol 812 was added to the AM1 solution to a final oil composition of 2% v/v. This mixture was sonicated in an Eppendrof tube by the Branson Sonifier 450 Ultrasonicator (www.emersonindustrial.com) using four 45 s bursts. Emulsions with a polydispersity index 0.2 or below were accepted for subsequent

surface modification. PEGylated DAMP4 products were integrated drop-by-drop onto the AM1-stabilised emulsions (P0) with vigorous stirring at a 1:1 volumetric ratio. To prepare TNEs with different DAMP4-PEG densities, a one-step of addition of different concentrations of PEGylated DAMP4 to P0 was performed and included 2 µM (P1), 4 µM (P2), 10 µM (P5), 20 µM (P10), 40 µM (P20) and 400 µM (P200).

3.2.3 Preparation of targeted and un-targeted TNEs

To prepare untargeted TNEs, 40 µM PEG-DAMP4 was used as an initial addition to the AM1-stabilised emulsions to obtain the P20-TNEs. Subsequent addition of PEGylated DAMP4 (400 µM) to the P20-TNEs formulated the P200-P20-TNEs (untargeted). Targeted TNEs, prepared by sequential addition using the same technique, were made by mixing 40 µM PEG-DAMP4 with P0 emulsions, followed by 2 µM scFv-DAMP4 fusion and 400 µM. PEG-DAMP4. Size measurements with associated polydispersity indices and ζ-potentials were measured using a Malvern Zetasizer Nano ZS (www.malvern.com). All samples were diluted to 1:100 in Milli-Q water with ζ-potential measurements made using an electrophoretic cell (www.malvern.com).

3.2.4 Cargo retention within the TNE oil core

Cargo retention within the TNEs was assessed after surface modifications were made to the TNE interface by integrating various concentrations of PEGylated DAMP4 to AM-TNEs. A standard curve was established, using two-fold serial dilutions of DiI-labelled P20-TNEs (0.25 µg/ml DiI concentration), to estimate the difference between the fluorescence of DiI in hydrophilic (H2O) and hydrophobic (miglyol 812) media. Fluorescence was measured at excitation and emission wavelengths 535 and 570 nm respectively using the infinite® M200 Pro plate reader (www.thermofisher.com). Retention of DiI was evaluated by measuring the decrease in fluorescence from the TNE oil core. Cargo retention was investigated in the P0, P1, P2, P5, P10, P20 and P200 TNEs. Measurements were performed in triplicate for 13 days in water. Size of the same TNEs was also measured in a Malvern Zetasizer Nano ZS (www.malvern.com) using a 1:100 final dilution in milli-Q water. Size measurements were collected within 24 hours and at the final point of cargo retention at 13 days.

3.2.5 Stability of TNEs in different storage conditions

P0, P20, P50, P100 and P200 TNEs, prepared using the method detailed in section (3.2.2), were stored for one week at 4 different temperatures including 25 °C (room temperature), 4 °C (fridge), -20 °C (freezer) and -80 °C (freezer). The stored TNEs were diluted 1:100 in milli-Q water before dynamic light scattering (Malvern Zetasizer Nano ZS) was used to investigate TNE size.

3.2.6 Coating efficiency of EMPs by TNEs

P20 and P200 DiI-encapsulated TNEs were prepared as described in section 1.2.1. The hydrodynamic radius of the TNEs was determined using dynamic light scattering (Malvern Zetasizer Nano ZS). 50 µl of each P20 and P200 DiI-loaded TNEs was added to 25 mg powdered EMPs. Four different methods were used to coat EMPs with TNEs including wet coating (W), freeze-dry coating (F), alginate cross-linking plus freeze-dry coating (AF), and alginate cross-linking (A). Wet coating was conducted by adding EMPs to the TNE formulation for 4-5 hours. Freeze-dry coating was performed by vigorously vortexing TNEs with EMPs in an Eppendorf tube with the resulting suspension incubated for 24 hours at 4 °C. Excess supernatant was removed before freeze-drying was performed under a vacuum at -80 °C for 4-5 hours. TNEs were also added to alginate coated-EMPs, that were generously supplied by Miko Yamada, either with (AF) or without freeze drying (A). Average size of the DiI-encapsulated P20 and P200 TNEs was collected before coating the EMPs and following each coating method. The coating efficiency of each method was estimated by comparing the percentage of coated TNEs with the percentage of uncoated TNEs (supernatant) following resuspension of the TNEs-EMPs mixture in milli-Q water.

3.2.7 Release profile of 6-carboxyfluorescein (CFC)-encapsulated TNEs

The release profile of CFC-loaded P20 TNEs (25 µg/ml dye concentration) was measured in Costar® 96-well black polystyrene plates using the Infinite® M200 Pro plate reader (www.thermofisher.com) following the release of CFC from the TNEs oil core through dialysis membranes. Fluorescence of the released CFC was measured using excitation and emissions wavelengths of 492 and 530 nm respectively. Samples of the dye molecules released into the hydrophilic medium were collected at the following time points; 0, 6, 18, 24, 48 and 72 hours.

3.2.8 Expression and purification of DAMP4-antibody fusions

A synthetic gene encoding a scFv, based on an immunoglobulin light chain signal peptide, was fused to DAMP4 via a Gly4Ser linker and codon optimised for expression in chinese hamster ovary (CHO) cells. The gene was transferred into the pcDNA 3.1 (+) mammalian expression plasmid (www.thermofisher.com) for transient expression before 2 µg DNA/mL was transfected into $3x10^6$ cells/ml. DNA was complexed with polyethylenimine-Pro (www.polyplus-transfection.com) in Opti-Pro serum-free medium (www.thermofisher.com) using a DNA (µg) to PEI (µl) ratio of 1:4 for 15 minutes prior to transfecting suspension-adapted CHO cells. The transfected cells were cultured in chemically defined CHO medium (CDCHO; www.thermofisher.com) at 37 °C, 7.5% CO_2, 70% humidity with shaking at 130 rpm for 6 hours, before feeding with 7.5% CD CHO Efficient Feed A

(www.thermofisher.com), 7.5% CD-CHO Efficient Feed B (www.thermofisher.com) and 0.4% anti-clumping agent (www.thermofisher.com). The viability of the cells was evaluated by trypan blue staining from day 7 with cell culturing stopped when viability ≤ 50%.

After transfection, the cells were pelleted by centrifugation and the supernatant was filtered through a 0.22 µm membrane (www.sartorius.com). The scFv-DAMP4 was purified from the supernatant utilising a 5 ml Protein-L column (www.gehealthcare.com.au) and eluted from the column using 100 mM glycine pH 3.0. Elution fractions were buffer exchanged into phosphate buffered saline (PBS) pH 7.4 using the HiPrep 26/10 column (www.gehealthcare.com.au). The final product was filtered through a 0.22 µm membrane before concentration was determined by measuring absorbance at 280 nm. The fusion was further analysed by sodium dodecyl sulphate polyacrylamide gel electrophoresis (SDS PAGE) and size exclusion high-performance liquid chromatography (SEC-HPLC) using a TSK gel G3000SW column (www.tosoh.com). The respiratory syncytial virus (RSV1)-DAMP4 fusion was synthesised using a gene encoding RSV antibody that was fused to DAMP4. The expression and purification protocol of the RSV-DAMP4 fusion is similar to that used for the scFv fusion.

3.2.9 Epidermal growth factor receptor (EGFR) binding plate assays

Enzyme-Linked immunosorbent assays (ELISA) were performed for DAMP4-RSV1 and scFv-DAMP4 fusion proteins. Maxisorp plate wells were coated overnight with 100 µl 1 µg/ml antigen (EGFR-hfc). EGFR-fc was expressed in CHO cells and purified using protein A. After coating, the solution was decanted and the EGFR-hfc-coated wells were blocked with 2% (w/v) non-fat dry milk solution in PBST (PBS, 0.05 v/v % tween 20) for 1 hour. Blocking solution was decanted and each DAMP4 fusion (DAMP4-RSV1 and scFv-DAMP4) was diluted in PBS and added to the wells at 20 µg/ml for 2 hours at room temperature. Incubated wells were washed three times with 200 µl PBST before Anti-His-Horseradish Peroxidase (http://www.miltenyibiotec.com), diluted 1/2000, was added and incubated for 1 hour. Three washes with 200 µl PBST were performed before 100 µl 3,3′,5,5′-tetramethylbenzidine liquid substrate (https://www.sigmaaldrich.com) was added and incubated for 5-15 minutes to facilitate colour development. 100 µl 2 M sulphuric acid was added to stop the reaction before absorbance was measured at 450 nm using a SpectraMax-M4 plate reader.

3.2.10 Solid state EGFR binding assay

Targeted and untargeted TNEs were prepared using sequential addition as per section 3.2.3. Firstly, 40 µM PEG-DAMP4 was integrated onto AM1-stabilised emulsions before 2 µM scFv-DAMP4 fusion was added to the P20-TNEs. Lastly, 400 µM PEG-DAMP4 was applied following the addition of the scFv-DAMP4 fusion. Untargeted TNEs were also formulated with the same technique,

however the second addition was RSV-DAMP4 rather than scFv-DAMP4. The human EGFR, diluted in PBS to a final concentration of 5 µg/mL (www.sinobiological.com), was immobilised onto 96-well black polystyrene plates (www.corning.com) at room temperature for 4 hours. The immobilised EGFR was blocked using 2% (w/v) non-fat dry milk powder in PBS for 1 hour. TNE formulations were diluted to 0.05% oil, and incubated for 30 minutes at room temperature. Two PBS washes, containing 0.05% Tween-20 were used to remove unbound TNEs. A final PBS wash was used before adding PBS to the wells and measuring fluorescence in the infinite® M200 Pro plate reader (www.thermofisher.com) using emission and excitation wavelengths of 535 and 570 nm, respectively.

3.2.11 Flow cytometry

Targeted and un-targeted TNEs, prepared as per section 3.2.3, were diluted to a final oil concentration of 0.03125%. Prepared TNEs were incubated for 1 hour at 4 °C with the MDA-MB-468 (breast cancer cell line, generously supplied by Dr Christopher Howard) cell suspensions (1.5 x 10^6 cells/ml) in PBS containing 10% foetal calf serum (FCS) at 1:1 ratio for binding. Three wash steps were conducted to remove weakly bound TNEs. Flow cytometry measurements were set to 20000 events using BD Accuri C6 Flow Cytometer System (BD Biosciences). Cell gating and a full analysis were performed using Flowing software v2.5.1. Overnight dialysed and un-dialysed, targeted and un-targeted TNEs were compared for binding to MDA-MB-468 cell suspensions (1.5 x 10^6 cells/ml) in PBS containing 10% FCS at a 1:1 ratio.

3.2.12 *In vivo* targeting and biodistribution studies

The targeting and biodistribution studies were performed in compliance with the Australian National Health and Medical Research Council guidelines for the care and use of laboratory animals, and with the approval of the EnGeneIC Animal Ethics Committee under ethics application number: AIBN/400/13/ARC/NHMRC.

For the targeting study, 7 female Balb/C athymic nude mice 6 weeks of age were obtained from the Laboratory of Animal Services at the University of Adelaide, South Australia. 100 µl (4 x 10^7 cells/ml) of MDA-MB-468 cells in serum-free RPMI were injected in the mammary pad of 6 female Balb/C athymic nude mice. The mice were divided into three groups as follows: 3 mice were treated with targeted TNEs (200 µl, 0.25% oil); 3 mice were treated with un-targeted TNEs (200 µl, 0.25% oil); and one control mouse was not injected. The TNEs were injected when the tumour mass reached 4 mm^2. Molecular imaging of the mice was taken at 5 and 24 hours post-injection of TNEs using Carestream (www.carestream.com) and In-Vivo Xtreme (www.bruker.com).

For the biodistribution study, 12 female Balb/C athymic nude mice 6 weeks of age were obtained from the Laboratory of Animal Services at the University of Adelaide, South Australia. The mice were divided into two groups as follows: 10 mice were treated with un-targeted TNEs (200 µl, 1% oil); and two control mice were not injected. Molecular imaging of the mice was performed using Carestream (www.carestream.com) and In-Vivo Xtreme (www.bruker.com).

3.2.12.1 *Ex vivo* biodistribution and cytokine analysis of TNEs

Ex vivo analysis of TNEs was performed using two mice at each time point (30, 60, 90 and 120 minutes and 24 hours). The analysis included body organs (liver, kidney, heart, gut and lung), blood and urine. Blood samples were collected through cardiac puncture with serum isolated via centrifugation. Blood and urine samples were evaluated for the presence of DiI-loaded untargeted TNEs using the infinite® M200 Pro plate reader (www.thermofisher.com) (www.lifesciences.tecan.com) at emission and excitation wavelengths of 535 and 570 nm, respectively.

Cytokines were analysed by Sullivan Nicolaides Pathology using the Milliplex assay (www.merckmillipore.com) with kit number; MPMCYTOMAG-70K-06 (Mouse Cytokine/Chemokine Panel, 6-plex (IL2, IL-4, IL-6, IL-10, IFN-gamma and TNF-alpha). Cytokines were measured in blood samples collected from two mice at each time point (30, 60, 90 and 120 minutes and 24 hours). The control samples were collected after 4 and 24 hours using subcutaneous injections of OVA albumin-TNEs (Zeng et al., 2013).

3.2.13 DiI retention in simulated plasma fluid

DiI-labelled TNEs (P0, P5, P10, P20 and P200), prepared as per section 3.2.3, were evaluated for dye retention over time in a simulated body fluid (Marques et al., 2011). The ionic concentration of the simulated body fluid composition was as follows: 4.2 mM HCO_3^-, 5 mM K^+, 148.8 mM Cl^-, 142 mM Na^+, 2.5 mM Ca^{+2}, 1.5 mM Mg^{+2}, 1 mM HPO_4^{-2}, 0.5 mM SO_4^{-2}, 50 mM tris(hydroxymethyl) aminomethane and 45 mM hydrochloric acid.

3.3 Results

TNEs are O/W emulsions stabilised by the peptide surfactant AM1 (Malcolm et al., 2006) and incorporating the protein DAMP4 that is used to tune the interface and allow the addition of various functionalities to the system. PEGylation is one of the most common techniques used to provide proteins and NPs with stability (Roberts et al., 2002, Ikeda and Nagasaki, 2012). Chemical conjugation between DAMP4 and an NHS ester-labelled 5 kDa PEG, allowed PEG presentation onto the TNE interface to impart colloidal stability and allow investigations into surface properties.

3.3.1 Surface properties and cargo retention of the tailorable nanocarrier emulsions

Controlling the surface charge of nanomaterials is an important element of drug delivery. In this study, the surface charge of TNEs was controlled by the integration of different PEG densities onto the TNE interface. DiI-labelled AM1, P20 and P200 TNEs were utilised to determine the effect of different PEG densities on surface charge. AM1 (P0), P20 and P200 TNEs were formulated with average sizes of 173.9 ± 2.4, 175.1 ± 1.7 and 179.2 ± 4.2 nm respectively. Increasing DAMP4-PEG density on AM1-TNEs reduced their surface charge from 52.5 ± 1.1 to 47.3 ± 1.5 mV for P20, and from 52.5 ± 1.1 to 38.6 ± 1.2 mV for P200 TNEs (Figure 3.1). These results reveal an inversely proportional relationship between PEG surface density and the charge of TNEs. Varying PEG densities on the TNE interface also allowed an investigation into the *in vitro* release of a model-drug, DiI – a lipophilic carbocyanine dye.

To investigate the capacity of TNEs to retain cargo over time (13 days), DiI was encapsulated within the oil core (Miglyol812) of AM1, P20 and P200 TNEs. DiI has been widely applied to label cell membranes (Schlessinger et al., 1977, Struck and Pagano, 1980) and is only weakly fluorescent in aqueous solutions. Dilution curves of DiI in miglyol and water showed that DiI in water was more than 250 times less fluorescent than DiI in oil (Figure 3.2A). Therefore, cargo retention was evaluated by dispersing the TNEs in an aqueous buffer solution to enable any decline in the fluorescence to be observed and indicate leakage of DiI from the TNEs over time (Figure 3.2B). The results showed that P20 and P200 TNEs retained about 99% of their cargo for five days. However, naked AM1 emulsions showed a 10% release of DiI into the medium after only one hour, and an almost 80% loss of cargo from the oil core into the aqueous medium after 48 hours. Thus, even the low ratio of DAMP4-PEG on the TNE interface (P20 TNEs) enabled cargo retention for at least 120 hours, showing a remarkable difference from the unmodified TNEs (Figure 3.2B).

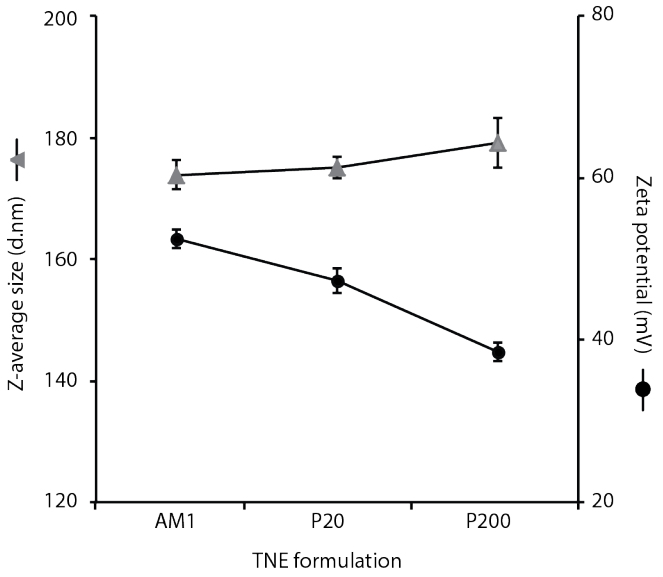

Figure 3.1. Size and charge characterisation of TNEs prepared with different PEG densities. It demonstrates the Z-average size and ζ-potential of AM1, P20 and P200 TNEs. The results are shown as average of triplicates (± standard deviation).

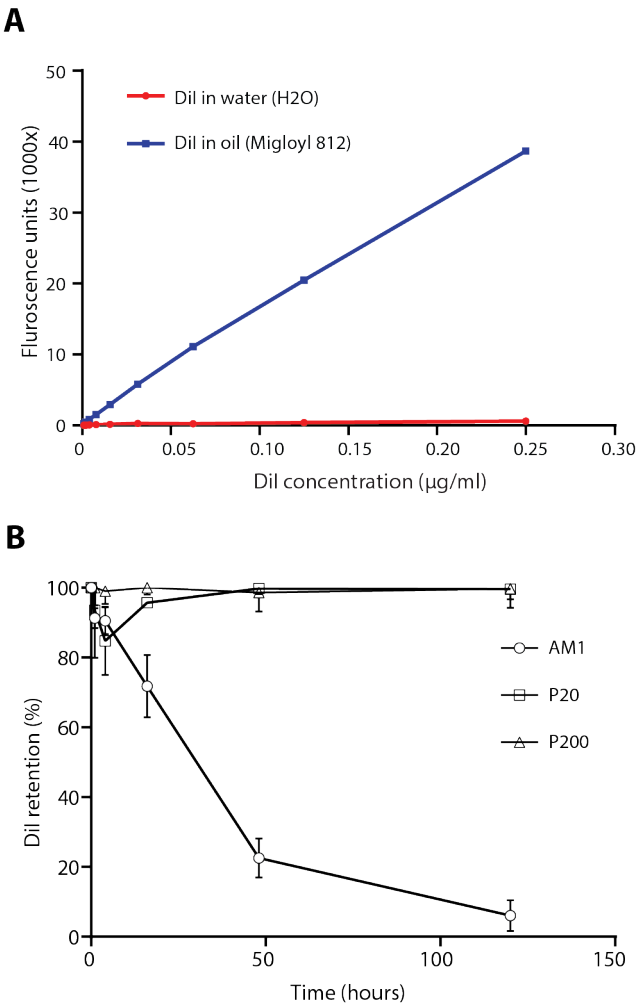

Figure 3.2. Effect of PEG density on the DiI retention profile of TNEs. (A) Shows the difference in DiI fluorescence between the hydrophilic and hydrophobic media (for measuring the percentage of dye retained within the oil core). (B) Shows the percentage of DiI retained within the oil core of the AM1, P20 and P200 TNEs, the results are shown as an average of triplicates (+ standard deviation).

These results suggested that by investigating the effect of changing the PEG densities on TNEs, the minimum amount of DAMP4-PEG required to maintain the physical stability of TNEs and cargo retention could be determined. Therefore, the cargo retention of lower DAMP4-PEG densities (P0, P1, P2, P5, P10, P20 and P200 TNEs) were analysed over 13 days. Results revealed that the amount of cargo retained over time increased with an increase in PEG densities on the TNE interface. For example, the P2 TNEs showed greatly improved cargo retention when compared to the P0 TNEs. Moreover, the P10, P20 and P200 TNEs retained over 90% of the encapsulated cargo for 13 days (Figure 3.3A).

The hydrodynamic size measurements at the first and last day of DiI-labelled TNEs have also reflected the effect of PEG density on stability and dye retention with the higher PEG densities producing more stable TNE droplets with better *in vitro* release profiles. For example, P0 and P1 emulsions showed an increase in size from approximately 170 nm to over 1000 nm. The observed size increase (instability) may account for the relatively high dye release from these TNEs over the first few hours. In contrast, P20 and P200 TNEs have retained their hydrodynamic stability over time (Figure 3.3B). Varying PEG density also affected the stability of TNEs under different storage conditions. TNEs with different PEG densities were stable at room temperature and 4 °C. In contrast, only P200 TNEs were stable at all freezing conditions, while P100 TNE were stable only at -80 °C. (Figure 3.4). TNEs with lower PEG densities (P0, P5 and P50) were unstable at -20 °C and -80 °C. This is probably due to the fact that storage conditions below 0 °C result in the formation of fat crystals within the oil phase, which reduce the stability of O/W emulsions (van Boekel and Walstra, 1981). These fat crystals protrude into the aqueous phase penetrating the film between adjacent oil droplets and causing partial coalescence (Harada and Yokomizo, 2000, Vanapalli et al., 2002, McClements, 2004). The slow freezing (-20 °) condition produces large fat crystals when compared to fast-cooling (-80 °) that results in smaller crystals formation. Consequently, the slow cooling process led to lower stability of TNEs at even high PEG densities (P100 TNEs). Therefore, tuning the integration of DAMP4-PEG density onto the TNE interface is an important factor in TNEs stability and their use in drug delivery, ultimately determining their structural and functional properties.

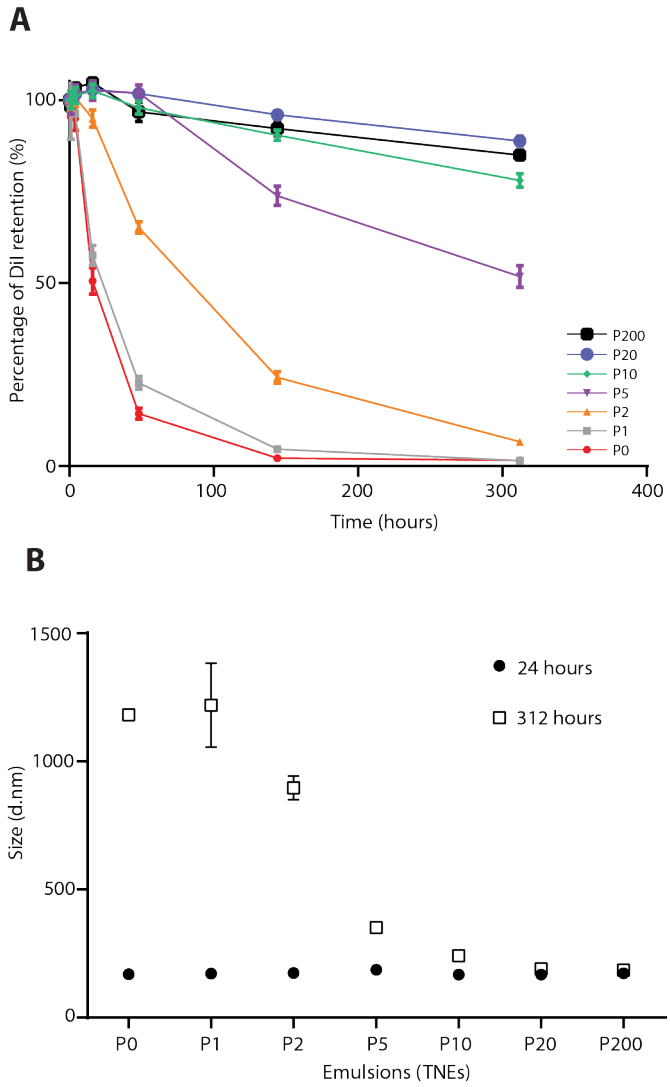

Figure 3.3. Size characterisation and DiI retention within the oil core of TNEs prepared with different PEG densities over time. (A) Retention of DiI over time by different TNEs formulations including: P0 (red), P1 (grey), P2 (orange), P5 (purple), P10 (green), P20 (blue) and P200 (black) shown as average of triplicates (± standard deviation). (B) Results reveal the size of TNEs based on their interfacial PEG density when loaded with a lipophilic tracer, DiI. Size was measured using dynamic light scattering and performed in aqueous solutions. The results are shown as an average of triplicates (± standard deviation).

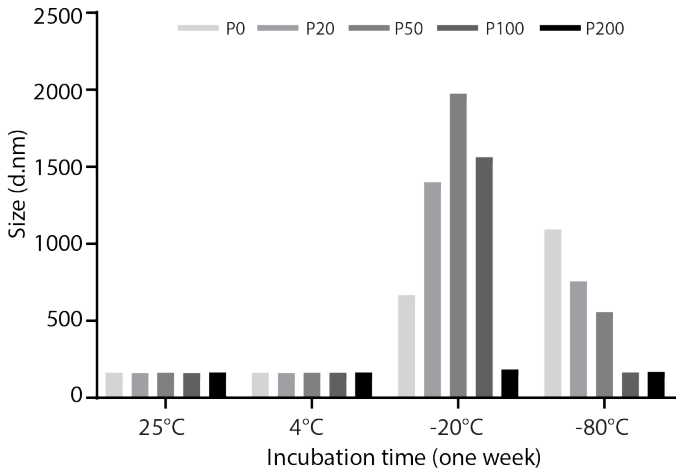

Figure 3.4. Size of TNEs in different storage conditions. The results show the effect of storage conditions, including room temperature (25ºC), 4ºC, -20ºC and -80 ºC, on TNE size (measured using dynamic light scattering).

3.3.2 Exploring the surface properties of TNEs toward topical (skin) applications

NEs are heterogeneous systems composed of dispersed and continuous phases that can be stabilised using emulsifiers or surface-active molecules (Mason et al., 2006). NEs are biodegradable, easily produced and show good safety profiles in food (Silva et al., 2012), pharmaceuticals (Singh et al., 2017) and cosmetics (Sonneville-Aubrun et al., 2004). They have been administered through different routes including parenteral (Araújo et al., 2011), ocular (Hagigit et al., 2012), nasal (Hosny and Banjar, 2013), oral (Beauchesne et al., 2007) and topical (skin) (Kelmann et al., 2016). These delivery routes were discussed in greater detail in chapters 1 and 2. The use of NEs to deliver hydrophobic compounds via the skin shows great potential. Topical administration is non-invasive and does not require highly trained medical professionals (Barry, 2004). However, topical delivery can be also challenging considering the different biological and physical barriers of the dermal layers (Paudel et al., 2010).

Controlling the surface charge of TNEs can be useful in several applications. In collaboration with Professor Tarl Prow's group in the University of Queensland's School of Medicine, we investigated the possibility of exploiting the tailorable surface charge of TNEs for topical drug delivery in humans. DiI-loaded TNEs were used to coat the negatively charged EMPs that were recently developed to enhance topical delivery (Raphael et al., 2013) and show remarkable penetration into the epidermis and dermis layers of pig skin. DiI was used as a model drug to demonstrate that TNEs could be used as a carrier for hydrophobic molecules on EMPs. The efficiency of the coating was investigated using TNEs with different surface charges achieved by varying the PEG-DAMP4 densities.

A variety of methods were used to coat the EMPs with TNEs including freeze-dry coating, wet coating, alginate cross-linking and alginate cross-linking with freeze-dry coating. Particle size analysis was performed to detect any change to the unbound TNEs after each coating method. The results showed almost no TNE size change associated with the wet and freeze dried coatings, whilst coating methods that involved alginate, a cross-linker, showed larger hydrodynamic radii (Figure 3.5A). This could explain why the total fluorescence of resuspended TNE-coated EMPs decreased after alginate cross-linking, suggesting some TNEs might be disrupted (Figure 3.5C). However, the alginate-coating methods using P20 TNEs had much higher percentages of coated EMPs compared to wet and freeze dried coatings. Interestingly, the PEG density of TNEs had a considerable impact on EMP coating efficiency with P20 TNEs producing less supernatant fluorescence and indicating more efficient coating (Figure 3.5C). The ability of EMPs to adhere better to P20 TNEs rather than P200 TNEs, is possibly due to a higher surface charge associated with P20 TNEs leading to stronger electrostatic interactions (Figure 3.5B).

The successful application of P20-TNEs as a drug carrier onto EMP surfaces suggests that this combined drug delivery system is promising for human use. To facilitate clinical translation, the release profile of a clinically relevant lipophilic fluorescent dye, CFC, was investigated after being encapsulated within the of TNEs oil core. The encapsulation efficiency of CFC was estimated at 75% with 48% of the dye released from the oil core of P20-TNEs after incubation in an aqueous solution for 24 hours (Figure 3.6). CFC-labelled P20 TNEs coated onto EMPs were applied to frozen human skin as well as human subjects in collaboration with Dr Miko Yamada and Professor Tarl Prow at the School of Medicine in TRI. The excised human skin from abdominoplasty was obtained from the Greenslopes hospital, Brisbane Australia, and approved by the University of Queensland Human Research Ethics Committee (Ethics approval number HREC_12_QPAH217). The excised human skin was also sourced from Massachusetts General Hospital, Boston, USA, with protocol number 2014P001345, and approval was provided by Harvard University Human Research Ethics committee. The patients involved in the study were healthy with no skin health problems, and this study was conducted in compliance with the National Health and Medical Research Council of Australia. The results show that the TNE formulation was well tolerated by the skin delivery route, and that TNEs have improved the delivery to the epidermis skin layer when compared to hydrophobic compounds alone (Miko Yamada, pers comm, 21 April 2018). These results suggest that TNEs have a promising future in pharmaceutical applications via the skin route.

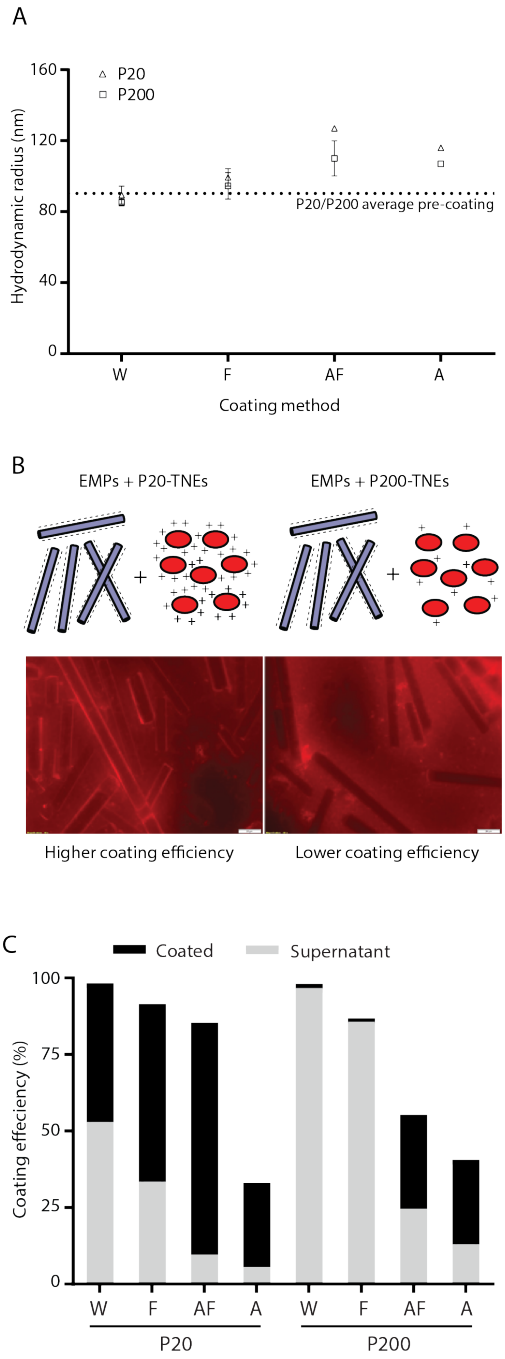

Figure 3.5. Coating efficiency of EMPs by TNEs. (A) Shows the hydrodynamic radius (nm) of unbound TNEs released from EMPs following coating (± standard deviation). (B) Illustration of the electrostatic interactions between TNEs and EMPs. (C) DiI fluorescence was measured from resuspended TNE-coated EMPs and from the supernatant following gravitational separation of EMPs. The coating methods used were wet coating (W), freeze-dried coating (F), alginate cross-linking plus freeze-dried coating (AF), and alginate cross-linking (A). Low supernatant values relative to total values indicate efficient coating.

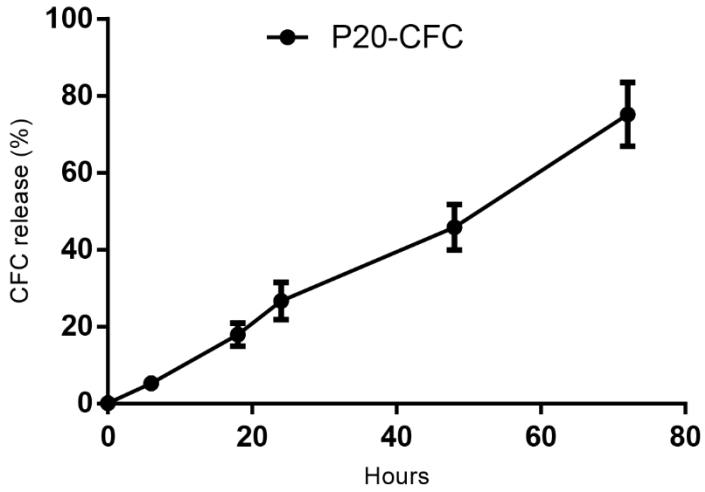

Figure 3.6. CFC release from the oil core of P20-TNEs. The increase in fluorescence of released CFC is presented as an average of triplicates (± standard deviation) in percentages (%) over 72 hours.

3.3.3 Tailorable nanocarrier emulsions toward intravenous applications

The delivery of hydrophobic drugs via the IV route is a major challenge for nanocarriers. Nanocarrier design should incorporate strategies that minimise phagocytosis and off-targeting (Gustafson et al., 2015). However, it is unknown to what degree these obstacles can be overcome, considering the wide spectrum of complexity encountered by nanocarrier design to meet the needs of each biological barrier in different delivery routes (Peer et al., 2007). Only a few *in vivo* studies involving targeted nanocarriers have shown improvements in the efficacy of their encapsulated drugs (Zhang et al., 2010, Xu et al., 2010) and provide evidence that targeted nanocarriers may become important treatment regimens for various diseases (Peer, 2014).

To investigate TNEs as a diagnostic tool and drug delivery vehicle via the IV route, experiments were designed to explore how TNEs can actively target cancer cells. To achieve active targeting a scFv antibody, specific to EGFR, was fused to the N-terminus of DAMP4 (DAMP4-VECT) via a short linker (Figure 3.7A). An isotype antibody against RSV was similarly linked to DAMP4 as a negative control (DAMP4-RSV). These experiments were performed to compare the targeting specificity of these DAMP4-antibody fusions to EGFR (that were measured using ELISA). The ELISA results were as expected for the EGFR-specific DAMP4 fusion and showed high binding specificity to EGFR, whereas the RSV-DAMP4 fusion only showed low non-specific binding to the receptor (Figure 3.7B).

DiI-labelled TNEs were functionalised with 1 μM DAMP4-VECT, and RSV-DAMP4 fusions resulting in VECT-1 and RSV-1 TNE formulations with droplet sizes 172.4 ± 0.4 and 186.4 ± 2.8 nm respectively (Figure 3.9A). Both formulations were compared to control TNEs (P200 TNEs) to investigate their binding specificity to EGFR-coated plate wells. The results demonstrate that the anti-EGFR labelled TNEs (VECT-1) have much higher binding specificity for the EGFR receptor compared to the negative controls, suggesting that DAMP4-VECT is accessible and presented on the TNE interface (Figure 3.7.C).

In the next step, flow cytometry was utilised to examine the functionality of VECT-1 compared to P200 TNEs and TNEs displaying the isotype antibody (RSV) with respect to receptor-specific targeting of EGFR-expressing cancer cells (MDA-MB-468). At the optimal dilution, fluorescence showed that while the negative TNE controls showed some DiI signal, there was a clear positive shift for VECT-1 TNEs. These results demonstrated that the targeted TNEs specifically bound to the EGFR-expressing cells and therefore had a higher median fluorescence than the controls (Figure 3.8A).

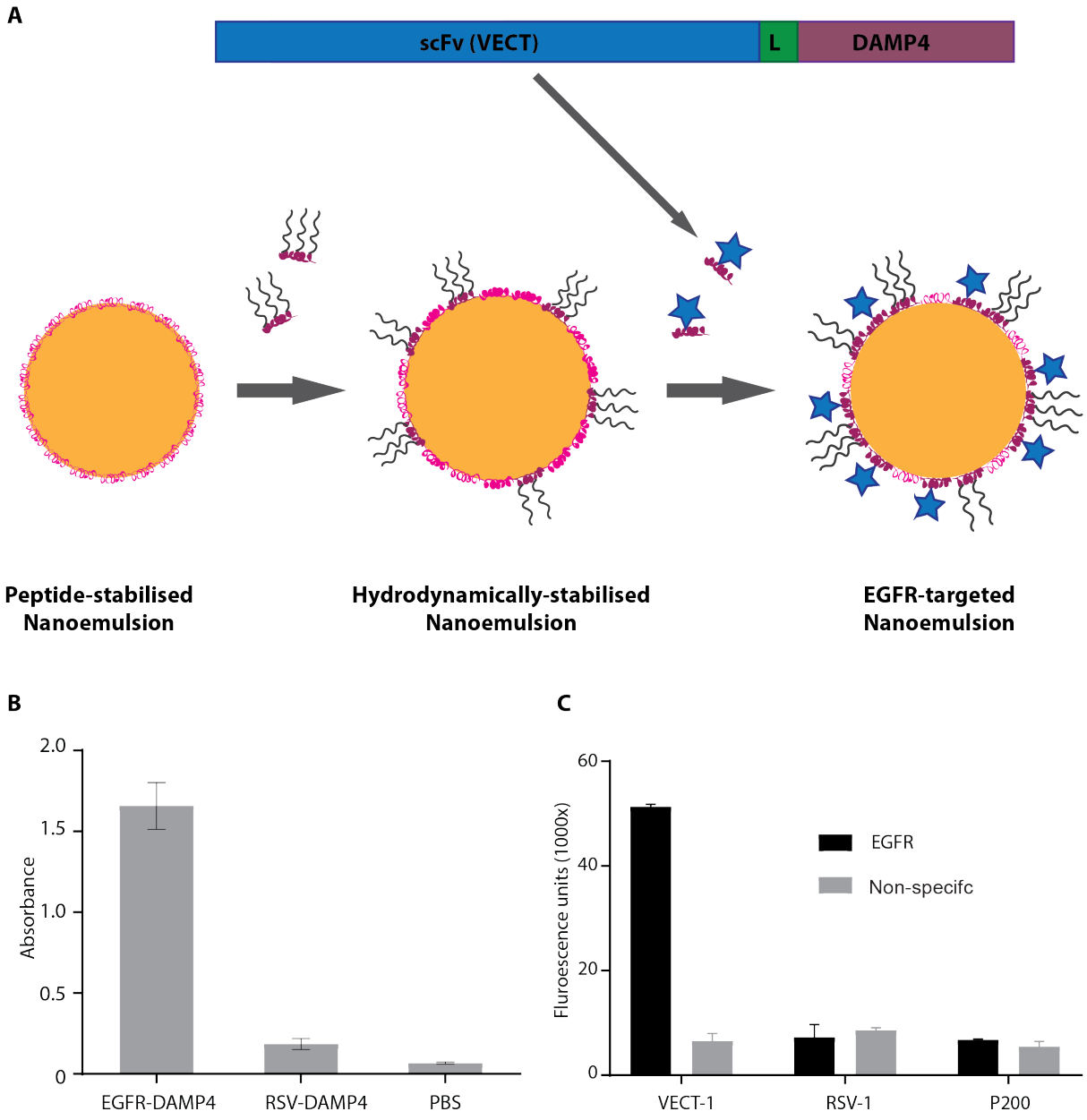

Figure 3.7. Functionalisation of peptide-stabilised TNEs with DAMP4 ScFv fusions. (A) Shows functionalisation of the peptide-stabilised TNEs with an anti-EGFR (DAMP4-ScFv fusion, VECT-1) targeting ligand to actively target MDA-MB-468 breast cancer cell lines. (B) ELISA results of EGFR-DAMP4, RSV-DAMP4 (an isotype antibody labelled TNEs) and PBS (control) shown as average of triplicates (± standard deviation) (against EGFR-immobilised plate). (C) Binding assay of P200, EGFR-DAMP4 and RSV-DAMP4 TNEs (0.05% oil concentration) to EGFR-coated plate shown as average of triplicates (± standard deviation).

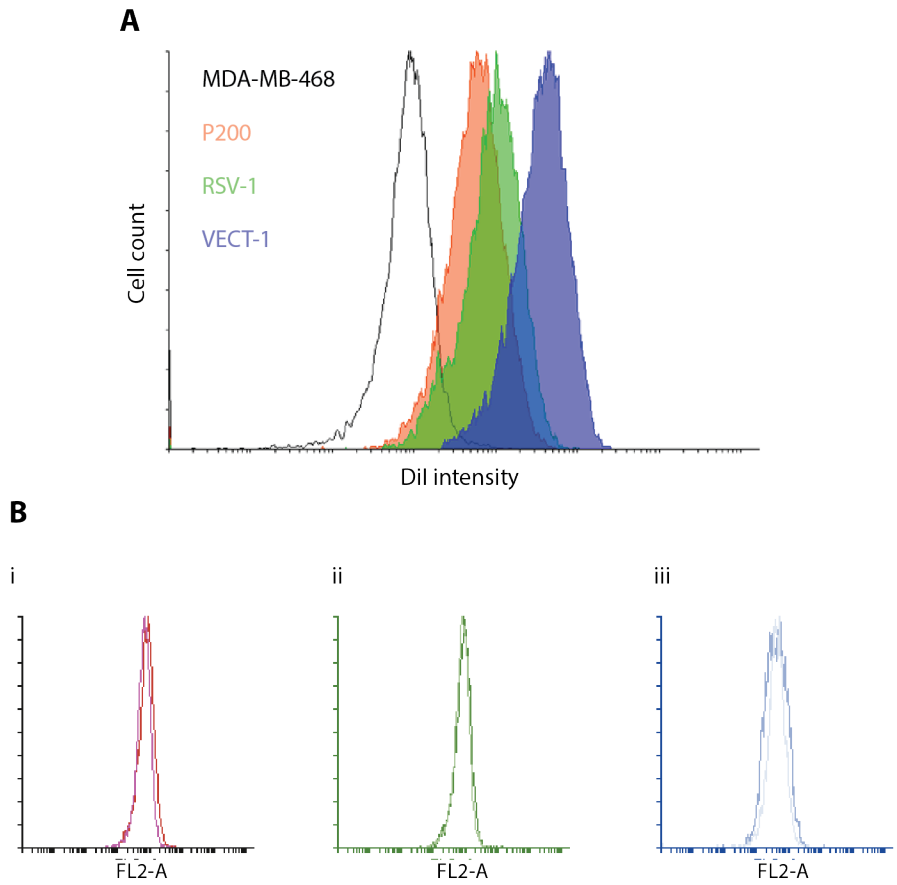

Figure 3.8. Binding of TNEs to MDA-MB-468 cells using flow cytometry. (A) An overlay histogram of DiI-loaded VECT-1, RSV-1 and P200 (untargeted) TNEs that were applied to MDA-MB-468 cells and analysed using a flow cytometry software. (B) Comparisons of dialysed (light colour) and undialysed (dark colour) TNE samples. DiI-loaded P200 (pink and light pink) (i), RSV-1 (green and light green) (ii) and VECT-1 (blue and light blue) (iii) TNEs were applied to MDA-MB-468 cells.

Dialysed and undialysed TNEs were compared to confirm that TNEs were stable during incubation with the cells, helping to validate the comparison between targeted and untargeted TNEs by ruling out the presence of free dye in their preparations. Both dialysed and undialysed TNEs showed similar results, suggesting no leakage occurred (Figure 3.8B).

A pilot in vivo study was conducted to evaluate the feasibility of using TNEs in the active targeting of breast cancer cells via the IV route. Tail vein injection with VECT-1 TNEs (targeted) and P200 TNEs (control), at 0.25% oil produced fluorescence in the tail and urinary tract areas, particularly in the bladder, five hours post-injection. The injected TNE volume was approximately 10% of mouse blood volume, resulting in 0.025% final blood oil concentration. As shown in Figure 3.9B, active targeting was not successful using injected TNEs as they were excreted in urine within 2 - 4 hours post-injection as evidenced by fluorescence in the legs and feet. However, the potential rapid clearance and biocompatibility of TNE formulations could possibly contribute to a satisfactory safety profile.

TNEs with different PEG densities were then tested for stability as a carrier of hydrophobic drugs within simulated plasma fluids. The results shown in Figure 3.10A illustrate how the P200 TNEs (control) retained their cargo for at least 48 hours. Size measurements were also used to evaluate the stability of TNE droplets before and after incubation in the simulated body fluids. The control P200 TNEs remained stable during the incubation period with no change to the hydrodynamic radius of the emulsions, however all other TNEs increased in size following the incubation (Figure 3.10B). These findings prompted investigations into the biodistribution of P200 TNEs over 24 hours, although due to the fast clearance profile of TNEs demonstrated in the pilot study, the biodistribution study also included short time intervals post-injection.

To explore the biodistribution profile of TNEs across short time intervals, 12 mice were injected with DiI-loaded P200 TNEs (control) before organ, blood and urine samples were taken every 30 minutes for the first two hours. Final measurements were then taken 24 hours post-injection. The results showed very low fluorescence in the liver from DiI-labelled TNEs after only 2 hours post-injection, suggesting that the hepatic path was not the main excretion route (Figure 3.11). Fluorescence was also detected in the gut that was possibly caused by food-related substances. Serum fluorescence revealed that TNEs remained in circulation for at least 120 minutes (Figure 3.12A). Urine fluorescence showed that renal excretion of TNEs was detectable from 60 to 120 minutes post-injection (Figure 3.12B). The fluorescence of DiI in the urine strongly suggested that the TNEs were intact as the DiI remained in the oil (based on the weak fluorescence in hydrophilic media).

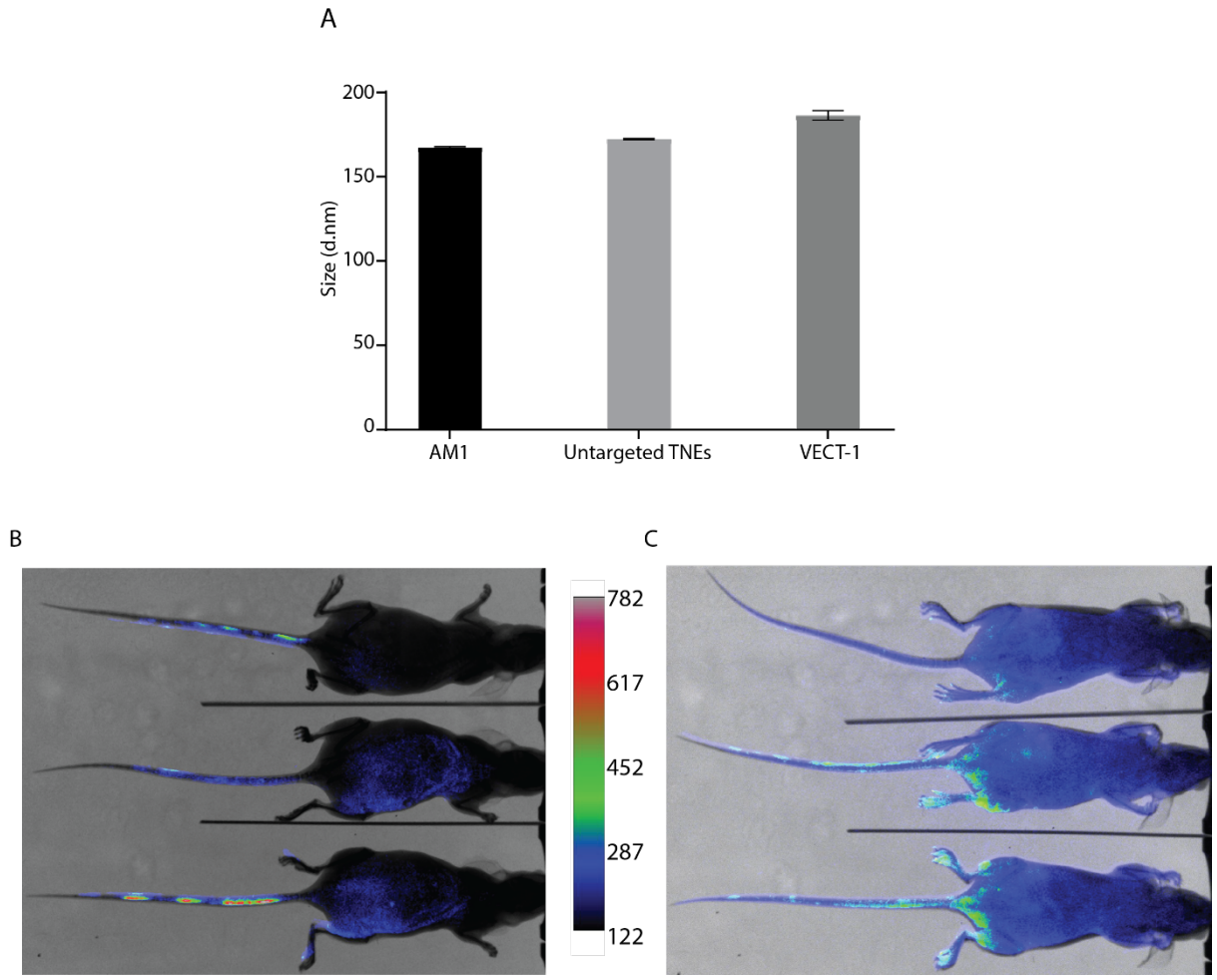

Figure 3.9. *In vivo* evaluation of TNEs targeting cancer cells. (A) Size measurement of AM1, untargeted (control) and targeted TNEs (VEC1-1) shown as average (± standard deviation). (B) Mouse back images 4 hours post-injection of targeted TNEs. (C) Mouse back images 4 hours post-injection of untargeted TNEs.

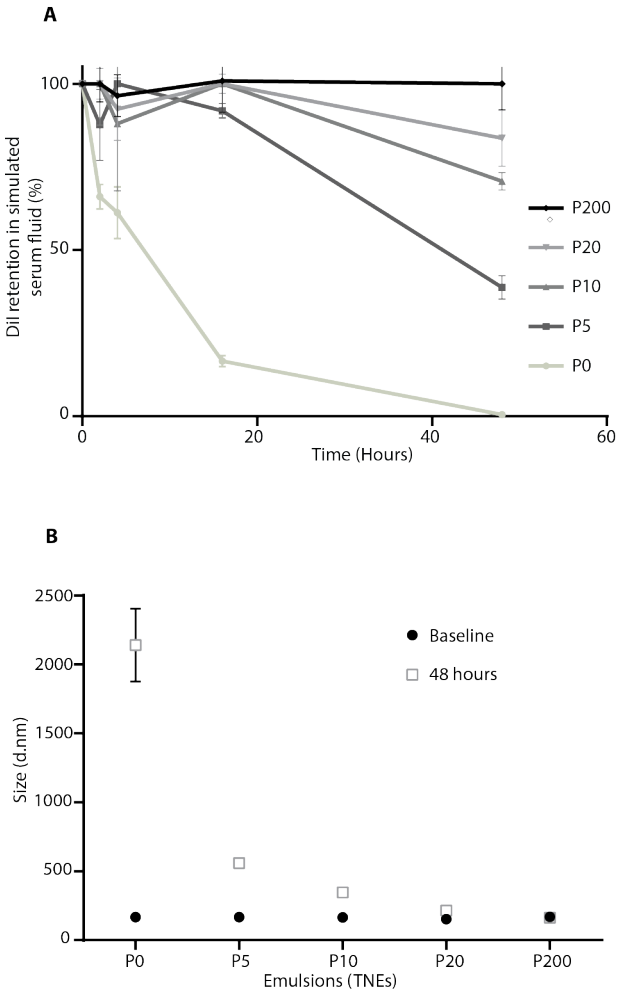

Figure 3.10. Evaluation of DiI retention in TNEs in simulated serum fluid. (A) Evaluation of DiI retention in TNEs with different PEG densities (P0, P5, P10, P20 and P200) in the simulated serum fluid over time. (B) Shows the size of TNEs loaded with DiI, based on their surface PEG density, measured before and after 48 hours incubation in the simulated body fluid (using dynamic light scattering). Results are expressed as an average of triplicate measurements (± standard deviation).

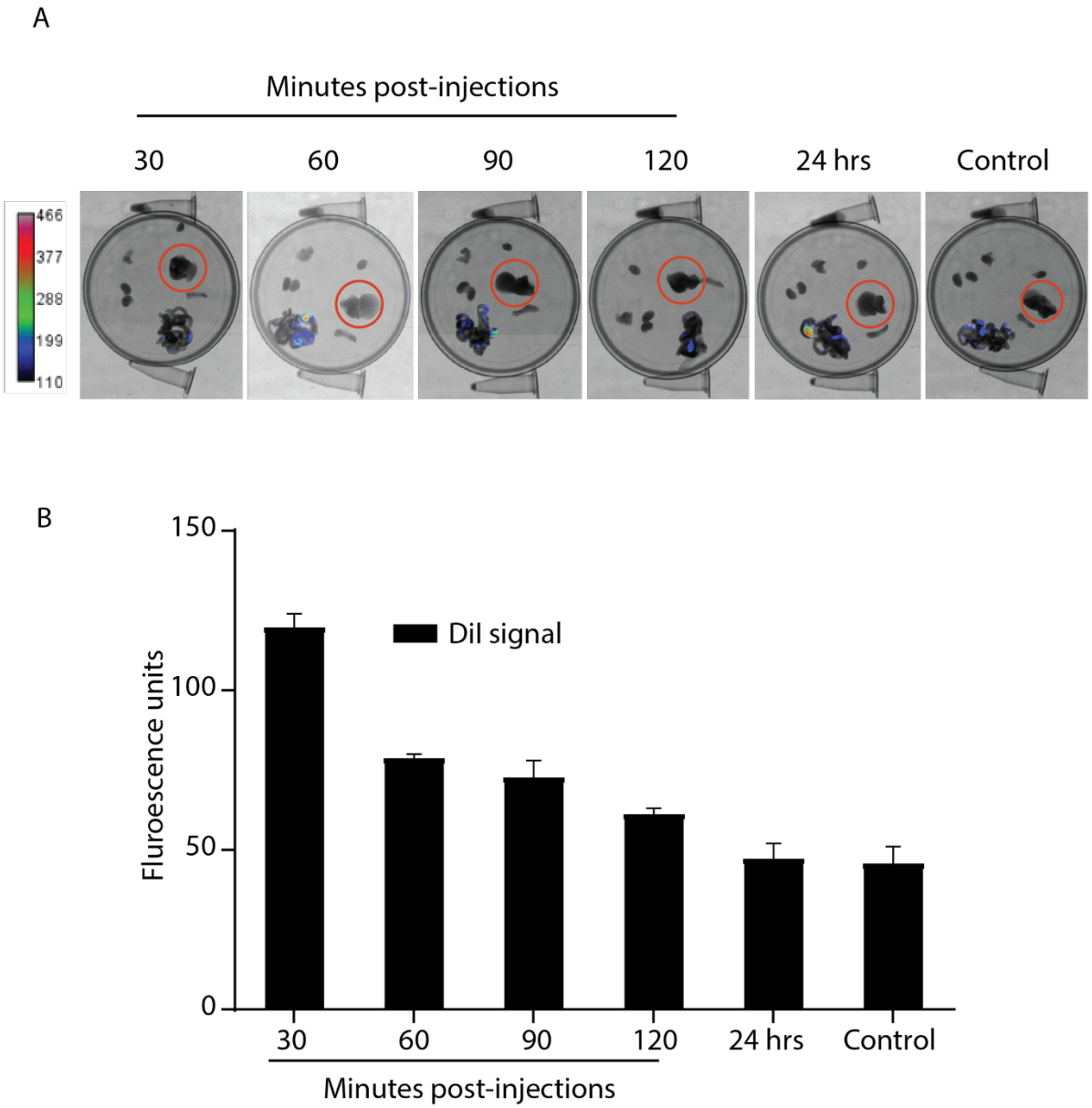

Figure 3.11. Ex-vivo analysis of TNE biodistribution. (A) Shows organs collected organs from the ex-vivo analysis with the liver highlighted by red circles. (B) The data (fluorescence of DiI-labelled TNEs) obtained from the liver in each petri-dish over different time points. The control mice were not injected with TNEs (n= 2). The number of mice for each time point was 2. The results are shown as average of duplicates (± standard deviation).

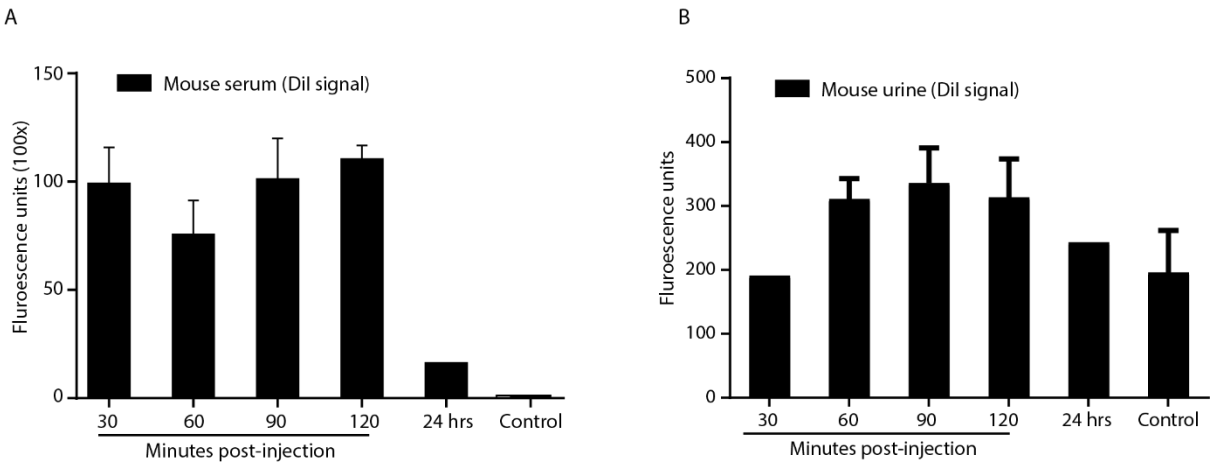

Figure 3.12. Biodistribution of TNEs in mouse sera and urine. (A) DiI signal in collected mice sera over time. The control sample is a non-injected mouse. (B) DiI signal in collected urine from two mice at each time point. The results are shown as average of duplicates (± standard deviation).

The immunotoxicity potential of nanomaterials following IV injection is an important aspect and requires attention because of the adverse reactions that could occur. Here, the immunotoxicity profile of TNEs was evaluated by measuring the serum levels of six cytokines (IFN-γ, IL-2, IL-4, IL-6, IL-10, TNF-α) at each time point post-injection. IFN-γ and IL-4 could not be detected at any time point following TNE injection, or in the control. IL-2 was not detected above control levels and was close to the assay limit of detection at any time point. Proinflammatory TNF-α and IL-6, as well as the anti-inflammatory cytokine IL-10, showed a spike in concentration at 60 minutes followed by an immediate decrease and return to control levels. The decrease was more intense for IL-6 compared to TNF-α and IL-10. The decline in cytokine production suggests these cytokines were produced as a non-specific stress response rather than an immune response (Figure 3.13).

The mice used in this study were athymic, therefore macrophages and endothelial cells were the main sources of cytokine production in the initial responses. The very low fluorescence from DiI-labelled TNEs in the liver post-injection, that was not observed in the control mice, suggests this organ, which is a major site of IL-6 production, was not involved in the immune response. If TNEs stimulated inflammatory cytokines beyond the immediate stress caused by the injection, then the prolonged circulation and persistent, low level accumulation in the liver, would cause at least IL-6 to continually increase. Therefore, the low cytokine levels and sudden decline could suggest there were no adverse reactions. Possibly the response was inflammatory provoked by the formulation components. Although TNEs show short circulation times and no active targeting following IV administration, the safety profile substantiates their use in other drug delivery applications through IV injection and possibly different routes of administration.

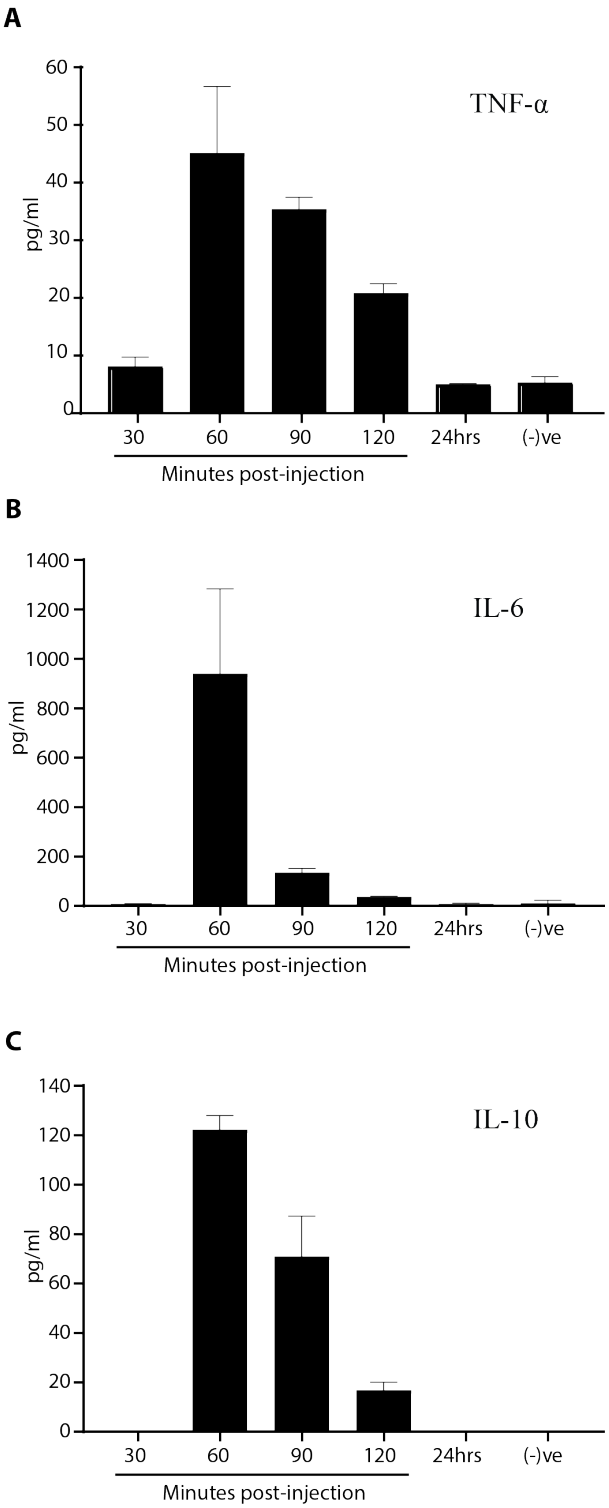

Figure 3.13. Release of cytokines over time from mice post-TNE injection. The results are shown as an average of duplicates (± standard deviation).

3.4 Discussion

Nanomaterials are being developed in different sizes, shapes, and surface designs to improve the therapeutic and diagnostic outcomes of hydrophobic compounds. However, there are currently no guidelines that specify the use of an appropriate NPs design for a specific application or route of administration. Therefore, the present comparative screening methods are just considered speculative and investigating the use of a specific NP design is still needed to obtain a promising drug delivery application. NEs possess various advantages including biocompatibility, payload protection and high loading capacity, making them promising drug carriers in food production, skin care and pharmaceutical applications. TNEs are promising peptide-stabilised NEs developed by Professor Anton Middelberg's group and have been administered subcutaneously for targeting dendritic cells to obtain specific immune responses (Zeng et al., 2013). In this chapter, TNEs were investigated as a topical and IV drug delivery system.

Controlling the surface properties is an important factor for applying TNEs as a drug delivery system. To study the capacity of TNEs to encapsulate hydrophobic compounds and to tune the TNE surface charge, PEG density on the TNE interface was varied. This led to promising results for combining TNEs with EMPs via electrostatic interactions toward topical drug delivery, where PEG density was found to be indirectly related to surface charge. These interesting results suggest that TNEs can be promising drug carriers for topical administration.

Cargo retention within the oil core of the TNEs was also found to be related to TNE surface properties, specifically PEG density. Varying the PEG density on the TNE surface directly affected the stability of DiI-labelled TNEs and subsequently, DiI retention.

The solubility of compounds within the oil core of TNEs is an important factor that determines retention/release of cargo. The high log P (partition coefficient) value of DiI (+20), that represents lipophilicity of compounds, explains the high retention by stable TNEs. Conversely, CFC was released from the oil core of the TNEs at a linear rate where a lower log P value may have contributed to faster dye partitioning from the oil to the water phase.

Another possible explanation for the different leakage profiles of DiI and CFC may have been the different testing methods used to assess the amount of cargo retained with the oil core of TNEs over time. That is, the amount of DiI retained within the oil core was measured by exploiting the fluorescent signal of DiI in oil, compared to a negligible signal in aqueous solutions. In contrast, the amount of released CFC was measured using dialysis. It is possible that the linear release profile of CFC was indicative of diffusion across a consistent surface area into a non-saturating solution, whereas the exponential release of DiI in the presence of lower PEG densities may have been due to

coalescence. Reorganisation of surfactants (desorption/adsorption) during coalescence of oil droplets might have also contributed to leakage of DiI-labelled TNEs with lower stability (lower PEG densities).

FRET (Förster resonance energy transfer) is a common tool in biochemistry, biophysics and molecular biology (Jares-Erijman and Jovin, 2003), and it is applied to measure intra-molecular distances or to study co-localisation at a nanometer scale. FRET can occur between two different or identical donor and acceptor fluorophores (Homo-FRET) (Bader et al., 2011). It has been shown previously that the release of hydrophobic probes, such as DiI, from their carrier can be monitored via FRET effects (Chen et al., 2008). Thus, Homo-FRET might be another possible technique for characterising the release of hydrophobic fluorophores from the oil core of emulsions.

PEG density also affected the stability of TNEs under different storage conditions. TNEs with different PEG densities were stable at 4 °C and room temperature, however, P200 only was stable at all freezing conditions, and P100 showed stability only at -80 °C. TNEs with lower PEG densities (P0, P5 and P50) showed instability at -20 °C and -80 °C. This is because storage below 0 °C temperatures produces fat crystals within the oil phase (crystallisation) that reduce the stability of O/W emulsions (van Boekel and Walstra, 1981). The fat crystals can protrude into the water phase penetrating the film between adjacent oil droplets and causing partial coalescence (Harada and Yokomizo, 2000, Vanapalli et al., 2002, McClements, 2004). A slow freezing (- 20°C) process results in the formation of larger fat crystals when compared to fast-cooling (- 80°C) that produces smaller fat crystals. Subsequently, slow-cooling led to lower stability of TNEs at even high PEG densities (P100) as shown in Figure 3.4.

Polymer surface coatings are commonly used to improve the *in vitro* and *in vivo* performance of nanomaterials. Polymers such as PEG can reduce non-specific binding and provide stability for nanomaterials during incubation with surrounding biological environments. Even though *in vitro* binding assays involving P200 TNEs (PEG-decorated emulsions) showed non-specific binding possibly caused by ionic interactions with cells, PEG display on nanomaterial surfaces can help to minimise these ionic interactions. It is also well known that surface coating nanomaterials with PEG can provide hydrodynamic stability and help emulsions evade phagocytosis potentially extending their blood circulation. However, the complexity of biological barriers, including plasma proteins (protein corona), can adsorb onto nanomaterial surfaces and affect the *in vivo* fate of nanomaterials inferring that the short circulation time observed in this study may have been due to the interaction of TNE surfaces with plasma proteins following IV injections.

The biodistribution study of P200 TNEs suggested clearance through urination, however the droplet size of TNEs (170 nm) is bigger than the pore size (10 nm) of kidney filters. In contrast, TNE droplets are soft contractible materials with mechanical properties that allow them to shrink and relax back to normal shape without affecting their stability (Zeng et al., 2013). The other explanation for renal clearance may be cargo (DiI) partitioning from the oil phase, however this is less likely because DiI is weakly fluorescent in aqueous solutions, therefore partitioning and clearance through urine should not produce a high signal. Consequently, the results from this study demonstrated urine fluorescence indicating TNEs (oil droplets-containing DiI) were cleared as intact droplets. The likely interactions between TNEs and biological systems strongly suggest that a deeper understanding of TNE interfaces and their interactions with surrounding environment is needed. This exploration can be facilitated by the tuneable interfacial properties of TNEs.

To conclude, TNEs were successfully directed toward *in vitro* receptor-specific targeting of cancer cells. However, the *in vivo* application of TNEs through the IV route for active targeting was not successful due to short circulation times, subsequently these findings present opportunities for further research. Distribution studies of un-targeted TNEs at short time intervals suggests TNEs were mostly cleared via the renal route, and to some extent, through the hepatic path within 24 hours. These results, combined with the absence of enduring cytokines levels and the biocompatible design, all contribute to an acceptable safety profile for TNEs as a drug carrier of lipophilic drugs. However, the rapid clearance of TNEs, due either to bound serum proteins or phagocytosis, suggests that their surface decoration, that encodes TNEs functionalities, requires better understanding (and will be discussed in further detail in chapter 4).

4 Chapter 4: Insights into the Interfacial Structure–Function of Poly(ethylene glycol)-Decorated Peptide-Stabilised Nanoscale Emulsions

The entire chapter 4 is composed of a journal article published as following:

Hossam H. Tayeb, Stefania Piantavigna, Christopher B. Howard, Amanda Nouwens, Stephen M. Mahler, Anton P. J. Middelberg, Lizhong He, Stephen A. Holt and Frank Sainsbury (2017). Insights into the interfacial structure–function of poly(ethylene glycol)-decorated peptide-stabilised nanoscale emulsions. *Soft Matter,* 13 43: 7953-7961. doi:10.1039/c7sm01614j

The rapid clearance of TNEs that minimised the success rate of active targeting, due either to bound serum proteins or phagocytosis, suggests that their surface decoration, encoding TNEs functionalities, requires better understanding. the following chapter addresses this. The physio-chemical properties of a tuneable model interface are related to ligand accessibility and receptor-binding performance of nanoscale emulsions. Polyethylene glycol (PEG)-mediated surface shielding is commonly applied to impart anti-fouling and immune-evading characteristics on interfaces and NPs. Using precise control over the surface decoration of peptide-stabilised emulsions the interfacial properties of a PEG-modified oil-water interface were investigated. In particular, how the physical parameters of the PEG layer impact the accessibility of a co-decorated single-chain fragment antibody were determined. The interfacial properties of soft nanomaterials are fundamental determinants of their performance and the structure-function findings presented in this chapter also provide a general understanding of interfaces. By defining a trade-off window in molecular design space, this work paves the way for the rational design of sophisticated nanomaterials that interact with their environment in controlled and predictable ways.

4.1 Abstract

The interfacial properties of nanoscale materials have profound influence on biodistribution and stability as well as the effectiveness of sophisticated surface-encoded properties such as active targeting to cell surface receptors. Tailorable nanocarrier emulsions (TNEs) are a novel class of oil-in-water emulsions stabilised by molecularly-engineered biosurfactants that permit single-pot stepwise surface modification with related polypeptides that may be chemically conjugated or genetically fused to biofunctional moieties. We have probed the structure and function of poly(ethylene glycol) (PEG) used to decorate TNEs in this way. The molecular weight of PEG decorating TNEs has considerable impact on the ζ-potential of the emulsion particles, related to differential interfacial thickness of the PEG layer as determined by X-ray reflectometry. By co-modifying TNEs with an antibody fragment, we show that the molecular weight and density of PEG governs the competing parameters of accessibility of the targeting moiety and of shielding the interface from non-specific interactions with the environment. The fundamental understanding of the molecular details of the PEG layer that we present provides valuable insights into the structure–function relationship for soft nanomaterial interfaces. This work therefore paves the way for further rational design of TNEs and other nanocarriers that must interact with their environment in controlled and predictable ways.

4.2 Introduction

Soft nanomaterials, such as emulsions, are attractive for various biomedical applications such as drug delivery (Hörmann and Zimmer, 2016), molecular imaging (Rosenblum et al., 2010) and engineered vaccines (Leleux and Roy, 2013). Nanoscale emulsions have evolved as robust carriers for a broad range of hydrophobic drugs, although until recently they have been at the lower end of the design sophistication spectrum. Emulsions offer several advantages over other NPs such as ease of fabrication, high loading capacity and colloidal stability (Koo et al., 2005, Solans et al., 2005, Tadros et al., 2004). However, approaches to engineering the surface of emulsions have been limited to bottom-up integration of functional moieties during emulsification or to deposition by electrostatic interactions (Sainsbury et al., 2014). The potential to overcome this limitation exists with peptide-stabilised emulsions (Dexter et al., 2006) where emulsification is decoupled from subsequent controlled functionalisation via the spontaneous integration of a designer protein anchor-surfactant onto the interface of kinetically stable emulsions (Sainsbury et al., 2014, Zeng et al., 2013). This top-down approach to nanoscale emulsion engineering imparts remarkable flexibility on the range and number of surface modifications now possible.

Surface modification of NPs for therapeutic and diagnostic use is commonly performed to optimise formulation stability and *in vivo* performance. PEG is an FDA-approved nonionic and hydrophilic polymer commonly used to modify liposomal and NP surfaces to improve their pharmacokinetics. PEG provides steric stabilisation during storage and application and may also reduce the adsorption of serum proteins (Harris and Chess, 2003), potentially prolonging circulation time in the blood stream via immune shielding (Pasut and Veronese, 2007, Knop et al., 2010). A recent report shows that PEG also affects the com position of the protein corona surrounding nanocarriers and in doing so decreases their non-specific cellular uptake, highlighting the importance of understanding the physical properties of NP surfaces (Schöttler et al., 2016).

The influence of PEG on protein adsorption, as well as the storage and serum stability of PEGylated NPs is affected by the molar mass, density and conformation of the PEG moiety (Vonarbourg et al., 2006, Georgiev et al., 2007). Furthermore, in the case of sophisticated particles possessing one or more functional moieties in addition to PEG, the physical characteristics of the PEG layer impact the density, accessibility and conformation of additional molecules, such as targeting ligands (Wang and Thanou, 2010). The effect of PEG modification on biodistribution, active targeting, and *in vivo* stability are important questions in soft matter engineering that still require fundamental research into the physical basis for interpreting the role of PEG.

Understanding how the structure–function of nanomaterial interfaces governs their interactions with the environment would enable rational design from first principles. Here we seek to understand the interfacial structure of a unique tailorable nanocarrier emulsion (TNE), thereby gaining insights into the remarkable interfacial self-assembly process of a poly(ethylene glycol)-decorated protein. The amphiphilic surface active peptide, AM1 (Malcolm et al., 2006) can be used to stabilise nanoscale O/W emulsions (Chuan et al., 2012). Surface modification is enabled by the subsequent spontaneous integration of a protein anchor-surfactant, DAMP4 (Middelberg and Dimitrijev-Dwyer, 2011), onto pre-adsorbed AM1 interfaces (Zeng et al., 2013, Dwyer et al., 2013). Genetic fusion or chemical conjugation of functional molecules to DAMP4 thereby facilitates their display on the aqueous phase of the emulsion. Thus, the TNE surface is tuneable in a sequential step-wise fashion, offering great flexibility to control the characteristics of the oil–water interface. Following the detailed characterisation of PEGylated DAMP4, we confirm the sequential addition of functionalised biosurfactants onto the interface. The effects of varying PEG length and density on TNE size, surface charge and interfacial thickness were evaluated to systematically assess their influence on the accessibility of co-displayed functional moieties.

4.3 Experimental section

4.3.1 DAMP4 expression, purification and quantification

DAMP4, a protein surfactant, sequence (MD(PSMKQLADSLHQLARQ VSRLEHAD)4) was expressed and purified as previously described (Middelberg and Dimitrijev-Dwyer, 2011). Briefly, DAMP4 was purified in three sequential chromatographic steps; immobilised metal affinity chromatography taking advantage of the eight histidine residues, ion exchange chromatography at pH 7.0 and reversed-phase (RP)HPLC. RP-HPLC fractions were lyophilised, quantified using analytical HPLC against a DAMP4 standard curve and stored at -80 °C.

4.3.2 DAMP4 PEGylation

DAMP4 was rehydrated with 25 mM HEPES, pH 7.0 and PEGylated using NHS-functionalised polyethylene glycol mPEG–NHS; (www.nanocs.com). PEGylation of DAMP4 using 5000 Da mPEG:NHS, was carried out at two different molar ratios of PEG : DAMP4 (20 : 1 and 50 : 1) and incubated for approximately 16 hours at 4 °C with continuous stirring.

DAMP4 was also PEGylated with the 10 000 Da mPEG–NHS at a 20 : 1 molar ratio under the same conditions. DAMP4 mixtures were analysed by SDS-PAGE using the Any-kD TGX Precast Protein Gels (www.bio-rad.com). Samples (3.55 μg of DAMP4) were loaded in triplicate and stained using

Coomassie brilliant blue R-250 and densitometric analysis was performed using Image J software following destaining to determine the mean percentage contribution of each band in the sample.

4.3.3 Matrix-assisted laser desorption/deionisation

5000 Da PEG-labelled DAMP4 was separated from free DAMP4 using size exclusion chromatography on a S75 column (www.gelifesciences.com) in 25 mM HEPES, pH 7 at 0.5 mL min^{-1}. Collected fractions were desalted with a C4 ziptip (www.merckmillipore.com.au), where the ziptip was first wet with 80% acetonitrile (ACN)/0.1% formic acid (FA), equilibrated with 1% ACN/0.1% FA, the sample loaded, washed with 1% ACN/0.1% FA, and eluted first with 80% ACN/0.1% FA followed by 100% ACN. Eluted material was dried in a speed vac, and resuspended in 3 mL 1% ACN/0.1% FA. An aliquot (0.5 mL) was spotted to a polished steel MALDI target plate along with 0.5 mL DHB matrix (7 mg mL^{-1}) in 50% ACN) and allowed to dry. MS data was acquired on an Autoflex III MALDI-TOF/TOF mass spectrometer (www.bruker.com) in positive linear mode. MS data were externally calibrated using a mix of cytochrome C and myoglobin.

4.3.4 Interfacial tension analysis

The IFT kinetics for PEGylated DAMP4 mixtures were measured using a DSA-10 droplet-shape analysis unit (www.kruss.de). Each sample of DAMP4 solution was loaded onto an 8 mL quartz cuvette (www.hellma-analytics.com) at 10 mM. A known diameter U-shaped stainless steel capillary fed by a glass syringe was used manually to form droplet of Miglyol® 812 (www.axoindustries.be) of approximately 9 mL. Interfacial tension was derived by the Young-Laplace equation using images of the droplet collected by a connected camera at a rate of about 1 measurement per second.

4.3.5 Quartz crystal microbalance

Quartz crystal microbalance with dissipation monitoring (QCM-D) experiments were performed using the E4 system with flow cells (Q-Sense, Västra Frölunda, Sweden). The QCM-D instrument measures the relative changes to the resonance frequency (f) and energy dissipation (D) of the sensor over the course of the experiment. Δf and ΔD were measured simultaneously at the fundamental frequency and the 3rd, 5th, 7th and 9th harmonics. The original data was processed in QTools (www.biolinscientific.com) before being exported for further analysis in OriginPro 8 (www.originlab.com). All experiments were conducted at a temperature of 24 ± 0.05 °C and repeated at least twice. In a typical experiment, firstly, a solution of AM1 0.1 mg mL^{-1} was flushed, flow rate 50 mL min^{-1}, over the surface of a silicon dioxide sensor chip surface modified with a layer of trichloro(octadecyl)silane (OTS; www.sigma-aldrich.com). After the flow was stopped, the peptide solution was left to incubate for 30 minutes and the chamber rinsed with HEPES buffer 25 mM pH 7

to remove any unbound material. After a stable baseline was reached, a solution of 0.1 mg mL^{-1} 10K-PEG DAMP4 was flushed through the chamber at the same flow rate and left to incubate for 30 minutes. The experiment concluded with the rinse of the chamber with HEPES buffer.

4.3.6 Preparation of the tailorable nanosized emulsions (TNEs)

Lyophilised AM1 (molar mass 2473 Da, ≥ 95% purity) was custom synthesised by Genscript (www.genscript.com) and dissolved using 25 mM HEPES containing 800 mM of $ZnCl_2$, to reach a final concentration of 400 mM. 1,1'-Dioctadecyl-3,3,3',3' tetramethylindocarbocyanine perchlorate (DiI; www.thermofisher.com) stock was prepared by dissolving the DiI powder in 100% ethanol at 10 mg mL^{-1}. DiI stock was diluted in Miglyol to a final concentration of 1 mg mL^{-1}. Miglyol was added to the AM1 solution to a final oil composition of 2 v/v%. The mixture was sonicated four times at 45 seconds using the Branson Sonifier 450 Ultrasonicator (www.emersonindustrial.com). Only emulsions with a polydispersity index below 0.2 were accepted for surface modification. The integration of PEGylated DAMP4 products onto emulsion surfaces was achieved by drop-by-drop addition of AM1-stabilised emulsions to vigorously stirring PEG–DAMP4 at a 1 : 1 volumetric ratio. To prepare untargeted TNEs, PEG–DAMP4 was used at a DAMP4 concentration of 400 mM. Targeted TNEs were prepared by sequential addition using the same technique. First, PEG–DAMP4 was used at 40 mM, followed by scFv-DAMP4 fusion at 2 mM and a final addition of PEG–DAMP4 at 400 mM. Hydrodynamic radii with associated polydispersity indices and ζ-potentials were measured using a Zetasizer ZS (www.malvern.com). All samples were diluted to 1 : 100 in Milli-Q water and ζ-potential measurements were made using an electrophoretic cell (www.malvern.com).

4.3.7 Interfacial thickness

The thickness of the air–liquid interface was obtained through X-ray reflectometry measurements done with the Panalytical X'Pert Pro reflectometer (Cu-Kα X-rays, λ = 1.5418 Å) at the Australian Centre for Neutron Scattering (Sydney, Australia). The intensity of monochromatic X-rays reflected from the smooth air–liquid interface was measured as a function of momentum transfer, Q [$Q = (4\pi/\lambda)\sin\theta$, where θ is the incidence angle].

The samples used for these measurements were 0.05 mg mL^{-1} DAMP4, 0.1 mg mL^{-1} 5 kDa or 10 kDa mPEG–NHS, and 0.05 mg mL^{-1} PEGylated DAMP4 (5K-PEG DAMP4 and 10K-PEG DAMP4). Each of these samples was dissolved in 25 mM HEPES pH 7 buffer. Thirteen mL of this solution was poured into a teflon trough, 8 × 5 cm × 0.2 cm deep and left to equilibrate for at least 10 minutes before commencing the measurements. After alignment, measurements were performed by scanning from an angle of incidence of 0.007 to 0.56 in 0.001 $Å^{-1}$ steps for a total time period of 45

minutes. In order to ensure complete equilibration scans were repeated at least twice. The data fitting was carried out using Motofit macros (Nelson, 2006) operating in the Igor Pro environment where the interface is described as a series of layers parallel to the interface. Each layer is described by three parameters its thickness, scattering length density (SLD), and a Gaussian interfacial roughness. The SLD is related to the electron density as follows;

$$SLD = \frac{\lambda 2}{2\pi} r_0 \rho_e$$

where λ is the wavelength, r_0 the classical electron radius and ρ_e the electron density. Data were then fitted to a single layer using a least-squares genetic algorithm routine by varying the layer parameters within physically reasonable bounds.

4.3.8 scFv-DAMP4 expression and purification

A synthetic gene encoding an scFv based on panitumumab34, preceded by an immunoglobulin κ light chain signal peptide and fused to DAMP4 via a Gly4Ser linker was codon optimised for expression in Chinese hamster ovary (CHO) cells. The gene was transferred into the pcDNA 3.1 (+) mammalian expression plasmid (www.thermofisher.com) for transient expression. Plasmid DNA was transfected using 2 mg of DNA per mL of cells at a concentration of 3 x 10^6 cells per mL. DNA was complexed with polyethylenimine-Pro (www.polyplus-transfection.com) in Opti-Pro serum free medium (www.thermofisher.com) at a DNA (μg) to PEI (μL) ration of 1: 4 (w: v) for 15 minutes prior to transfecting suspension-adapted CHO cells. The transfected cells were cultured in chemically defined CHO medium (CD-CHO; www.thermofisher.com) at 37 ^oC, 7.5% CO_2, 70% humidity with shaking at 130 rpm for 6 hours, before feeding with 7.5% CD CHO Efficient Feed A (www.thermofisher.com), 7.5% CD-CHO Efficient Feed B (www.thermofisher.com) and 0.4% anti-clumping agent (www.thermofisher.com). Viability of the cells was evaluated by trypan blue staining from day 7 and culturing was stopped when viability ≤ 50%.

Following transfection, the cells were pelleted by centrifugation and the supernatant was filtered through a 0.22 μm membrane (www.sartorius.com). The scFv-DAMP4 was purified from the supernatant utilising a 5 mL Protein-L column (www. gehealthcare.com.au), eluting the protein with 100 mM glycine pH 3.0. Elution fractions were buffer exchanged into PBS pH 7.4 using the HiPrep 26/10 column (www.gehealthcare.com.au). The final product was filtered through a 0.22 μm membrane and the concentration was determined by measuring absorbance at 280 nm. The fusion was further analysed by SDS PAGE and size exclusion HPLC using a TSK gel G3000SW column (www.tosoh.com).

4.3.9 Biolayer interferometry

Biolayer interferometry was used to determine the binding affinity constants of the scFv-DAMP4 fusion protein for recombinant EFGR (rEGFR)-Fc targets. The Octet-Red (www.fortebio.com) platform was used to evaluate binding using 96 well black plates (www. greinerbioone.com). Each well was prepared with 200 μL of sample, the reactions were conducted at 30 ^{o}C and 1000 rpm agitation was used for each step. Biosensors were hydrated in 200 μL of PBS for 10 minutes prior to the start of the binding assay. Anti-human Fc-specific biosensors (www.fortebio.com) were immobilised with 100 μg mL^{-1} rEGFR-hFc (www.sinobiological.com). The assay conditions included an initial baseline step in PBS for 5 minutes, followed by loading 100 μg mL^{-1} rEGFR-Fc for 10 minutes, PBS baseline for 5 minutes and then an association step with scFv-DAMP4 for 10 minutes followed immediately by a 10 minutes dissociation step in PBS. The scFv-DAMP4 was titrated from 500–6.25 nM to measure the binding kinetics for EGFR using a 1: 1 binding kinetic model.

4.3.10 Solid state EGFR binding

The human epidermal growth factor receptor (5 μg mL^{-1}) in PBS (www.sinobiological.com) was immobilised onto 96-well black polystyrene plates (www.corning.com) at room temperature for 4 h. Then, the immobilised EGFR was blocked using 2% milk PBS for 1 hour. Diluted TNEs (0.05 oil%) formulations were applied and incubated for 30 minutes at room temperature. Unbound TNEs were removed with two washes of PBS, containing 0.05% Tween-20, and a final wash using PBS, before re-filling the wells with PBS. Fluorescence intensity was measured using an M200Pro TECAN plate reader (www.lifesciences.tecan. com) with emission and excitation wavelengths of 535 nm and 570 nm, respectively.

4.3.11 Flow cytometry

Targeted and un-targeted TNEs prepared using each DAMP4–PEG species were diluted (0.025–0.015 oil%) and applied at 1 : 1 volumetric ratio to the MDA-MB-468 cell suspension (1.5 × 10^{6} cells per mL) in PBS containing 10% Foetal Calf Serum (FCS). Cells were then incubated 1 hour for binding at 4 ^{o}C, followed by three washing steps to remove weakly bound TNEs. FACS measurements were limited to 20 000 events, cells gating and a full analysis were performed using flowing software v2.5.1.

4.4 Results and discussion

4.4.1 Characterisation of protein co-surfactant PEGylation

The protein co-surfactant DAMP4, is a tetrameric repeat of the peptide surfactant AM1 joined by designed fold-permissive linkers. In solution it is a hyper-stable 4-helix bundle formed by hydrophobic interaction of the amphipathic helical AM1 units. PEGylation by NHS-coupling is used to bioconjugate to the free amines of the four lysine residues plus the amino terminus and this generic approach results in mixed species of DAMP4 with varying numbers of conjugated PEG (Figure 4.1). SDS-PAGE was used to separate the PEGylated species from un-conjugated DAMP4, which, although it could not be used to determine molecular weight of each species (Zheng et al., 2007), did allow quantification by densitometry. Matrix assisted laser desorption/ionisation time of flight (MALDI TOF) mass spectrometry (Supplementary Figure 4.1) showed that the four species including the free DAMP4 (11116 m/z) (Dimitrijev Dwyer et al., 2014) resulting from the conjugation of 5 kDa PEG correspond to DAMP4 + 1PEG (16551 *m/z*), DAMP4 + 2PEG (21537 *m/z*) and DAMP4 + 3PEG (27378 *m/z*).

Enriching the DAMP4–PEG conjugate yield could be achieved by increasing the PEG: DAMP4 ratio and also by using longer length polymers. The low PEG: DAMP4 ratio (20:1) reaction yields approximately 50% PEGylated DAMP4 species (5K-PEG-Lo). However, increasing the PEG: DAMP4 ratio (50 : 1) shows a significant increase in the yield of the PEGylated forms to approximately 90% (5K-PEG-Hi). The use of 10 kDa NHS–PEG results in more than 90% PEGylated DAMP4 at the same 20:1 molar ratio as 5K-PEG-Lo. We suspect that this is due to different reactivity of the functional groups of the two NHS–PEG reagents. Due to the presence of multiple free amines on DAMP4, the NHS–coupling performed here results in a mixture of products. Although we find that the relative abundance of species is consistently obtained, further engineering of DAMP4 could permit site-specific and potentially, with the use of click chemistry, stoichiometric bioconjugation (Salmaso et al., 2009, Sato, 2002, Kolb et al., 2001, Fee and Van Alstine, 2006)

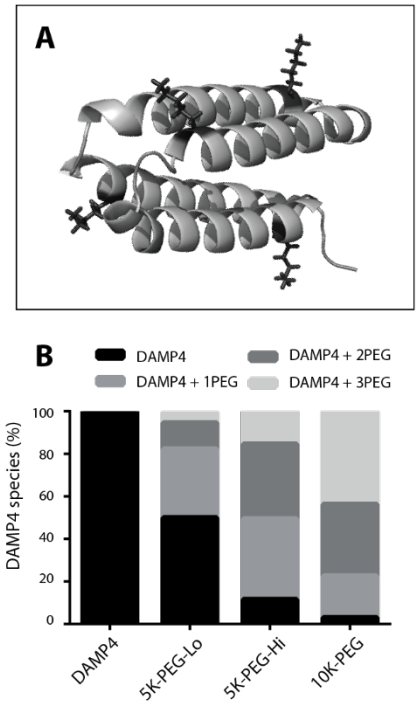

Figure 4.1. Bioconjugation of NHS-mPEG to DAMP4. (A) Cartoon of DAMP4 showing the position of the four lysine residues. (B) Densitometric analysis of DAMP4–PEG mixtures including DAMP4 conjugated to 5000 Da NHS– PEG using the low (5K-PEG-Lo) and high (5K-PEG-Hi) ratio reaction, and DAMP4 conjugated to 10 000 Da NHS–PEG (10K-PEG). Values represent the mean percentage composition of the different reaction products from 3 independent reactions, which each varied by no more than 10% between conjugation reactions.

4.4.2 Interfacial tension of PEGylated DAMP4

Due to the kinetic mass transfer limitations of large surfactant molecules on interfacial activity we analysed the IFT of the PEGylated DAMP4 species to determine the impact of the bioconjugate. The oil–water IFT kinetics of DAMP4 and the various PEGylated ensembles are shown in (Figure 4.2). A drop in surface tension from 31 mN m^{-1}, that of a pristine oil droplet, indicates adsorption of the biosurfctant. While an increase in average size due to DAMP4 conjugation results in lower mass velocity and migration to the interface, all PEGylated DAMP4 mixtures are interfacially active. The increase in PEG length from DAMP4 to 5K-PEG to 10K-PEG reduces the adsorption as would be expected due to the decrease in diffusion coefficient (Cussler, 2009). The increasing density of conjugated PEG does result in slightly lower interfacial activity, although the different DAMP4 samples give similar final reductions in surface tension, (Figure 4.2). The IFT is lowest for DAMP4 at 13.8 mN m^{-1} whereas for the 5K-PEG-Lo PEGylated DAMP4 mixture it is 15.5 mN m^{-1}. The 5K-PEG-Hi and 10K-PEG preparations, which have similar PEGylation reaction yields, also have similar IFT measurements of 17.3 and 17.8 mN m^{-1}, respectively. Interestingly, therefore, steady state IFT values appear to depend more on the number of conjugated PEG moieties per DAMP4 than the MW of the conjugate, indicating an impact of the bioconjugated state of individual residues on interfacial activity.

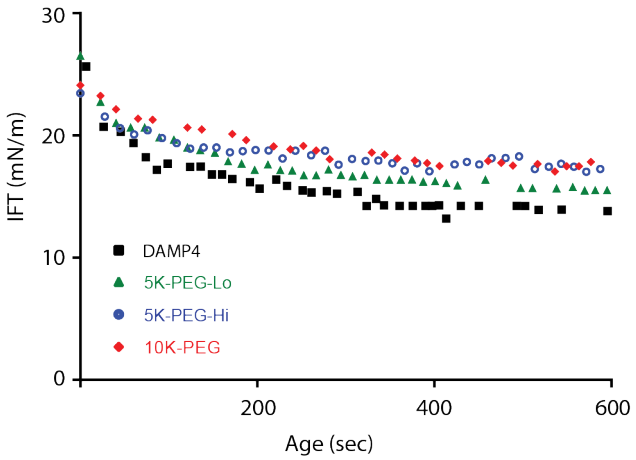

Figure 4.2. Interfacial tension analysis of the DAMP4:PEG conjugates. Measurement of the interfacial tension (mN $m^{-}1$) against time (s) was performed for DAMP4 (black squares), 5K-PEG-Lo (green triangles), 5K-PEG-Hi (blue circles) and 10K-PEG (red diamonds) at 10 mM.

4.4.3 Sequential addition of DAMP4 conjugates

Previous work has shown that AM1-stabilised O/W emulsions can be modified by the spontaneous integration of PEGylated DAMP4 onto the interface (Zeng et al., 2013). Here we investigated the interaction of PEGylated DAMP4 with a pre-formed AM1 layer by monitoring the mass variation on a hydrophobic interface using QCM-D (Figure 4.3). A decrease in frequency, corresponding to mass addition, from -6 Hz to -37 Hz shows that 10K-PEG–DAMP4 adsorbs at the AM1 layer. This interaction is stable and irreversible as the signal is unchanged after initial adsorption during the incubation time (Figure 4.3; step c), with only a small amount of material removed by the buffer wash (Figure 4.3; step d), which was continued until the signal was stable for two minutes. The response of the three harmonics is very similar suggesting that the DAMP4 penetrates the AM1 layer rather simply adsorbing on top. The observed stable increase in dissipation (ΔD) may be due to the PEG tails protruding in the bulk solution.

To relate the addition to AM1-stabilised nanoscale emulsions we sought to confirm the stable adsorption of PEGylated DAMP4 by quantifying the amount of free AM1 and DAMP4 following sequential assembly. Modification with increasing amounts of PEG–DAMP4 showed that up to approximately 40 pmol cm^{-2} DAMP4 can be integrated onto a 1% (v/v) AM1-stabilised Miglyol emulsion (Supplementary Figure 4.2). At 57 pmol cm^{-2} some AM1 is displaced from the interface and this increases with higher density of DAMP4. However, even a low amount of PEG–DAMP4 can confer hydrodynamic stability on the emulsions; preventing coalescence in PBS where electrostatic repellent effects are negated, or in the presence of EDTA (Supplementary Figure 4.3), which disrupts the cohesive interfacial peptide network (Malcolm et al., 2006). This indicates that PEG is functionally displayed on the interface, creating a steric barrier to coalescence. Therefore, PEG–DAMP4 is stably integrated onto AM1-stabilised TNEs, presumably with PEG oriented into the bulk phase.

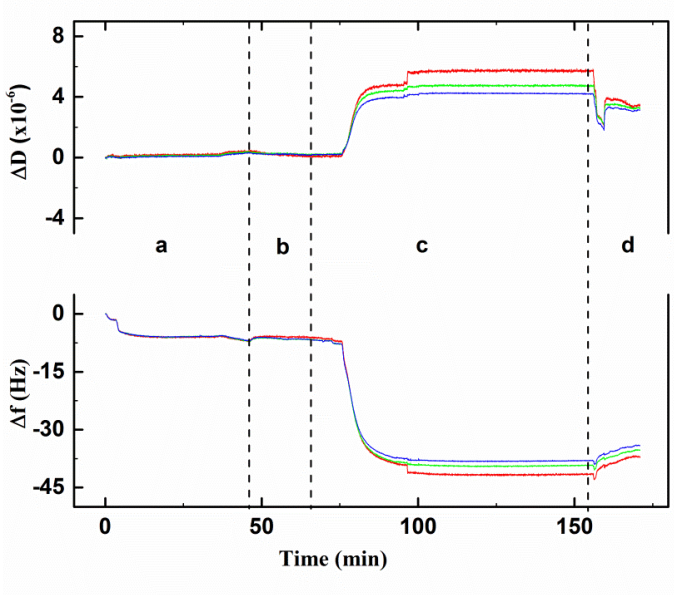

Figure 4.3. Typical Δf and ΔD versus time plots of 10K-PEG–DAMP4 interacting with AM1 peptide. The dashed lines mark the end of each phase. Phase a corresponds to the flow and incubation of AM1 solution, whereas c denotes the flow and incubation of PEG–DAMP4. The rinse with HEPES buffer solution corresponds to phase b and d. The 5th (red), 7th (green) and 9th (blue) harmonics are displayed.

4.4.4 Impact of DAMP4 PEGylation on the size and ζ-potential of TNEs

To investigate the influence of variable DAMP4 PEGylation on the surface properties of TNEs we modified the interface of AM1-stabilised emulsions with the DAMP4 mixtures. Application of the DAMP4–PEG conjugates results in predictable changes to the size and ζ-potential values of TNEs (Figure 4.4). While there is no change in size following the addition of 5K-PEG-Lo DAMP4, from 165 ± 2 to 166 ± 3 nm, there is a variable size increase following the addition of 5K-PEG-Hi DAMP4 to 171 ± 7 nm and a considerable and consistent increase with 10K-PEG DAMP4 to 178 ± 2 nm. Emulsion preparations remain monodisperse (polydispersity index ≤0.2) following the integration of DAMP4–PEG indicating that colloidal stability of the emulsions is maintained. The increase in size corresponds to the amount and size of PEG moieties displayed on the surface of each TNE preparation. However, recent estimations of the density and linear dimension of anchored PEGs in the extended brush format (Damodaran et al., 2010, Meng et al., 2004), suggest that the PEG molecules here are displayed in a compressed conformation or even oriented parallel to the TNE oil–water interface.

The addition of 5K-PEG (Lo or Hi) also changes the electrophoretic mobility of TNEs (Figure 4.4) by masking the positive charge carried by surface-exposed residues of the hydrophilic face of AM1/DAMP4 helices (Dexter et al., 2006). Integration of PEGylated DAMP4 reduces the ζ-potential of AM1 emulsions from 62.7 to 38 and 39.6 mV for the 5K-PEG-Lo and 5K-PEG-Hi formulations, respectively. The integration of the 10K-PEG onto TNEs further reduces the ζ-potential to 24.3 mV, indicating that 10K-PEG better shields AM1 and DAMP4 helices at the oil–water interface. Since the two 5K-PEG preparations result in the same ζ-potential despite presumed differences in PEG density, the effect on apparent surface charge could be due to expansion of the surface double layer such that less charge is able to ‘‘shine through’’ from the 10K-PEG TNEs relative to 5K-PEG-Hi TNEs (Pasche et al., 2005), as opposed to simply an effect of overall PEG mass. Reducing the ζ-potential of NPs is a significant factor for minimising non-specific interactions with serum proteins and cells (Lane et al., 2015), thus it is imperative to understand the physical basis for control of this parameter.

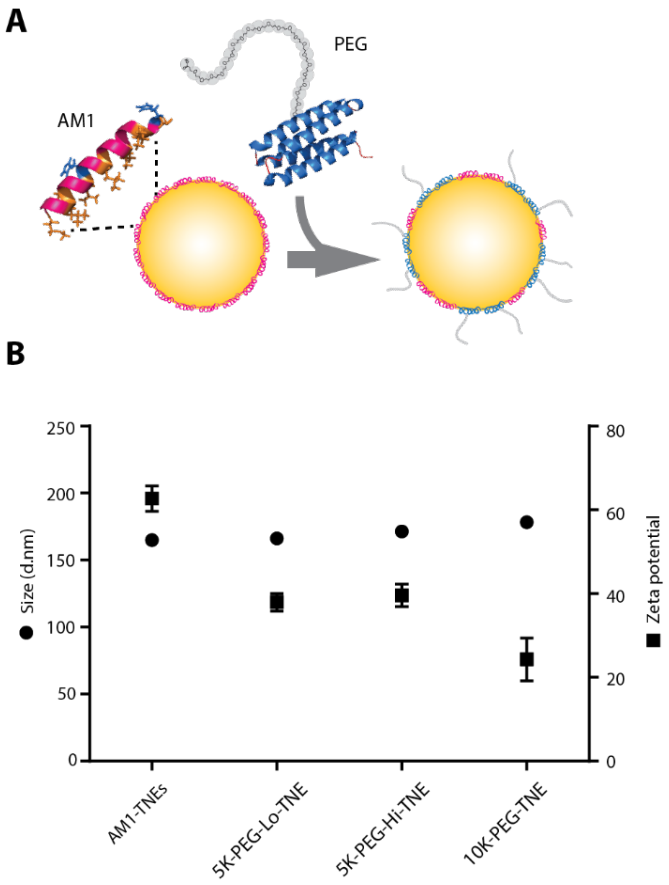

Figure 4.4. Dynamic light scattering and ζ-potential measurements of TNEs prepared with DAMP4-PEG conjugates. (A) Schematic representation of the spontaneous integration of DAMP4 conjugates onto the surface of AM1-stabilised emulsions. (B) Z-averaged size and ζ-potential of the AM1-stabilised emulsion, as well as the 5K-PEG-Lo, 5K-PEG-Hi and 10K-PEG TNEs. Values represent the mean of three emulsions ± SD.

4.4.5 Interfacial thickness of the PEG layer

Using an air–water interface as a model that closely mimics the oil–water interface, we have applied X-ray reflectometry to probe the thickness and relative density of the PEG layer in the aqueous phase. This was compared to interfaces with DAMP4 or PEG only. Figure 4.5 shows the layer fit (see Table 4.1 for parameters) and the scattering length density (SLD) profile, which is effectively a scaled electron density perpendicular to the interface as a function of distance where ‘‘0’’ represents the interface and positive values are moving into the bulk solution. The data were fitted simultaneously where the upper layer (layer one) was constrained to have the identical thickness across the three datasets. As DAMP4 consists of four AM1 units it is not possible to distinguish between them by XRR. This modelled density profile showed that for DAMP4, there is a surface excess layer about 11 Å thick with a higher electron density than pure water, as has been previously observed (Dwyer et al., 2013, Li et al., 2016). For a solution containing 5K-PEG-Hi PEGylated DAMP4 there is a surface layer with a slight reduced electron density suggesting that the surface packing of the DAMP4 may be disrupted. With the 10K-PEG DAMP4 an initial layer similar to that from DAMP4 is observed but with a second layer of material and corresponding density gradient extending into solution over a distance of about 50 Å. This ‘tail’ is attributed to the 10 kDa PEG molecules extending into the bulk solution and is not observed for the 5 kDa PEG. It should be noted that the scattering from this second layer is very weak and its inclusion imparts a marginal improvement to the data fitting.

This intriguing difference in the interfacial structure resulting from PEGs of different molecular weight may explain the observed differential influence on physical properties of TNEs. The extension of 10 kDa PEG into the aqueous phase is consistent with the marked increase in hydrodynamic radius of TNEs modified with 10K-PEG DAMP4. In addition, substantially decreased ζ-potential following the addition of 10K-PEG DAMP4 is consistent with expansion of the electrical double layer due to the extended density profile of the neutral polymer. On the other hand, negligible or variable size changes of TNEs modified with 5 kDa PEG together with density-independent impact on ζ-potential and a potential influence on DAMP4 packing, suggest that the 5 kDa PEG is indeed oriented parallel to the TNE oil–water interface or remains in an otherwise compressed state. If this were the case, then an effect on PEG spacing of DAMP4, as suggested by the SLD profile, would be expected to lower the average charge density at the interface. Knowledge of the biophysical properties of the PEG layer is fundamental to molecular understanding of the TNE interface and, therefore, the potential for rational design of functional interfaces.

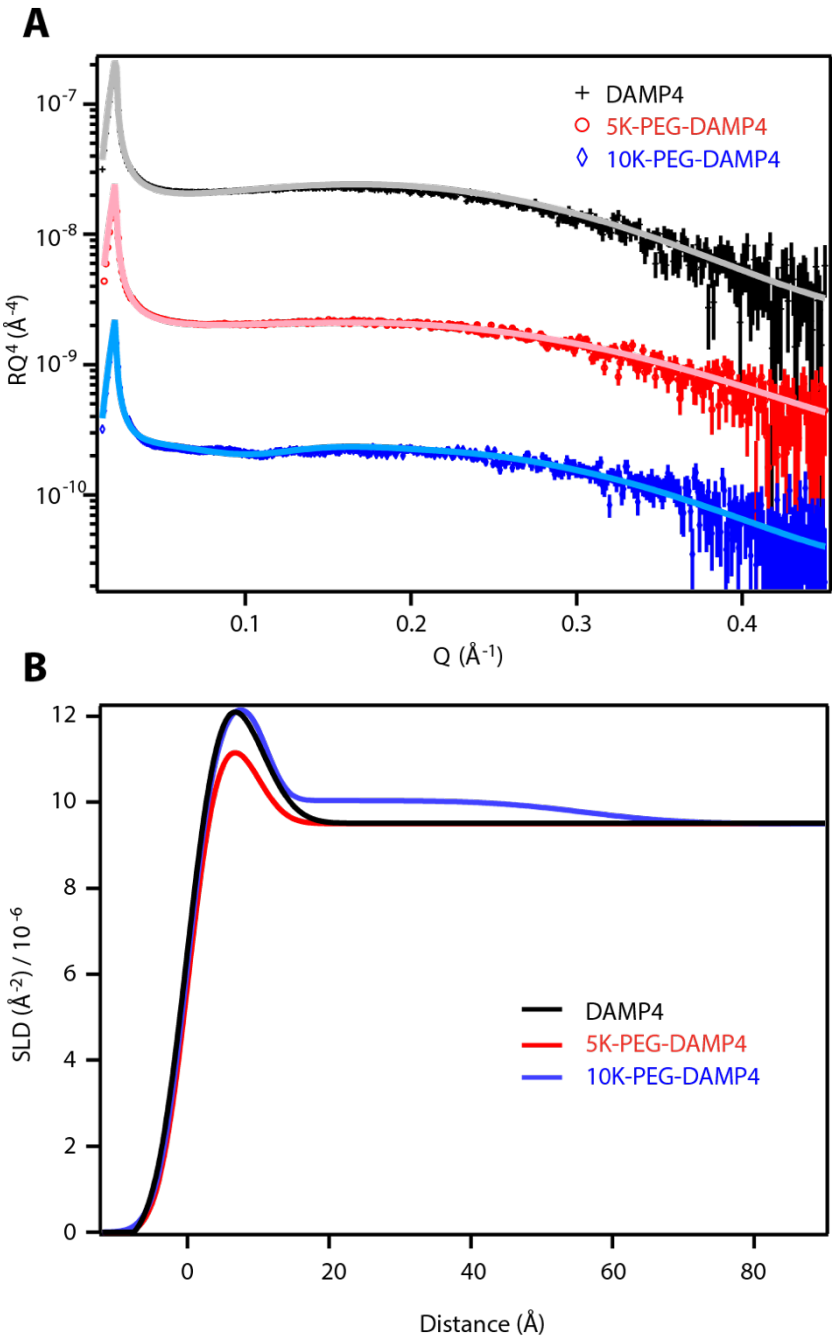

Figure 4.5. X-Ray reflectivity data and the real space fit to the datasets. (A) Reflectivity data multiplied by Q4 for DAMP4, 5K-PEG-DAMP4 and 10K-PEG–DAMP4 where the points represent the data and the lines the fit to the data, error bars not shown where they are smaller than the symbol. (B) The real space SLD profile according to the data fits presented in (A).

Table 4.1. Parameters from the fit to the XRR data sets. Where there are two layers layer one is against the air and layer two against the subphase.

Parameter	DAMP4	5K-PEG DAMP4	10K-PEG DAMP4
Layer 1 thickness (Å)	11	11	11
Layer 1 SLD ($Å^{-2}$)	11.9	11.0	12.6
Layer 1 roughness (Å)	3.3	3.5	3.8
Layer 2 thickness (Å)	-	-	49
Layer 2 SLD ($Å^{-2}$)	-	-	10.3
Layer 2 roughness (Å)	-	-	6.5

4.4.6 Presentation and accessibility of functional moieties on TNEs

As we have verified herein, surface modification of TNEs is as simple as adding DAMP4 conjugates to a single reaction pot. This approach was used to sequentially introduce cell-specific targeting to TNEs, in addition to PEG-mediated shielding from non-specific uptake (Zeng et al., 2013). To generate a simple model for surface presentation of functional moieties on TNEs we constructed a single-chain variable fragment-DAMP4 fusion as a ligand- binding reporter. As designed, the fusion is competent for epidermal growth factor receptor (EGFR) binding, with a 1 nM dissociation constant measured by biolayer interferometry (Supplementary Figure 4.4). Following the integration of a low density PEG layer to confer hydrodynamic stability on the emulsions, the surface was further modified with the scFv-DAMP4, followed by backfilling with PEGylated DAMP4 as previously described (Zeng et al., 2013).

The integration of the 38 kDa scFv fusion onto the TNEs results in an increase in size and while the ζ-potential of 5K-PEG-Hi and 10K-PEG TNEs is slightly reduced by the presence of the scFv, there is a marked impact on the variability of the 5K-PEG- Lo TNE ζ-potential (Supplementary Figure 4.4). Although all preparations again remained monodisperse, this size change suggests some impact on the colloidal stability of 5K-PEG-Lo TNE.

To show that the targeting moiety was functionally presented at the oil–water interface and assess the impact of PEG length and density on accessibility of the scFv we devised a solid state binding assay to the ligand. The 5K-PEG-Lo TNE shows no specificity in ligand binding (Figure 4.6B). In contrast, both the 5K-PEG-Hi and 10K-PEG TNEs display scFv-dependent binding to the receptor in this controlled environment. However, the more complex surface of the cell imparts a more stringent test for specificity and the coverage of the TNE surface by PEG. Using EGFR-positive breast cancer cells and a high emulsion concentration (32.7 droplets per cell) to assess both specific and non- specific binding, no difference in median fluorescence can be seen between 5K-PEG-Lo formulations with and without the targeting moiety (Figure 4.6C). While the 5K-PEG-Hi targeted formulation only improves binding 1.8-fold, the use of 10K-PEG is substantially more effective at preventing non-specific binding and the display of the scFv on 10K-PEG TNEs results in a 2.6-fold increase in median fluorescence. These results show that the scFv was functionally displayed on the surface of TNEs and that the specificity of binding can be controlled by the density of PEG at the surface.

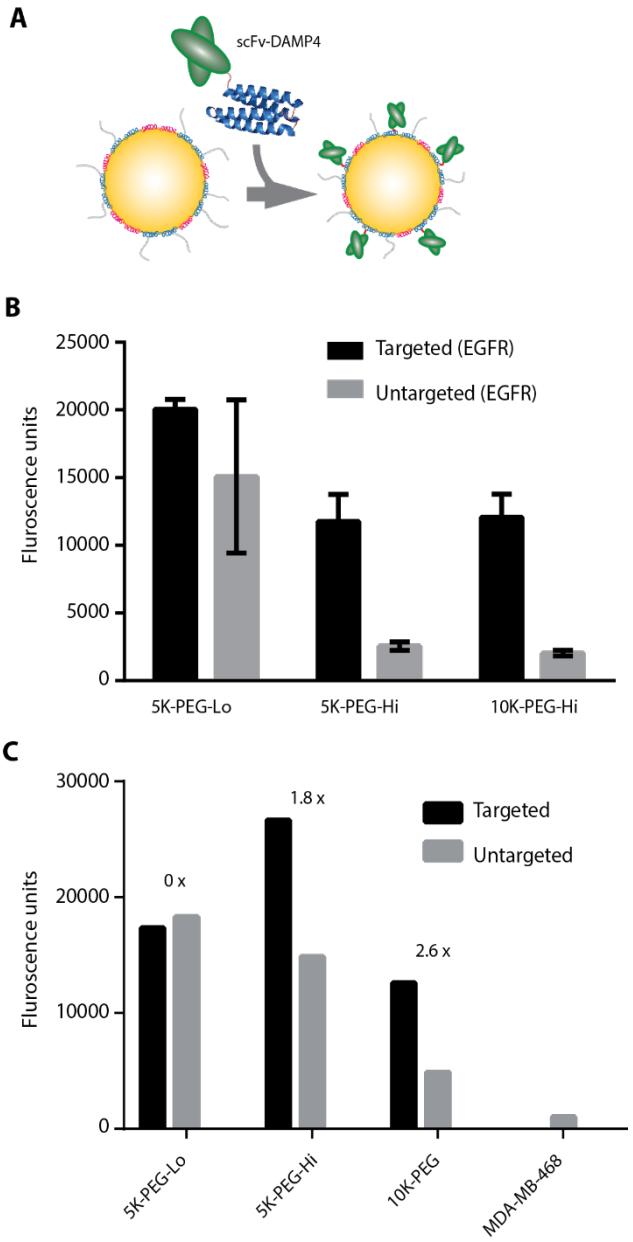

Figure 4.6. Functionalising TNEs with a ligand-binding reporter. (A) Schematic representation of the spontaneous integration of the scFv-DAMP4 fusion protein onto the surface pre-PEGylated TNEs. (B) Solid-state binding assay of the functionalised TNEs. Depicts the binding of fluorescent TNEs assembled using the 5K-PEG-Lo, 5K-PEG-Hi and 10K-PEG DAMP4 mixtures both with and without the scFv displayed on their surface, applied to EGFR-coated wells. (C) Flow cytometry showing the binding to EGFR-positive MDA-MB-468 cells of targeted (black) and control (grey) TNEs assembled using the different DAMP4 mixtures. The values shown are median fluorescence values (from 20000 events). Values represent the mean of three emulsions ± SD.

4.5 Conclusions

The interfacial properties of NPs comprise a set of key determinants for how they interact with their environment. For multifunctional particles, the complexity of this interaction is compounded by the impact of the functional moieties on one another, defining a competition trade-off window in molecular design space. Here we have used a unique model system that permits the controlled assembly of multifunctional NPs to probe the structure-function relationship of an interface modified with the competing influences of PEG and a targeting moiety. TNEs have been shown to be a potentially powerful *in vivo* delivery system (Zeng et al., 2013) and here we present a detailed analysis of their building blocks, preliminary verification of their assembly mechanism and determination of the molecular characteristics of the aqueous phase. Despite the expected differences in thickness of their respective PEG layers demonstrated by X-ray reflectometry, a solid state binding assay suggests that the scFv is equally accessible at the surface of 5K-PEG-Hi TNEs and 10K-PEG TNEs. However, the PEG layer proved vital in reducing non-specific interactions. Summarising these results in a simplistic model (Figure 4.7) allows us to entertain the possible future rational interfacial design of multifunctional TNEs. Continuing work on exploring the assembly and display capacity of TNEs, as well as controlled functionality and performance *in vivo*, is on-going.

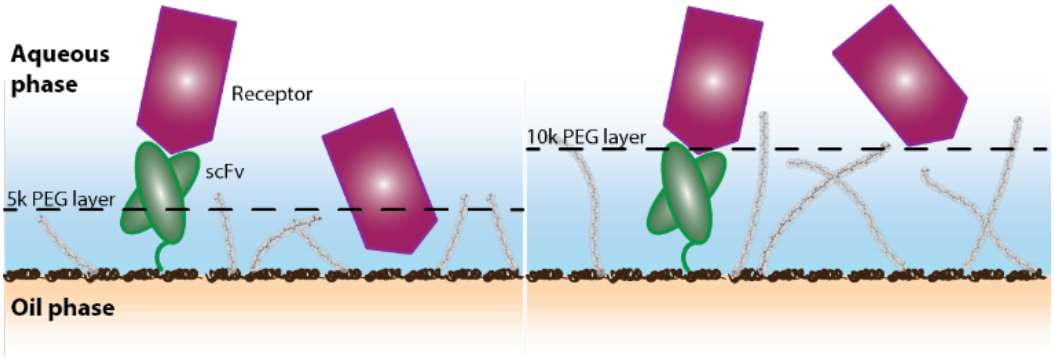

Figure 4.7. Schematic model of the competing influences on EGFR binding of PEG and an anti-EGFR scFv at the oil-in-water interface of TNEs.

4.6 Acknowledgements

This work was supported in part by ANSTO-University of Queensland-Monash University strategic alliance. F. S. acknowledges support from the Australian Research Council (DE140101553) and a University of Queensland ECR Grant. H. H. T. acknowledges financial support from the King Abdul Aziz University, Ministry of Higher Education, Saudi Arabia. The authors gratefully acknowledge Karyn Wilde and Anthony Duff at the National Deuteration Facility (ANSTO) for technical assistance in producing and purifying DAMP4 used in X-ray reflectometry experiments.

4.7 Supplementary materials

Supplementary Figure 4.1

Matrix assisted laser desorption/deionisation. The figure represents the mass spectrometry traces and mass-to-charge ratio (*m/z*) of DAMP4, DAMP4+1PEG, DAMP4+2PEG and DAMP4+3PEG.

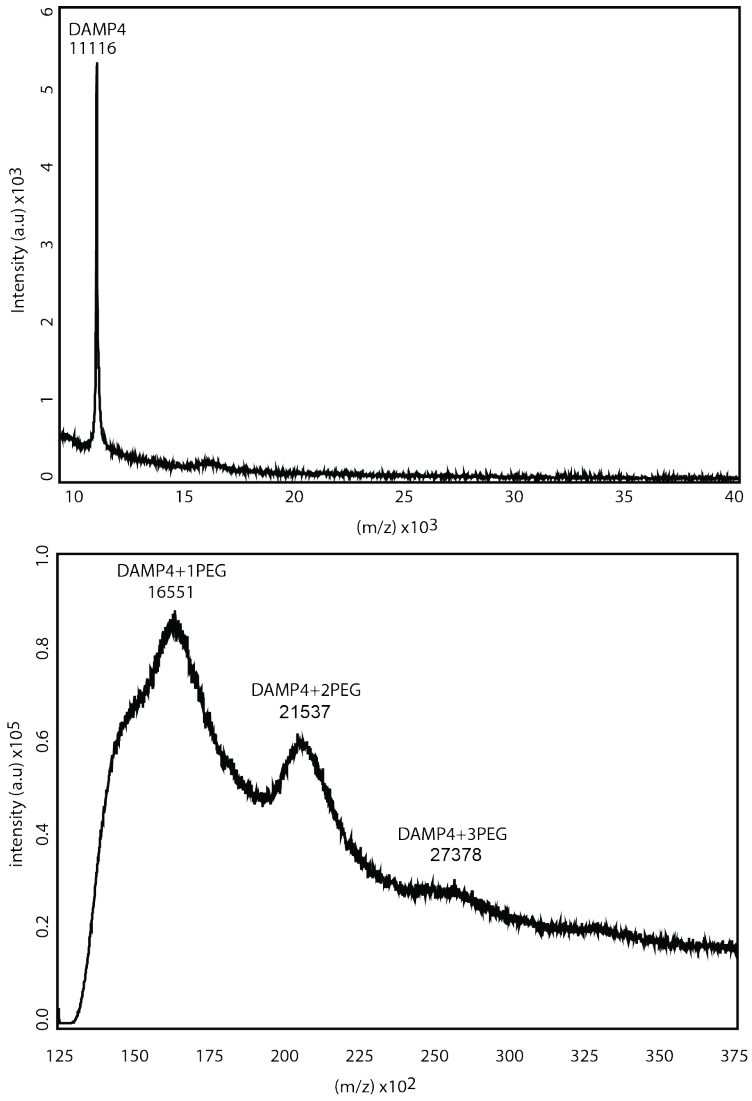

Supplementary Figure 4.2

Concentrations of free AM1 and DAMP4 following the adsorption of PEG-DAMP4 onto AM1-stabilised emulsions. Triplicate emulsions, dispersed in the presence of 400 μM AM1 were mixed with PEG-DAMP4 at the indicated μM concentrations. Taking the surface area corresponding to the subsequent 1% O/W emulsion, the DAMP4 surface densities were as follows: P50 = 14 pmol/cm^2, P100 = 28 pmol/cm^2, P200 = 57 pmol/cm^2, P400 = 113 pmol/cm^2.

A sample of the continuous phase was isolated using a centrifugal ultrafiltration device (100 MWCO) and peptide concentrations determined by HPLC. Values represent the mean of three emulsions ± SD.

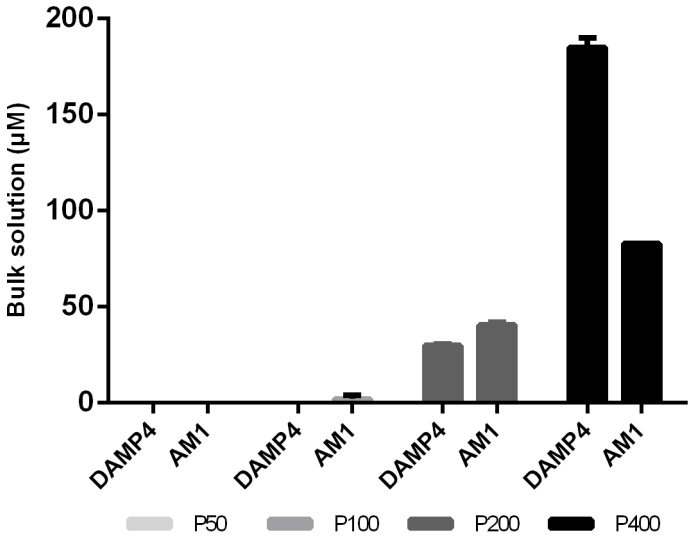

Supplementary Figure 4.3

Stability of TNEs following the addition of DAMP4-PEG. Emulsions containing DiI, dispersed in the presence of 400 µM, were mixed with DAMP4-PEG to obtain the indicated final µM concentrations (5 µM and 10 µM). Each emulsion prepared with DAMP4, 5K-PEG-Lo, 5K-PEG-Hi and 10K-PEG was mixed 1:1 with 100 mM EDTA. The unPEGylated DAMP4 addition at both concentrations shows clear aggregation. The addition of the different DAMP4-PEG preparations at 10 µM stabilises the emulsions, making them resistant to the aggregation in the presence of EDTA. While the addition of 10K-PEG also stabilises the emulsion at 5 µM, 5K-PEG-Lo and 5K-PEG-Hi did not, resulting in reduction in the colouration of the solution due to aggregation of the droplets.

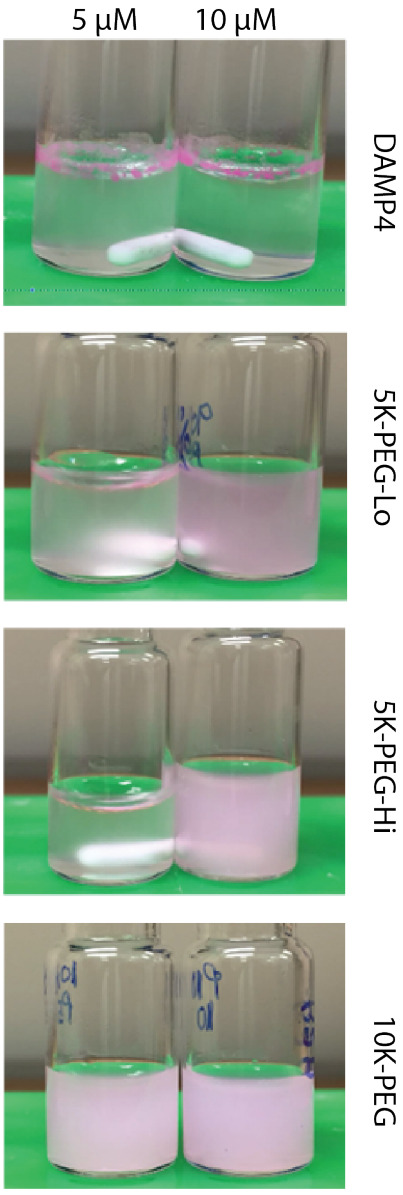

Supplementary Figure 4.4

(A) Schematic representation of the spontaneous integration of the scFv-DAMP4 fusion protein onto the surface pre-PEGylated TNEs. (B) Biolayer interferometry sensogram showing the association and dissociation of the scFv-DAMP4 fusion to EGFR. (C) Z-averaged size and ζ-potential of the 5K-PEG-Lo, 5K-PEG-Hi and 10K-PEG versions of scFv-functionalised TNEs. Values represent the mean of three emulsions ± SD.

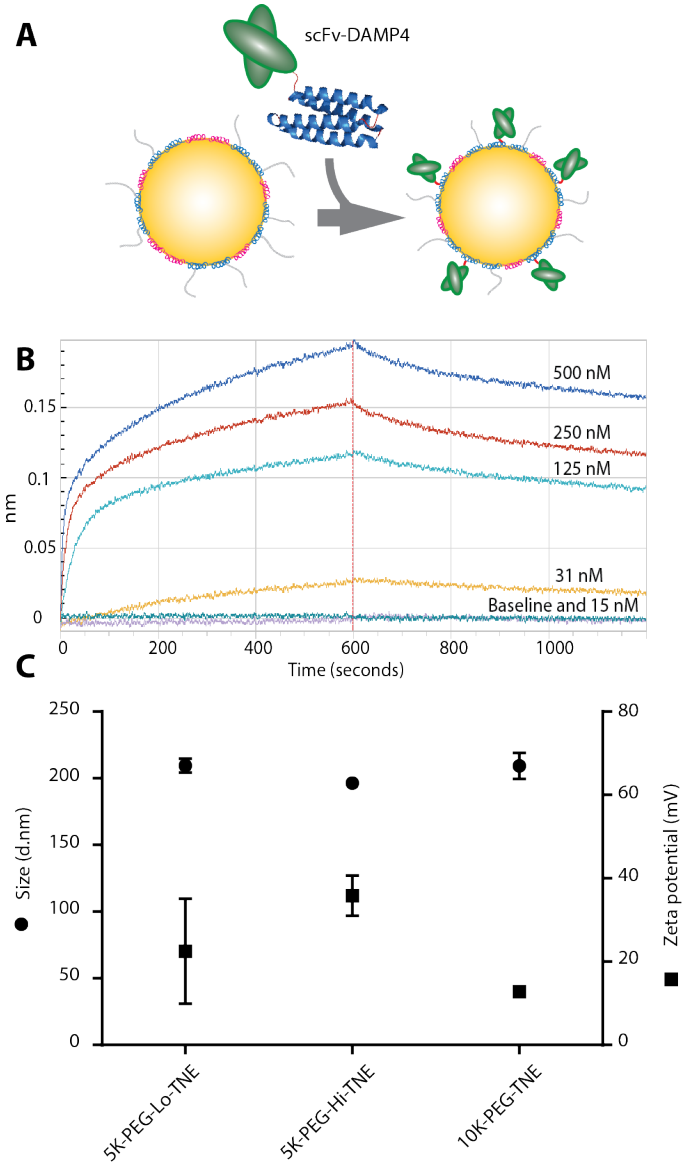

5 Chapter 5: Site-Specific Bioconjugation with Poly(Ethylene Glycol): Impact on the Interfacial Activity of a Protein Biosurfactant

The entire chapter 5 is composed of a journal article submitted 12/01/18 as following:

Hossam H. Tayeb[a], Marina Stienecker[a], Anton P. J. Middelberg[a1] and Frank Sainsbury[a]* (2018) Site-specific bioconjugation with poly(ethylene glycol): impact on the interfacial activity of a protein biosurfactant. Submitted to Colloids and Surfaces B: Biointerfaces Manuscript ID: COLSUB-D-18-00076.

[a] *The University of Queensland, Australian Institute for Bioengineering and Nanotechnology, St Lucia, QLD 4072, Australia.*

[1] Present address: Faculty of Engineering Computer & Math Sciences, The University of Adelaide, Adelaide, SA 5005, Australia.

In the previous chapter it became apparent that the precise bioconjugation of functional moieties to DAMP4 is necessary for effective design of sophisticated interfaces as well as for the more controlled determination of their biophysical properties. This chapter describes the creation of a second generation of DAMP4. Rationally designed cysteine variants by amino acid substitution or addition were generated to enable specific and efficient bioconjugation of maleimide-functionalised PEG.

5.1 Abstract

Biosurfactants are surface active molecules that can be produced by renewable, industrially scalable biological processes. DAMP4, a novel designer biosurfactant, enables the modification of interfaces via genetic or chemical conjugation to functional moieties. However, inconsistent bioconjugation introduces heterogeneity that limits the precision of functionalisation and the resolution of interfacial characterisation. In this work, we successfully designed DAMP4 variants with cysteine point mutations to allow for site-specific bioconjugation. These designed DAMP4 variants were shown to retain the structural stability and interfacial activity of the parent molecule, while permitting efficient and specific conjugation of polyethylene glycol (PEG). PEGylation results in a considerable reduction on the interfacial activity of the single and double mutants. Comparison of conjugates with one or two conjugation sites shows that both the number of conjugates as well as the mass of conjugated material impacts the interfacial activity of DAMP4. As a result, the ability of DAMP4 variants with multiple PEG conjugates to impart colloidal stability on peptide-stabilised emulsions is reduced. We suggest that this is due to constraints on the structure of amphiphilic helices at the interface. Specific and efficient bioconjugation permits the exploration and investigation of the interfacial properties of designer protein biosurfactants with molecular precision. Our findings should therefore inform the design and modification of biosurfactants for their increasing use in industrial processes, and nutritional and pharmaceutical formulations.

5.2 Introduction

Self-assembling biosurfactants have been extensively applied in different areas including food science (McClements, 2015, McClements and Rao, 2011), pharmaceuticals (Brokx et al., 2002, Gudiña et al., 2013, Rodrigues et al., 2006), cosmetics (Vecino et al., 2017, Varvaresou and Iakovou, 2015) and the petroleum industry (Perfumo et al., 2010). Biosurfactants offer many advantages when compared to chemically-synthesised equivalents such as biocompatibility, biodegradability, and sustainable manufacture (Marchant and Banat, 2012, Pacwa-Płociniczak et al., 2011). The interfacial activity of biosurfactants is defined by intermolecular and intramolecular electrostatic and hydrophobic interactions, as well as hydrogen bonds and van der Waals forces. These interactions, that the drive the assembly of protein biosurfactants into supramolecular interfacial arrays, are determined by the primary sequence that dictates their fold into α-helices or β-sheets. Genetic or chemical modifications provide an opportunity to expand the functional repertoire of protein biosurfactants, but they must also consider the possibility of structural alteration and resulting biophysical implications on function.

DAMP4 is an 11.1 kDa protein biosurfactant that was generated by linking four copies of a designer amphiphilic peptide into an anti-parallel four-helix bundle (Middelberg and Dimitrijev-Dwyer, 2011). It is extraordinarily stable in bulk solution (Schaller et al., 2015) and amenable to industrially relevant purification procedures (Dimitrijev Dwyer et al., 2014). Yet it is a highly functional surface-active molecule that has the ability to mediate switchable foaming under variable solution conditions (Dimitrijev-Dwyer et al., 2012). Highly expressed in *Escherichia coli*, DAMP4 can be functionalised via genetic fusion or chemical conjugation and possesses the unique ability to integrate into interfacial films pre-stabilised by the helical monomers that constitute DAMP4 (Dimitrijev Dwyer et al., 2014). These features have seen DAMP4 used to modify O/W emulsions providing functionality for inorganic shell deposition (Wibowo et al., 2015), immune-shielding (Zeng et al., 2013) and cell-receptor targeting (Zeng et al., 2013, Tayeb et al., 2017). The extent of non-specific interactions between the emulsion interface and the surrounding environment can be controlled by the mass and density of decorating polyethylene glycol (PEG) molecules (Tayeb et al., 2017).

PEGylation is widely applied to improve the performance biopharmaceuticals and NPs by reducing immunogenicity, and increasing serum half-life and stability (Mateo et al., 2000, Herman et al., 1995, Jokerst et al., 2011). However, PEGylation of proteins has many challenges including polydispersity of PEG during chemical synthesis or inefficient reaction yield (Fee and Van Alstine, 2006). We recently showed that modification of DAMP4 using NHS-functionalised PEG yields heterogeneous reactions products resulting in limitations on the physico-chemical characterisation of DAMP4-

populated interfaces as well as on the precision of surface modification (Tayeb et al., 2017). However, bioconjugation chemistries offer a range of possible modifications dependent on the accessibility of suitable amino acid side chains (Stephanopoulos and Francis, 2011). For example, conjugates can be coupled to proteins through functional groups including hydroxyl, carboxyl, and thiol-reactive compounds. thiol-maleimide chemistry is widely applied to obtain site-specific bioconjugation (Nair et al., 2014) due to the less frequent occurrence of solvent-exposed cysteine residues allowing for their rational insertion by site-specific mutagenesis.

Bioconjugation should impart the desired modification on a biomolecule whilst preserving its activity. In the case of biosurfactants, function is achieved via adsorption at an interface between two phases. This generally occurs in two steps; (A) transfer or transportation of the protein molecule to the interface; (B) protein unfolding and rearrangement at the interface (Tcholakova et al., 2006). TNEs are peptide-stabilised O/W emulsions that can be functionalised by the spontaneous integration of genetically or chemically modified versions of DAMP4 (Zeng et al., 2013, Sainsbury et al., 2014). During the assembly of TNEs with multifunctional interfaces, DAMP4 conjugated to polyethylene glycol (PEG) is used to provide steric stability during additional functionalisation steps. Here we genetically engineered DAMP4 to improve the accuracy with which it can be used to impart functionality to the surface of peptide-stabilised emulsions. The rational introduction of cysteine residues at select positions designed to retain structure and function of DAMP4 resulted in highly efficient site-specific bioconjugation using the maleimide-thiol reaction. We report the impact of single and double cysteine insertions on interfacial activity and are able to address whether the number of conjugates or the total mass of conjugated polymer affect this parameter. This work shows how genetic and chemical modification of amphiphilic structural features relates to the design of functional interfaces stabilised by biosurfactants using the TNE model.

5.3 Materials and methods

5.3.1 Molecular cloning

DAMP4-encoding sequences were ordered from Integrated DNA Technologies (www.idtdna.com) with extensions homologous to the flanking insertion site of the E.coli expression vector pET48b+ (Novagen; www.merckmillipore.com). Coding sequences were amplified with upstream (5`-ACTTTAAGAAGGAGATATACAT-3`) and downstream (5`-TGTACAGAATTCGGATCC-3`) oligonucleotides corresponding to the extensions and the vector was amplified with their reverse complements. Expression constructs were assembled using the NEBuilder HiFi DNA assembly master mix (New England Biolabs; www.neb.com) and clones were verified by Sanger sequencing.

5.3.2 Expression and purification of DAMP4 variants

DAMP4 variants were expressed and purified in *E.coli* as previously described except where indicated (Dimitrijev Dwyer et al., 2014). Briefly, each variant was purified using sequential chromatography steps; immobilised metal affinity chromatography by taking advantage of the presence of eight histidine residues in each protein sequence, ion exchange chromatography at pH 7.0 and reversed-phase (RP) HPLC. Purified proteins were lyophilised and analyzed for purity and concentration using analytical HPLC against DAMP4 standard curve. Accurate concentrations were determined by amino acid analysis conducted by the Australian Proteome Analysis Facility (APAF).

5.3.3 PEGylation of DAMP4 variants

DAMP4 variants were resuspended with 25 mM HEPES (pH 7.0), 2 mM tris(2-carboxyethyl)phosphine (TCEP) and PEGylated using 5 kDa maleimide-functionalised methoxy polyethylene glycol (www.sigmaaldrich.com). PEGylation of DAMP4 variants was carried out at 4 °C for approximately 16 hours. The PEGylation reaction for all DAMP4 variants was evaluated by SDS-PAGE using the Any-kD TGX Precast Protein Gels (www.bio-rad.com).

5.3.4 Interfacial tension analysis

The IFT kinetics for the DAMP4 variants were measured using a DSA-10 droplet-shape analysis unit (www.kruss.de). The sample volume of each protein (10 µM) is 8 ml in 25 mM HEPES (pH 7.0) loaded onto a quartz cuvette (www.hellma-analytics.com). Approximately 10 µl Miglyol® 812 (www.axoindustries.be) droplets were manually formed using a known-diameter U-shaped stainless steel capillary fed by a glass syringe. The obtained interfacial tension was based on the Young-Laplace equation through images captured by a connected camera for each oil droplet at an

approximate rate of 1 measurement/second. The surface tension of a mature pristine oil droplet was 31 mN/m and IFT values were derived by averaging the final 100 seconds of measurement.

5.3.5 Circular dichroism (CD) spectroscopy

To analyze the secondary structure (Helicity level) of each DAMP4 variant, at 0.25 mg/ml in 2.8 mM HEPES (pH 7.0), 2 mM TCEP, we determined the CD spectra using (http://www.jascoinc.com) at 190-260 nm. CD spectra measurements (300 s) were conducted in a 1 mm path length glass cuvette (www.starnacells.com) at 20 and 90 °C to evaluate the stability against high temperature for all DAMP4 variants. Molar ellipticity was derived from collected data of each variant.

5.3.6 Differential scanning calorimetry (DSC)

DSC analysis was performed to evaluate the thermal stability of the DAMP4 mutants before and after PEGylation. The experiment was conducted using the MicroCal VP- DSC Microcalorimeter (http://www3.gehealthcare.com) and the VPViewer 2000 DSC software. The test and reference samples were treated using the ThermoVac degassing station at 25 °C for 5 minutes to eliminate air bubbles. The molar ratio of DAMP4 mutant samples (0.75 mg/ml) to TCEP was maintained at 1:10. DSC measurements were conducted at scan rate ranging from 25 °C to 125 °C. The collected data were analyzed using the MicroCal-enabled Origin data analysis package.

5.3.7 Preparation and characterisation of TNEs

Lyophilised AM1 (molar mass 2473 Da, ≥ 95% purity) was custom synthesised by Genscript (www.genscript.com) and dissolved using 25 mM HEPES (pH 7.0) containing 800 μM of $ZnCl_2$, to reach a final concentration of 400 μM. Miglyol was added to the AM1 solution to a final oil composition of 2% v/v. The mixture was sonicated four times at 45 seconds using the Branson Sonifier 450 Ultrasonicator (www.emersonindustrial.com). AM1-stabilised emulsions were added drop-by-drop onto to each PEGylated DAMP4 variant (100 μM) while vigorously stirring in a 1:1 volumetric ratio. Prepared TNEs were analyzed using dynamic light scattering and ζ-potential (www.malvern.com).

For stability analysis the concentration used of each PEGylated DAMP4 variant was 10 μM. TNEs modified by PEG-S28C and PEG-D4C2 were diluted in 25 mM HEPES (pH 7.0) or 0.1 M EDTA in the same buffer at 1:1. Emulsions were labelled with 1,1′-dioctadecyl- 3,3,3 0 3 0 -tetramethylindocarbocyanine perchlorate (DiI; www. thermofisher.com) and monitored over time to evaluate TNEs stability.

5.4 Results and discussion

5.4.1 DAMP4 variants

The protein biosurfactant, DAMP4 (11.1 kDa), is composed of four repeats of the helical amphiphilic peptide AM1 (Figure 5.1A). Each repeat is linked by a short sequence designed to break the helix and provide the conformational flexibility that allows the overall 4-helix bundle structure of the protein (Middelberg and Dimitrijev-Dwyer, 2011). In order to insert unique sites for efficient bioconjugation, cysteine mutations were generated by replacing serine residues within the linkers. Selecting this location should not affect the structure and interfacial activity of DAMP4 given the similarity between the substituted side chains. In addition, the C99 variant was created by adding a cysteine residue to the carboxy (C)-terminus of DAMP4 (Figure 5.1B). All variants were successfully expressed and purified (Supplementary Figure 5.1).

5.4.2 Structure, stability and activity of cysteine mutants

DAMP4 is an extremely stable four-helix bundle in solution (Dimitrijev Dwyer et al., 2014) and its helicity is preserved at high temperature (Schaller et al., 2015). However, it is possible that even rational modifications to the sequence might interfere with the structure or function of DAMP4. Therefore, to investigate the structure and stability of the cysteine variants we performed CD spectroscopy. At 20 °C, all single cysteine mutants showed similar CD spectra to DAMP4, characterised by the double absorption minima at 222 nm and 208 nm (Supplementary Figure 5.2). This indicates that all variants show a similar level of helicity. Thermal stability was also performed by CD spectroscopy for each protein at 90 °C, which showed that the variants retained the remarkable stability of DAMP4 (Figure 5.2A). To evaluate the impact of these changes to the primary structure on interfacial activity of each DAMP4 variant, we determined interfacial tension of an O/W bubble in the presence of the biosurfactants. Interfacial tension in the presence of DAMP4 shows an immediate drop, levelling off to 11.32 Nm/m consistent with the adsorption of the protein at the interface (Tayeb et al., 2017). The variants all resulted in a similar surface tension drop indicating that all DAMP4 variants possess similar interfacial activity at the oil-water interface (Figure 5.2B). This is expected as the interfacial activity of DAMP4 is governed by the designed helical structuring present in both the four-helix bundle in bulk and of the repeated helices of the unfolded protein at the interface (Middelberg and Dimitrijev-Dwyer, 2011, Dwyer et al., 2013). This shows that the genetic modification/substitution with cysteine residues at rationally chosen positions does not have an effect on the overall interfacial activity at the oil-water interface. Preserving the interfacial activity for DAMP4 variants allows their further use in the stabilisation and functionalisation of TNEs.

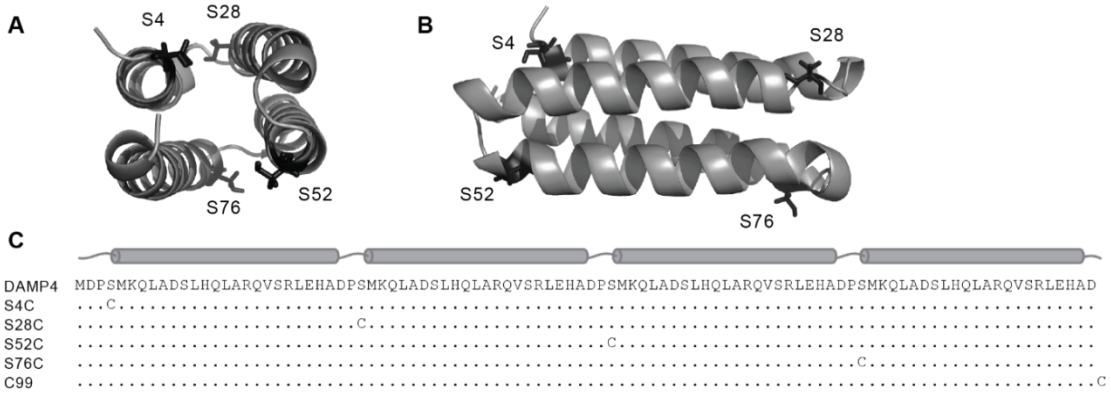

Figure 5.1. Sequence design for DAMP4 cysteine variants. End (A) and side (B) views of a molecular model of the four-helix bundle DAMP4 protein with mutated serine residues indicated. (C) The sequence variation between single cysteine mutants developed in this study. Dots represent conserved residues.

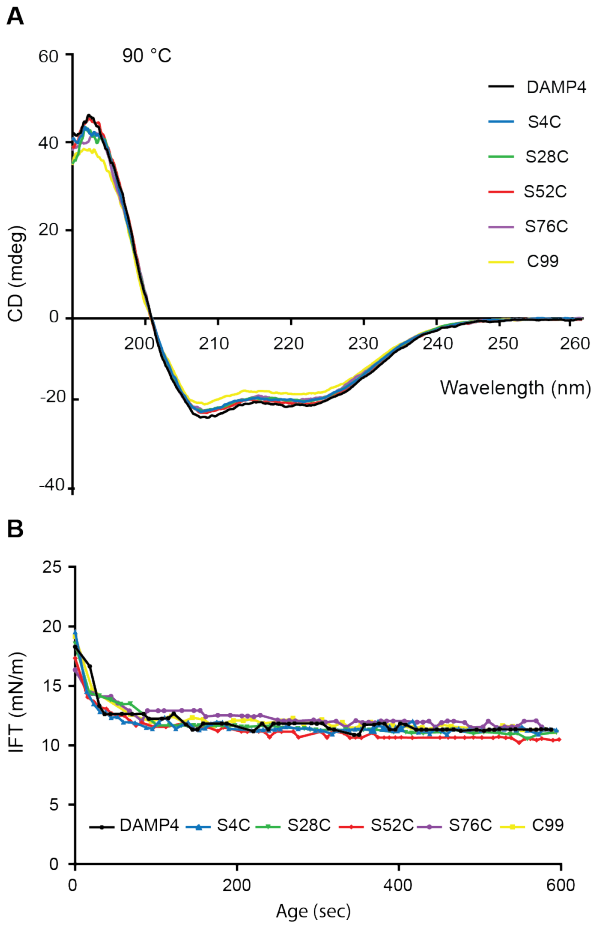

Figure 5.2. Thermal stability and interfacial activity of DAMP4 single cysteine variants. (A) CD spectra of DAMP4 variants at 90 °C. (B) Interfacial tension analysis of DAMP4 variants.

5.4.3 Functional bioconjugation to DAMP4 variants

The single cysteine mutants were genetically engineered through the substitution/addition of cysteine residues to obtain site-specific bioconjugation. In previous work we showed that the density and mass of PEG molecules presented on the surface of nanoscale emulsions was central to the properties of the interface and accessibility of co-presented functional moieties (Tayeb et al., 2017). Here we PEGylated each DAMP4 variant using maleimide-functionalised methoxy PEG (5 kDa). The efficiency of the PEGylation reaction was evaluated using SDS-PAGE and showed successful PEGylation at a yield approaching 100% (Supplementary Figure 5.3). The precise and efficient modification of DAMP4-derived biosurfactants with maleimide-thiol chemistry is a significant improvement on the variable amine labelling previously employed. Such defined conjugates will enable controlled evaluation of the structure and function of DAMP4-modified interfaces.

DAMP4 facilitates the presentation of a wide range of biomolecules via the spontaneous integration onto an AM1-stabilised interface (Figure 5.3A). To test the interfacial activity of PEG conjugates of the DAMP4 variants, we assessed their ability to impart colloidal stability on AM1-stabilised emulsions. The positive surface charge of individual droplets results in a net repulsion effect that prevents coalescence on the timescale of days. However, dilution of the peptide-stabilised emulsion into a high salt solution negates the positive charge leading to rapid coalescence in the absence of a stabilising modification. The adsorption of PEGylated DAMP4 onto the TNE interface was thus confirmed by comparing them to the AM1 stabilised emulsion in PBS. While AM1-emulsions rapidly coalesce, TNEs stabilised with PEGylated DAMP4 mutants remain stable (Supplementary Table 5.1). PEGylated DAMP4 variants were used at a final surface density of 14 pmol/cm^2, which is well below the capacity for DAMP4 integration (Tayeb et al., 2017). The presentation of each PEGylated DAMP4 variant resulted in a slight increase in the droplet size when compared to AM1-emulsions (Figure 5.3B) attributed to an increased hydrodynamic diameter of TNEs with PEG presented into the aqueous phase (Tayeb et al., 2017). Furthermore, PEG presentation decreased the ζ-potential of TNEs following the integration of each PEGylated DAMP4 variant (Figure 5.3B) due to the effect of PEG shielding surface charge. Interestingly, the drop in ζ-potential was variable even though each protein carries a single PEG. This suggests that the orientation and/or conformation of the PEG is affected by its position, probably due to the orientation of the cysteine insertions within the DAMP4 sequence. For example, brush-like or mushroom-like orientation of PEG can affect the electrophoretic mobility of NPs (Jokerst et al., 2011). Future studies involving PEG orientation and architecture when presented on TNE interfaces are required and are enabled by the specifically modifiable biosurfactants reported herein.

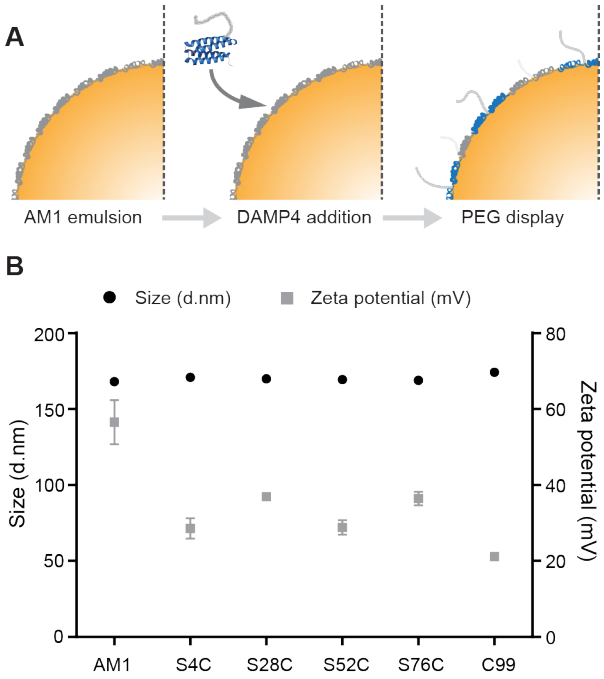

Figure 5.3. Functionalisation of TNEs by PEGylated DAMP4 variants. (A) Schematic representation of the spontaneous integration of DAMP4 onto the surface of an AM1-stabilised Miglyol emulsion. (B) DLS and ζ-potential measurements of the TNEs modified with PEGylated DAMP4 cysteine mutants. TNEs size and ζ-potential measurements are presented as black circles and grey squares respectively and values represent the average of three independent assembly steps.

5.4.4 Stability, interfacial activity and bioconjugation to a double cysteine variant

Devising an emulsion platform with controlled variability in PEG density gives maximum flexibility in interface design and will lead to greater understanding of the interactions between soft matter interfaces and the surrounding environment. Therefore we designed a DAMP4 variant that combines two of the cysteine insertions to enable the comparison of TNE formulations with varied PEG densities. Combining the S28C and S76C mutations created D4C2, with cysteines positioned at one end of the four-helix bundle (Figure 5.1A). We also cloned a variant that combined the S28C and S52C mutations (at opposing ends of the four-helix bundle), but did not pursue this variant due to low level expression and a strong propensity to aggregate, even in the presence of high concentrations of reducing agents.

D4C2 is also predominantly helical although it was shown to have less pronounced 222 nm and 208 nm CD spectroscopy minima compared to DAMP4 (Figure 5.4A). Nevertheless, the helicity is preserved at 90 °C indicating that the double variant maintains high thermal Stability. Despite the small difference in the helical structure of D4C2, the interfacial activity at the oil-water interface is similar to the constituent single mutants and DAMP4 (Figure 5.4B). It is possible that the interaction of hydrophobic side chains aligned on one side of the four helices with the oil phase imposes a constraint on helical conformation, reinforcing the same structural feature that imparts interfacial activity. In any case, the IFT results of D4C2 shows that the slight changes in the level of helicity did not interfere with its spontaneous integration onto an oil-water interface, which also suggests that it could also be used to modify an AM1-stabilised emulsion. SDS-PAGE separation of PEGylation reactions showed that bioconjugation via maleimide-thiol chemistry also efficiently reacts with the thiols of both inserted cysteines of D4C2 (Figure 5.5A). We have previously shown by mass spectrometry that the additional molecular weight of the conjugates conferred by PEG appears to be 2-fold higher than expected on a PAGE gel (Tayeb et al., 2017). Thus, the single and double cysteine mutants are conjugated to 1 and 2 PEGs, respectively. We investigated the size and charge of TNEs stabilised with PEGylated D4C2, S28C and S76C to evaluate the influence of different PEG densities on the interface. Again, the adsorption of each PEGylated variant of S28C, S76C and D4C2 was confirmed by TNE stability in PBS, which showed that while PEGylated D4C2 was able to stabilise TNEs there was a slight increase in hydrodynamic radius (Supplementary Table 5.2). This was mirrored in the size variability among replicate emulsions stabilised by this conjugate (Figure 5.5B). Despite the two-fold increase in PEG at the interface, there are no significant surface charge differences between the TNEs formulated with the single and double PEGylated DAMP4 variants (Figure 5.5B). Together this suggested that interfacial activity of DAMP4 variant could be differentially altered by PEGylation.

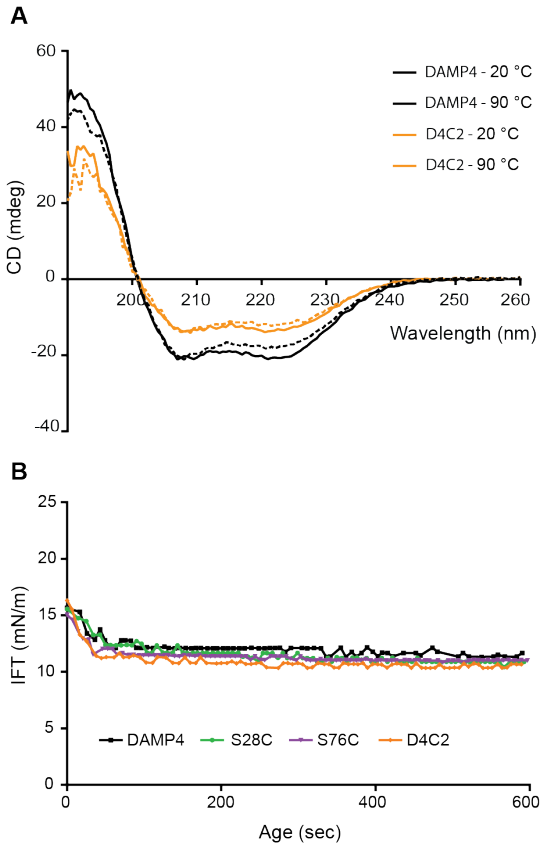

Figure 5.4. Thermal stability and interfacial activity of D4C2, a double cysteine variant of DAMP4. (A) CD spectra of DAMP4 and D4C2 recorded at both 20 °C and 90 °C. (B) Interfacial tension analysis of D4C2 and variants possessing its constituent single mutations compared to DAMP4.

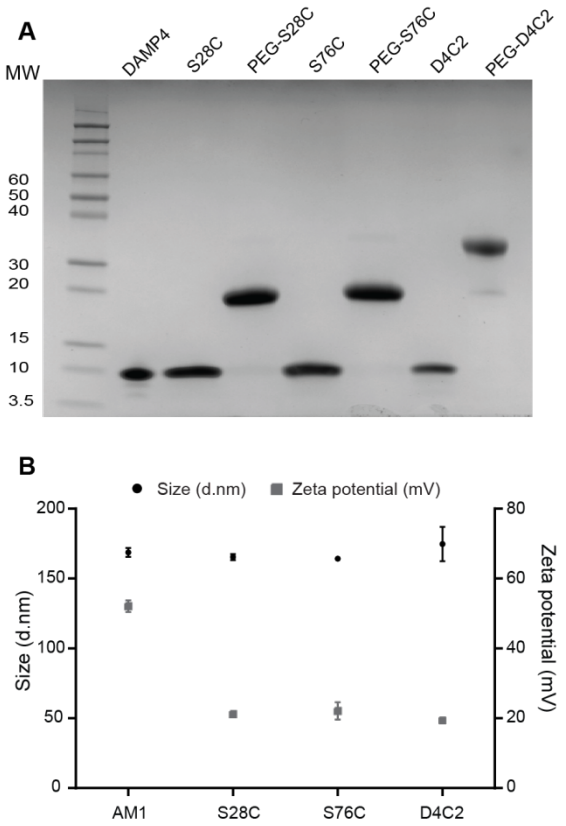

Figure 5.5. PEGylation and TNE functionalisation by D4C2. (A) SDS-PAGE analysis of PEGylated D4C2 and its constituent single mutations. (B) DLS and ζ-potential of TNEs formulated with these variants.

5.4.5 Interfacial activity is affected by both the mass and number of conjugates

Conjugation of the relatively large PEG molecules to DAMP4 is expected to have a significant impact on the kinetic mass transfer and, therefore, adsorption rate of DAMP4. However, how the mass and position of the conjugate impacts steady-state interfacial activity is unknown and highly relevant to the design and deployment of tailored interfaces. Comparing the single (S28C) and double (D4C2) cysteine variants with either 5 kDa (5K) or 10 kDa (10K) conjugated PEG, revealed that not only does the mass of the conjugate impact interfacial activity, so too does the number of conjugates (Figure 5.6). While S28C-5K-PEG reduces IFT from the 31 mN/m of a pristine oil droplet to 15.8 mN/m, S28C-10K-PEG only reduces IFT to 17.2 mN/m. In comparison, the unconjugated protein reduces IFT to 11.1 mN/m. PEGylated D4C2 reduced IFT to 19.3 and 21.9 mN/m when conjugated to 5K and 10K PEG, respectively. This additional insight enables us to refine our previous interpretation using heterogeneous conjugate mixtures (Tayeb et al., 2017), here we show that the mass of the conjugate has a considerable impact on IFT in addition to the number of conjugates. The efficient, site-specific bioconjugation now achievable allows us to compare the D4C2-5K PEG (19.3 mN/m) with S28C-10K-PEG (17.2 mN/m), which possess the same theoretical mass of polymer and show that the number of PEGs has a considerable impact on IFT. These results highlight the utility of the DAMP4 variants and their precise conjugation in enabling the fundamental study of biosurfactants and their interfacial properties. To rule out an effect of PEG on the unfolding of DAMP4, which is necessary for its adsorption onto the interface, we subjected the PEGylated variants to differential scanning calorimetry.

The transition temperature of both S28C and D4C2 were found to be unaffected by the conjugated PEG (Supplementary Figure 5.4), indicating that the polymer has negligible impact on the stability of the proteins and, therefore, its capacity to unfold at the interface. Furthermore, although we have not enumerated the initial rate of the reduction in IFT, the drop is similar for D4C2-5K PEG and S28C-10K-PEG, indicating that as with protein unfolding, transit to the interface is dependent on mass and is not affected by the number of conjugates. To examine the functional impact of the interference with interfacial activity due to PEG conjugation, we assembled TNEs with a low (1.4 pmol/cm^2) density of PEG-DAMP4. Incubation with 0.1 M EDTA disrupts the cohesive interfacial peptide film by chelating the Zn^{2+} that acts to cross-link histidine-bearing AM1 peptides, resulting in susceptibility to coalescence (Tayeb et al., 2017, Malcolm et al., 2009). Using a low density of PEG-DAMP4 variant ensures that TNEs will coalesce within a reasonable timeframe. TNEs decorated with PEGylated S28C remained stable at least for 1 hour (Figure 5.7).

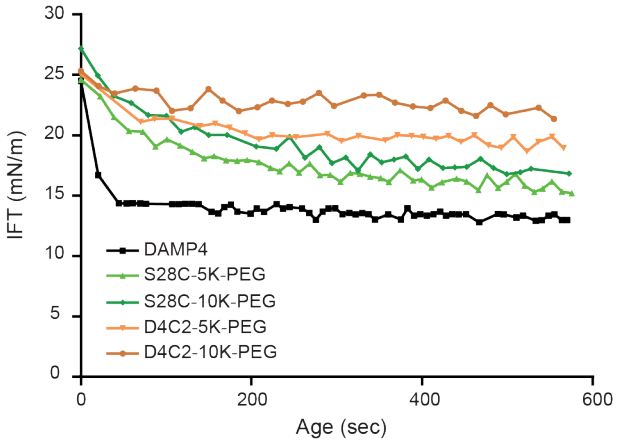

Figure 5.6. Interfacial activity of double and single PEGylated DAMP4. Analysis was performed on D4C2 and the single cysteine variant S28C conjugated to 5K and 10K PEG compared to DAMP4.

In contrast, and despite the two-fold increase in PEG density, phase separation of the PEGylated D4C2 stabilised TNEs was detectable at approximately 2 minutes, similar to the undecorated AM1 emulsion (Figure 5.7). Thus, the differences in the interfacial activity of PEGylated S28C and D4C2 result in a functional impact on their ability to stably decorate TNEs. As the conjugate does not appear to affect the unfolding of DAMP4, these results suggest rather that the PEG conjugate can affect the conformation of DAMP4 at the interface. This has implications on the effect of conjugates on the function of surfactants and, more broadly, the impact that PEGylation potentially has on pharmaceutical protein activity. It could be expected that a greater mass of PEG attached to a single conjugate could compensate for the reduced activity of the double conjugate, however, TNEs modified by S28C-10K-PEG are similarly unstable (data not shown). This leads us to an alternative explanation; that the increase in PEG density presents a steric constraint on the permissible density of DAMP4 at the interface, effectively preventing adsorption. Although we have previously found evidence to suggest the presence of PEG directly at the interface (Tayeb et al., 2017), the low density of DAMP4 used here means that this is unlikely to explain the reduced stabilisation of TNEs by preventing PEG-DAMP4 adsorption. Nor can we rule out the possibility that electrostatic interactions between the AM1 interface and DAMP4 are important for the integration of DAMP4 and that such interactions could be masked by the increased mass of PEG, thereby reducing the adsorption of the more highly PEGylated variant.

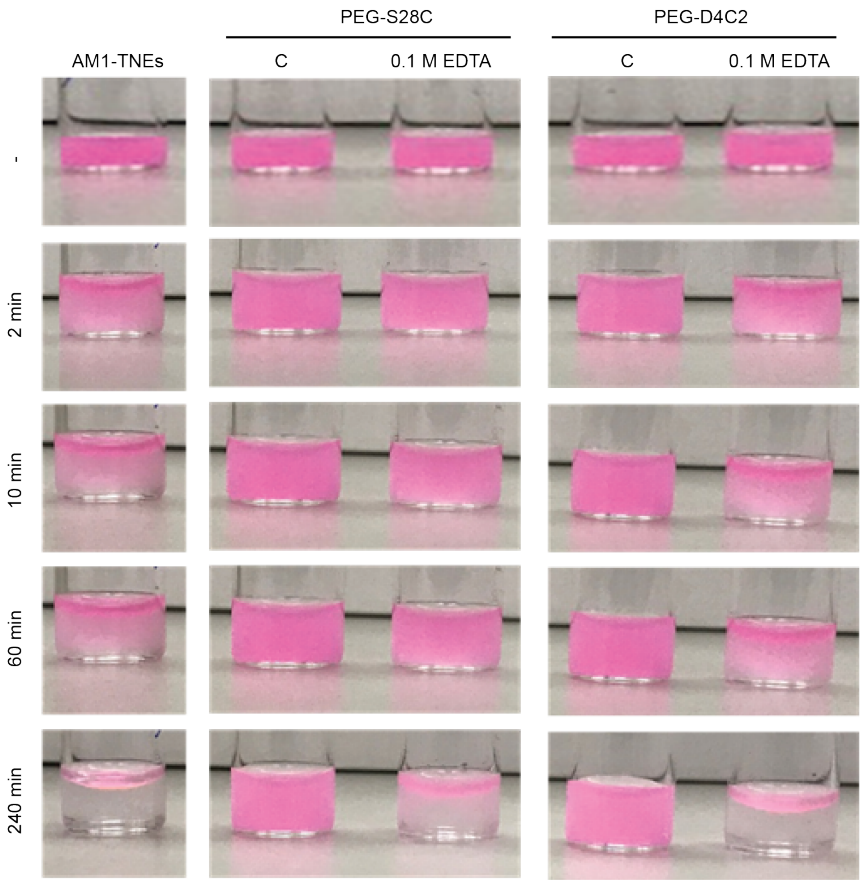

Figure 5.7. Stability of TNEs modified with PEGylated DAMP4 variants in the presence of EDTA. AM1 emulsions labelled with DiI, and those subsequently modified with PEG-S28C and PEG-D4C2 were diluted 1:1 in 25 mM HEPES (pH 7.0) as a control (C) or the same buffer with a final EDTA concentration of 50 mM, and monitored for stability over time.

5.5 Conclusion

Controlling the interfacial properties of nanomaterials is essential for understanding their interactions with the surrounding environment. Here we used a bioengineering approach to obtain biosurfactants amenable to site-specific bioconjugation. Rational design of cysteine mutants of the designer protein surfactant, DAMP4, yielded variants with preserved structure, stability and interfacial activity that could be specifically PEGylated with almost 100% yield. The biologically produced DAMP4 has potential as a renewable surfactant in industrial processes and as a co-surfactant useful in the top-down functionalisation of sophisticated interfaces for high-end applications. The present work demonstrates that the primary sequence can be tailored for specific applications requiring chemical modification and will, for example, allow more precise functionalisation of TNEs than was previously possible. Furthermore, controlled modification of these versatile biosurfactants will provide tools to investigate the fundamental relationship between structure and function of polypeptides at an interface. As an example, we showed that the number of conjugates as well as the mass of a conjugated polymer, PEG, influences interfacial activity, likely via perturbation of secondary structure of the biosurfactant at the interface. We expect that the outcomes of this study will provide the tools to further explore the design of functional interfaces and increase understanding of the relationship between the genetic and chemical modification of polypeptides and their function.

5.6 Acknowledgments

This work was supported by the University of Queensland ECR grant to FS. HHT acknowledges the financial support from the King Abdul-Aziz University, Ministry of Higher education, Saudi Arabia. Elements of this research utilised equipment and support provided by the QLD node of the National Biologics Facility (www.nationalbiologicsfacility.com), an initiative of the Australian Government being conducted as part of the NCRIS National Research Infrastructure for Australia. We also acknowledge the contribution of APAF staff and that the amino acid analysis was facilitated using the infrastructure provided by the Australian Government through the National Collaborative Research Infrastructure Strategy (NCRIS).

5.7 Supplementary materials

Supplementary Figure 5.1

SDS-PAGE analysis of the expression and purification of DAMP4 single cysteine variants. L = soluble fraction of cell lysate, P = purified DAMP4 variant.

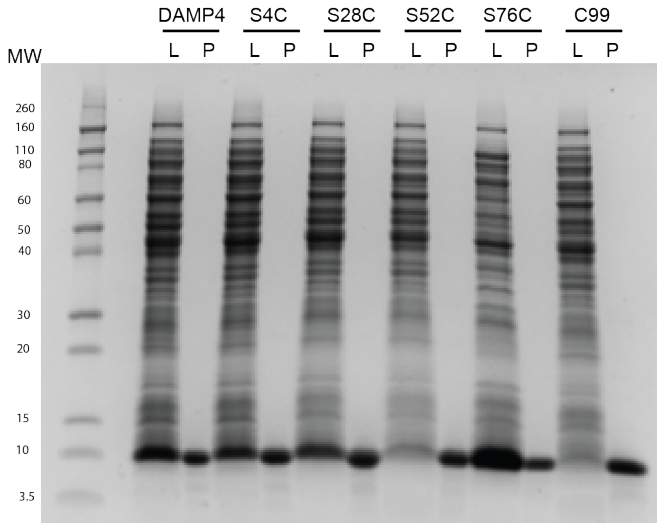

Supplementary Figure 5.2

Structural characterisation of DAMP4 single cysteine variants. CD spectra of DAMP4 variants at 20 °C.

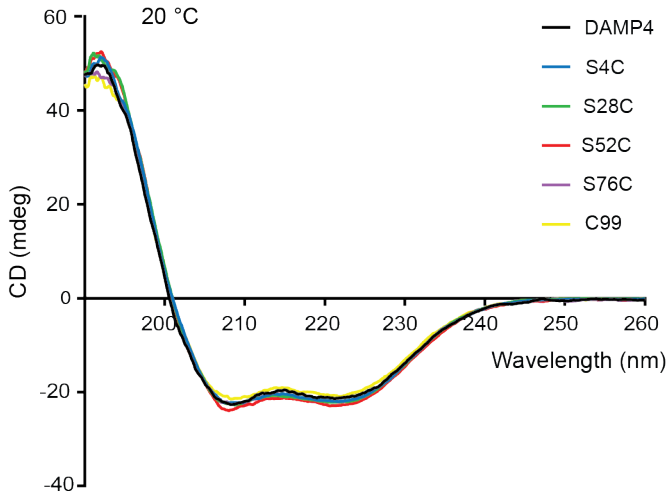

Supplementary Figure 5.3

SDS-PAGE analysis of the PEGylation of DAMP4 single cysteine variants. Each cysteine mutant is shown before and after incubation with and without maleimide-PEG.

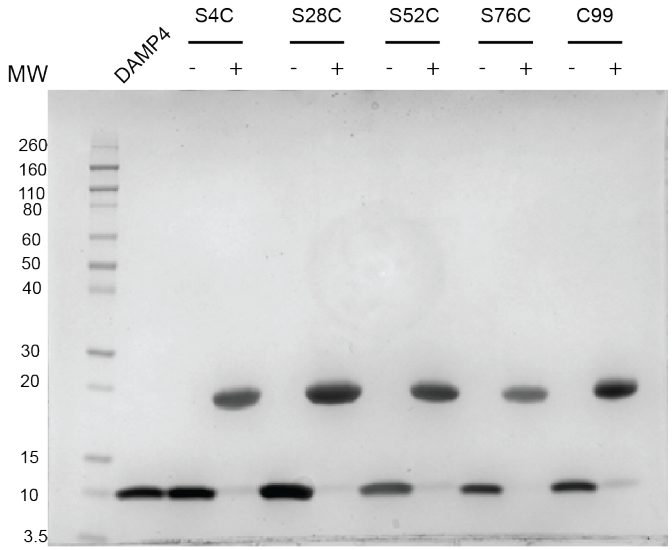

Supplementary Table 5.1. Stability of TNEs formulated with the PEGylated single cysteine variants following dilution in PBS.

TNEs (P50)	Size (d.nm)
AM1	1370.2 ± 1.6
S4C	168.3 ± 4.4
S28C	169.5 ± 4.2
S52C	165.4 ± 0.1
S76C	166.3 ± 2.6
C99	170.4 ± 2.0

Supplementary Table 5.2. Stability of TNEs formulated with the PEGylated single and double cysteine variants following dilution in PBS.

TNEs (P50)	Size (d.nm)
AM1	1299.3 ± 85.4
S28C	163.7 ± 1.1
S76C	165.6 ± 1.8
D4C2	172.5 ± 2.7

Supplementary Figure 5.4

Differential scanning calorimetry of PEGylated DAMP4 variants. The single cysteine variant (S28C) and double cysteine variant (D4C2) were analysed with and without PEGylation.

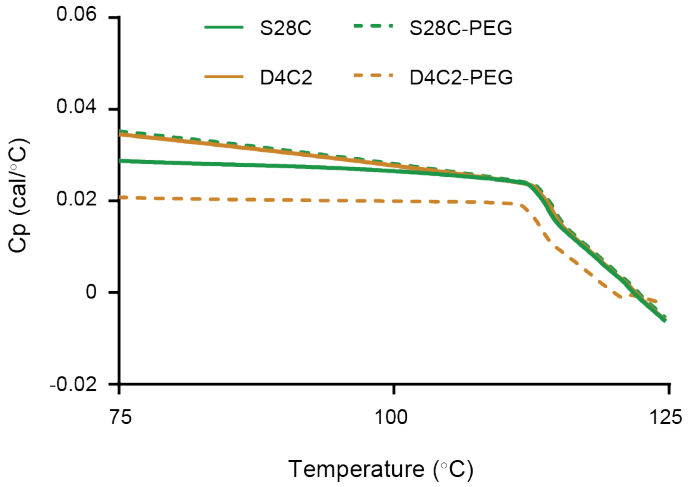

6 Chapter 6: Conclusion and Future Directions

Nanoparticle-mediated drug delivery involves the development of nanosized materials loaded with pharmaceutical compounds for specific therapeutic and diagnostic applications. Although nanomaterials are considered promising, they must overcome a series of complex physical and biological barriers encountered through different routes of administration. These barriers lead to instability during circulation, non-specific biodistribution, and cytotoxicity to healthy cells (Xin et al., 2017).

Recent studies involving mice report that less than 1% of injected NPs reach their target site (Wilhelm et al., 2016) clearly showing how active targeting of NPs is still unrealistic in living organisms. Therefore, a deeper understanding of the biophysical properties of a particular NP design, including the size, surface charge, and presentation of functional moieties, is required. The biological complexity encountered in delivery routes and the type and stage of disease are other aspects that must be considered in the design of NPs to enhance the effectiveness of nanomaterials in drug delivery. Exploring the potential of a particular drug delivery design through different applications or routes of administration can help reveal possible limitations. By addressing these limitations, the clinical translation of nanomaterials can be more realistic.

Despite all the challenges facing nanomaterials in drug delivery, there are few nanomaterials that have gained approval for clinical use against diseases such as cancer. For example, the liposomal formulation, Doxil®, was approved by the FDA for the treatment of Kaposi's sarcoma (Barenholz, 2012b). Lipid-based nanomaterials, including liposomes (Bulbake et al., 2017) and NEs (Singh et al., 2017), are considered promising vehicles for hydrophobic drugs. Emulsions offer a broad range of advantages including high solubilisation and loading capabilities, biocompatibility and ease of production, and have been applied with safe profiles in cosmetic, nutritional (Intralipid®) and pharmaceutical applications (Liple®).

The aim of my research project was to refine the use of TNEs toward pharmaceutical applications. TNEs were invented recently by the Middelberg group at the AIBN and have shown promising results in the targeted, subcutaneous delivery of antigens (Zeng et al., 2013). TNEs are easily formulated by the assembly of protein-based surfactants at the oil-water interface in a bottom-up fashion via the top-down sequential addition of reagents. The TNE core is made from a pharmaceutical-grade oil (Miglyol 812) that is generally recognised as safe (GRAS) and approved by the FDA.

In this project, the properties of TNEs were investigated as well as their administration through topical (skin) and IV routes. Specifically, PEGylation was used to alter the surface design of the TNEs and

determine the effect of PEG density on the interfacial properties furthering the refining of TNEs for drug delivery. PEGylation is a common technique that improves the stability and pharmacodynamics of drugs and is one of the most important aspects in drug delivery research. Controlling the surface charge of TNEs via PEG density enabled the successful coating of EMPs through electrostatic interactions. The combined system showed promising results as a carrier of hydrophobic drugs for human skin applications. IV administration of TNEs was also explored showing an acceptable safety profile, however circulation time was short and showed that the TNEs were mostly cleared via the renal route.

The research outcomes from my PhD project were divided into three chapters. The aim of the first experimental chapter (Chapter 3) was to broadly explore the use of TNEs as a vehicle of hydrophobic drugs for topical and IV administration. Exploring the use of TNEs via the IV route provided the basis of the second experimental chapter (Chapter 4) that delivered insights into the interfacial structure-function of poly(ethylene glycol)-decorated peptide-stabilised nanoscale emulsions. With a deeper understanding of the TNE interface provided by Chapter 4, the final experimental chapter (Chapter 5) aimed at gaining better control over the TNE interface through genetic engineering of DAMP4 for precise bioconjugation whilst maintaining interfacial activities. A summary of the key findings from each chapter will be discussed in the following sections.

6.1 Exploring the suitability of TNEs in diagnostic and therapeutic applications by employing different routes of administration.

Nanomaterials are being continuously developed into drug delivery systems with various surface designs to improve the therapeutic efficacy of lipophilic drugs. However, there are still no specific guidelines that help facilitate the fabrication of NP designs capable of overcoming most drug delivery challenges. These challenges include the biological barriers encountered within each route of administration, as well as the complexity of NPs designs. Subsequently, the feasibility of TNEs in diagnostic and therapeutic applications was considered through both topical and IV delivery routes. Firstly, by varying the PEG-DAMP4 density on the TNE interface, the surface properties of TNEs could be explored revealing that surface charge was inversely proportional to the integrated PEG density on the TNE interface.

To investigate the capacity of cargo retention, a hydrophobic dye was encapsulated within the oil phase of TNEs showing that over time the amount of retained dye was directly related to the DAMP4-PEG density. A leakage profile of the encapsulated cargo also revealed that PEG density was directly related to the stability of DiI-labelled TNE droplets over time. By tuning the surface charge, TNEs were combined with EMPs via electrostatic interactions and showed promising human skin

applications. The coating efficiency of EMPs with TNEs was investigated through different methods with results suggesting that freeze drying of DiI-loaded P20-TNEs (positively-charged) droplets onto powdered EMPs (negatively-charged), in the presence of alginate as a cross-linker, gave better coating results. Having control over the surface charge by simply varying PEG densities is attributed to the remarkable and inherent spontaneous integration capability of DAMP4 at the interface of AM1-pre-stabilised TNEs. These results suggest that TNEs have great potential in topical (skin) drug delivery applications.

The delivery of hydrophobic drugs using active targeting via the IV route is a major obstacle for nanomaterials. TNEs were successfully functionalised with DAMP4-scFv fusion for targeting EGFR on cancer cells. The fusion complex alone had high binding specificity to EGFR (which was validated through ELISA). DAMP4-scFv fusion was also successfully presented on the TNE interface, resulting in a VECT-1 formulation that showed high binding specificity to EGFR-coated wells in a fluorescence-based plate assay. Binding to EGFR using VECT-1 formulations was also demonstrated *in vitro* using the breast cancer cell line, MDA-MB-468. However to some extent, non-specific binding was observed and may have been due to increased targeting complexity going from proteins bound to a plate, to surface proteins in a more diverse cellular environment.

The potential of administering targeted TNE (VECT-1) formulations through the IV route was explored using an *in vivo* pilot study. This study showed that TNEs were mainly execrated via the renal route suggesting that TNEs only have a short circulation time that was insufficient to achieve active targeting. The rapid clearance of TNEs was then explored in more detail using a biodistribution study that involved serum, urine, and cytokines analyses. These analyses suggested that TNEs remained in circulation for at least two hours with renal excretion starting one-hour post-IV injection. TNEs were also detected in the liver two hours post-injection but at very low levels implying that the hepatic path was not the main clearance pathway. The very low cytokine levels, as well as their biocompatible design, suggested that TNEs did not cause adverse reactions and showed a safe profile during IV administration. However, given the instability of TNEs during circulation that might have been due to opsonisation or phagocytosis, it's obvious that a deeper understanding of the TNE interface is required for optimising the surface design for drug delivery.

6.2 Insight into the interfacial structure-function of the polyethylene glycol-decorated peptide-stabilised nanocarrier emulsions

Interfacial properties of nanocarriers directly influence the biodistribution, stability and efficiency of nanomaterials in drug delivery. Chapter 4 aimed to understand the interfacial structure of TNEs and gain insights into the molecular interfacial assembly of a poly ethylene-decorated protein

biosurfactant (DAMP4). The surface modification of TNEs was facilitated by the remarkable spontaneous integration feature of DAMP4 onto the pre-adsorbed AM1 oil-water interface. Genetic fusion or chemical modification of DAMP4 with functional molecules facilitates their presentation on the aqueous phase of TNEs. TNEs formulated in a sequential step-wise fashion have tuneable surface properties that offer great potential to gain control over the oil-water interface. DAMP4 PEGylation using different PEG lengths was characterised in detail and the sequential addition of functionalised DAMP4 molecules at the oil-water interface was confirmed. The influence of varying PEG density and length on TNE size, surface charge, and interfacial properties was evaluated by determining the accessibility of co-displayed targeting molecules.

For multifunctional nanomaterials, the complexity of the surrounding environment is compounded by the impact of functional molecules on one another, defining a competition-trade off window in molecular design space. As a unique model system, TNEs allow controlled assembly and were used to probe the structure-function relationship of the interface designed with the competing effects of two functional biomolecules: PEG and a targeting ligand. In this research, the building units of TNEs were analysed in detail along with verification of the assembly mechanism and determination of the molecular characteristics of the TNE aqueous phase. Regardless of the predicted differences in interfacial thicknesses with respect to the PEG layer, that were demonstrated using x-ray reflectometry, the solid state binding assay indicated that the targeting moieties presented on TNEs surfaces were equally accessible to their receptors. In contrast, the difference in PEG layer proved to have an essential role in minimising non-specific targeting. These findings validated the concept of designing multifunctional TNE interfaces. The next chapter continued to explore TNE assembly and presentation capacity of biomolecules at the interface. The use of a homogeneous population of DAMP4 conjugates should give better control over interfacial properties. Controlled functionalisation of the TNE interfaces using the protein biosurfactant, DAMP4, is discussed in the next section.

6.3 Site-specific bioconjugation with poly(ethylene glycol): impact on the interfacial activity of a protein biosurfactant

Controlling the interfacial properties of nanomaterials is vital for understanding their interactions with surrounding environments. Biosurfactants are amphiphilic surface active molecules that can be synthesised using industrially scalable, renewable biological processes. Biosurfactants also offer several advantages including biocompatibility, biodegradability, and sustainability. A novel designer protein biosurfactant, DAMP4, allows surface modifications through genetic engineering or chemical conjugation to functional molecules. However, inconsistent and unpredictable chemical conjugation

results in heterogeneous products that restrict precise functionalisation and the resolution of physio-chemical characterisation of interfaces.

In this research, we successfully bioengineered DAMP4 variants with single/double cysteine point mutations to obtain biosurfactants capable of site-specific bioconjugation. Rational point mutations of the designer protein surfactant, DAMP4, with cysteine residues produced variants with conserved structure and stability, and surface activity that can specifically conjugate to PEG with nearly 100% yield. Bio-synthesised DAMP4 holds great potential as a renewable biosurfactant in industrial applications, and as a valuable co-surfactant in the top-down modifications of interfaces for sophisticated applications. This work demonstrated that the primary sequence of DAMP4 could be tailored toward specific applications that require chemical modifications. For example, it allowed precise functionalisation of the TNE interface.

Controlled functionalisation of DAMP4 provided means to study the fundamentals of the structure-function relationship of polypeptides at the interface. For example, the number, as well as the mass of PEG conjugates, were found to influence the interfacial activity of the biosurfactant probably because the secondary structure at the interface was perturbed. Therefore, the capability of DAMP4 variants with multiple PEG conjugates to impart colloidal stability on peptide-stabilised emulsions decreased. This observation was made based on the possible constraints on the amphiphilic helices of DAMP4 at the interface that resulted from the attachment of multiple PEG conjugates.

Specific and efficient chemical modifications enable investigation of the interfacial properties of designer protein biosurfactants with molecular precision. The outcomes of this work are expected to contribute to further exploring the design of functional interfaces, and help understand more about the relationship between the genetic and chemical modifications of protein biosurfactants and their function. This research may help to inform the design and modification of biosurfactants for increasing their applications in industrial processes, and nutritional and pharmaceutical formulations.

6.4 Future directions

It is well known that the administration of APIs via different routes has various effects on therapeutic efficacy. Administered API can be affected by the harsh conditions encountered within biological systems including enzymatic secretions and pH changes. To help overcome the challenges of administered API, in particular hydrophobic compounds, nanomaterials like polymer-based NPs (Chan et al., 2010, Crucho and Barros, 2017), inorganic materials-based platforms (Giner-Casares et al., 2016, Ojea-Jimenez et al., 2013), and lipid-based NPs (Qi et al., 2017) have emerged as delivery vehicles to improve therapeutic outcomes.

These vehicles have improved the overall pharmacokinetics of drugs such as water-solubility and extended circulation times. However, these improvements, that fall under the umbrella of patient safety and lower morbidity rate, and have led to the successful clinical translation of nanomaterials like Doxil®, are still considered minimal. The main reason being that once nanomaterials are administered through different routes, they face complex environments involving various physical and biological barriers that limit their therapeutic efficacy. This evidence therefore suggests that the "magic bullet" hype surrounding nanomaterials remains unrealistic to date and that far more knowledge of the fundamentals of nanomaterial interfaces and how they relate to specific biological applications is still required.

Tailoring the surface properties of drug carriers is an important aspect of drug delivery and helps to contribute fundamental knowledge of the interface and possible solutions for overcoming the complexity of biological systems. One of the main obstacles that limits the study of, and precise control over, the surface design of nanomaterials is ensuring physical stability that limits the ability to functionalise surfaces with biomolecules. TNEs are O/W peptide-stabilised emulsions that are easily formulated, biodegradable and allow the decoupling of physical stability imparted during emulsification from subsequent functionalisation (Sainsbury et al., 2014).

AM1, a surface active peptide with rapid adsorption rate, is used to stabilise O/W droplets during emulsification (Dexter et al., 2006). AM1 also provides mechanical stability at the oil-water interface in the presence of metal ions via histidine residues (Malcolm et al., 2009). DAMP4, a protein biosurfactant, is made of four repeats of AM1 joined by linkers that permit folding in solution. DAMP4 spontaneously unfolds and integrates at the pre-adsorbed AM1 oil-water interface, allowing surface functionalisation via either genetic fusion or chemical conjugation. These remarkable features of the surface-active designer molecules (AM1 and DAMP4) provide TNEs with amenability to step-wise surface modification, independent of droplet formation.

Decoupling the biological functionalisation of TNEs from the emulsification process enabled PEG density to be varied at the TNE interface. This allowed the surface properties of TNEs to be controlled, which directly affected the stability of DiI-labelled TNEs and, concomitantly, cargo retention within the oil core. Other factors that may influence cargo retention include the solubility level of drugs within the oil phase. Controlling the surface properties of TNEs played an important role in coating EMPs with TNEs via electrostatic interactions. The TNE-coated EMPs that encapsulated a clinically relevant imaging agent, were explored in human skin applications. Future research could be aimed at investigating therapeutic applications of TNE-coated EMPs. For example, encapsulating therapeutic agents such as antifungal drugs targeted to specific skin layers for the treatment of fungal infections.

TNEs were successfully directed toward *in vitro* active targeting using the scFv-DAMP4 fusion that was synthesised by genetic engineering, however the accessibility of the scFv-DAMP4 fusion was affected by the display of PEG. Therefore, future studies are needed to investigate the accessibility of presented functional moieties on the TNE interface. The precise and site-specific bioconjugation of PEG to DAMP4 variants, such as S28C, allows greater control of bioconjugation to the protein biosurfactant. This should enable characterisation of the accessibility of functional moieties displayed at the TNE oil-water interface with greater precision. Improved accessibility might be achieved in the future through one of the following proposals:

1- Chemical modifications of the biosurfactant: the presentation of functional moieties using bifunctional PEG molecules where the targeting molecule is conjugated to the opposite end of PEG (e.g. via an NHS ester), and displayed on the TNE interface using a DAMP4 cysteine variant that can be conjugated to PEG using maleimide chemistry (Figure 6.1A).
    a. Advantages:
        i. It should eliminate the masking of functional molecules by the PEG, leading to better accessibility.
    b. Disadvantages:
        i. The need for extra purification steps to remove unconjugated bi-functional PEG molecules from DAMP4.
        ii. The interfacial activity of the biosurfactant might be affected.
2- Optimising the genetic fusion of the scFv to DAMP4 variants by increasing the linker length. The previously synthesised scFv-DAMP4 fusion has a single G4S linker and it may help to extend this with more copies (Figure 6.1B).
    a. Advantages:

i. Increasing the linker length might lead to better accessibility of the presented functional moiety by reducing the interference of presented PEG on the interface.

b. Disadvantages:

i. Folding and stability of the protein fusion might be affected.

ii. Changing the linker length might introduce challenges for the production of the fusion protein within mammalian cells.

iii. The additional flexibility may prove to be a disadvantage during sequential addition if it allows interaction of the targeting moiety with the interface.

3- Studying the interfacial properties of TNEs with shorter PEG length. Previously applied PEG masses on TNEs were 5 kDa and 10 kDa, whereas 2 kDa or 3.4 kDa PEG may be sufficient to impart stability (Figure 6.1C).

a. Advantages:

i. Less interference with other presented functional molecules.

ii. Possibly better interfacial activity when compared to DAMP4 variants conjugated to PEG with larger mass.

b. Disadvantages:

i. Possible increase in non-specific interactions with the surrounding environment due to changes in the surface properties, such as surface charge.

ii. Shorter PEG lengths might not impart sufficient colloidal stability to prevent coalescence or aggregation.

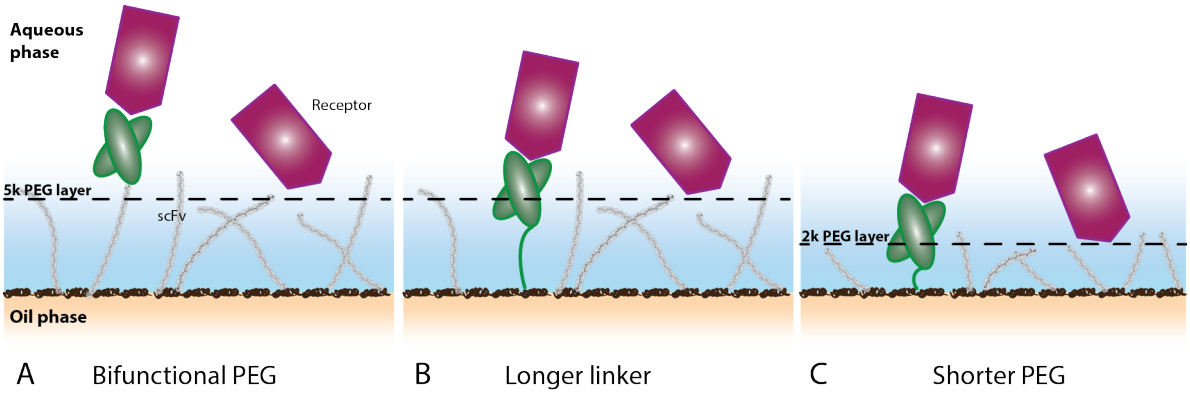

Figure 6.1. Accessibility of functional moieties displayed at the TNE interface. (A) Presentation of functional moiety with bifunctional PEG. (B) Illustrates the display of the functional moiety (scFv) genetically fused to DAMP4 by increasing the linker length. (C) Presentation of functional moieties fused to DAMP4 at the interface of TNEs functionalised with shorter PEG length.

The combined outcomes from this research show that TNEs have great potential in topical formulations for human skin applications. TNEs are also considered safe IV formulations for further biodistribution studies. Specific and non-specific TNE interactions are directly affected by their surface decoration. Site-specific bioconjugation of a biocompatible, renewable, and industrially-scalable protein biosurfactant, DAMP4, was obtained and permitted the investigation and tailoring of the TNE interface for specific applications with precision. The remarkable characteristics of these designer protein surfactants make TNE interfaces amenable to a wide range of genetic or chemical modifications ensuring that TNEs have a promising future in drug delivery. Based on the combined outcomes of my PhD project, further physiochemical and biophysical studies would contribute to better understanding of the TNE system and, potential of biosurfactants.

Physical chemistry, employs techniques to study and monitor the behaviour of a particular matter on a molecular and atomic level. Therefore, to reach this level of detail a precise understanding of a particular material or system is required. The Controlled site-specific bioconjugation of DAMP4 variants should facilitate precise fundamental interface studies. These include X-ray reflectometry to study interfacial thickness, which may help to elucidate the interaction of TNE surface design with the surrounding environment. Also, neutron reflectometry can be applied to determine the precise composition at the interface, the density of DAMP4 integration and whether DAMP4 integration results in AM1 displacement. Quartz crystal microbalance (QCM) can be used to monitor mass changes at the interface, which can provide insights into the molecular assembly of surfactants at air-fluid or fluid-fluid interfaces. These studies are currently ongoing in collaboration with colleagues at ANSTO and Monash University.

Harnessing the metal-binding properties of surface designer surfactants is another important property for the formulation of NEs with PET/MRI imaging agents. Based on the formation of a cohesive interfacial network via the coordination of metal ions, the possibility of incorporating additional functionality using the radioisotope, Cu^{64}, was investigated (data not shown). Perfluorocarbon emulsions are commonly applied as MRI agents but do not easily permit further surface modifications in a controlled way. Comparatively, TNEs enable spontaneous integration of a wide range of biomolecules in a step-wise fashion via DAMP4, that allows further surface modifications with functional moieties, such as PEG, to improve formulation stability and performance within a living organism. AM1 stabilises O/W droplets during emulsification and enables the incorporation of positron emitting isotopes (Cu^{64}) at the interface via the metal-binding residues (histidine). Employing the oil core of AM1-stabilised TNEs by incorporating MRI agents (perfluorocarbons), can potentially direct TNEs toward promising bimodal imaging applications. The idea of this work was aimed at paving the way for further applications of TNEs as bimodal imaging agents administered

through different routes. This research was conducted in collaboration with the research group of Professor Andrew Whittaker at the AIBN and the Centre of Advanced Imaging (CAI).

The potential of TNEs in both localised and systemic delivery can be explored by investigating alternative administration routes in the future. The local administration of hydrophobic drugs using emulsions offers strategies that can help avoiding biological and physical barriers by modulating their surface properties. For example, tailoring surface charge can permit penetration of biological membranes via electrostatic interactions in ocular or topical applications. The administration of nanomaterials via alternative routes for systemic delivery also offers various advantages including self-administration, being non-invasive (Sun et al., 2017), exploitation of high absorption surface areas such as the lung, and avoidance of first path-metabolism and enzymatic degradation (Mathias and Sridharan, 2017).

6.5 Concluding remarks

NEs have a safe history in food, cosmetic, and pharmaceutical applications. However, NE surface functionalisation is limited by the stabilisation process that takes place during emulsification. In this project, the use of novel TNEs was explored in both topical and IV delivery routes that allowed decoupling of physical stabilisation and functionalisation. TNEs showed promise as a platform for carrying hydrophobic drugs combined with the EMPs, that helped to overcome the physical barrier of skin. In contrast, the IV delivery of TNEs resulted in a short circulation time but an acceptable safety profile. These findings highlight the need for further research into the interfacial properties of TNEs to better understand molecular assembly. The spontaneous integration of DAMP4, that can be easily functionalised via genetic engineering or chemical modifications, at the interface enabled PEG in different masses and densities to coat the interface. These experiments revealed important information about the assembly and stability of TNEs, as well as the accessibility of targeting moieties.

Variants of DAMP4 were genetically engineered using rational design that allowed site-specific bioconjugation of a wide range of molecules with almost 100% yield of DAMP4-PEG products. This allowed a controlled number of biomolecules to be displayed on the TNE interface and showed how the interfacial activities of biosurfactants can be affected by the number and mass of their conjugates. Further investigations into how interfacial properties of TNEs relate to the different biological environments encountered in various routes of administration, are required to advance the use of TNEs in future drug delivery systems.

The potential of NPs in targeted drug delivery is yet to be realised, subsequently clinical translation of drug carrier candidates requires further research to better understand the surface design of nanomaterials, the physiology of different diseases, the biological complexity associated with each route of administration as well as the safety and biocompatibility of nanomaterials. Keeping the design of nanomaterial surfaces simple can improve the understanding of nanomaterial interactions with surrounding environments, and by addressing all of the considerations discussed above, better functional, affordable, safe, and biocompatible drug delivery candidates will be synthesised.

6.6 List of References

AALDERING, L. J., TAYEB, H., KRISHNAN, S., FLETCHER, S., WILTON, S. D. & VEEDU, R. N. 2015. Smart functional nucleic acid chimeras: enabling tissue specific RNA targeting therapy. *RNA Biol,* 12**,** 412-425.

ABDOU, E. M., KANDIL, S. M. & MINIAWY, H. 2017. Brain targeting efficiency of antimigrain drug loaded mucoadhesive intranasal nanoemulsion. *Int J Pharm,* 529**,** 667-677.

AHMAD, N., RAMSCH, R., LLINÀS, M., SOLANS, C., HASHIM, R. & TAJUDDIN, H. A. 2014a. Influence of nonionic branched-chain alkyl glycosides on a model nano-emulsion for drug delivery systems. *Colloid Surface B,* 115**,** 267-274.

AHMAD, Z., SHAH, A., SIDDIQ, M. & KRAATZ, H.-B. 2014b. Polymeric micelles as drug delivery vehicles. *RSC Adv,* 4**,** 17028-17038.

AHMAD, Z. A., YEAP, S. K., ALI, A. M., HO, W. Y., ALITHEEN, N. B. & HAMID, M. 2012. scFv antibody: principles and clinical application. *Clin Dev Immunol,* 2012**,** 980250.

ALLEN, T. M. & MARTIN, F. J. 2004. Advantages of liposomal delivery systems for anthracyclines. *Semin Oncol,* 31**,** 5-15.

ALLISON, A. C. 1999. Squalene and squalane emulsions as adjuvants. *Methods,* 19**,** 87-93.

ALLISON, A. C. & BYARS, N. E. 1986. An adjuvant formulation that selectively elicits the formation of antibodies of protective isotypes and of cell-mediated immunity. *J Immunol Methods,* 95**,** 157-168.

AMANI, A., YORK, P., CHRYSTYN, H. & CLARK, B. J. 2010. Evaluation of a nanoemulsion-based formulation for respiratory delivery of budesonide by nebulizers. *Aaps Pharmscitech,* 11**,** 1147-1151.

AMES, P. & GALOR, A. 2015. Cyclosporine ophthalmic emulsions for the treatment of dry eye: a review of the clinical evidence. *Clinical investigation,* 5**,** 267-285.

ANDERSON, B. 2005. *ESF scientific forward look on nanomedicine* [Online]. European Science Foundation. Available: http://archives.esf.org/fileadmin/Public_documents/Publications/Nanomedicine_01.pdf [Accessed 29 January 2018].

ANSELL, S. M., HARASYM, T. O., TARDI, P. G., BUCHKOWSKY, S. S., BALLY, M. B. & CULLIS, P. R. 2000. Antibody conjugation methods for active targeting of liposomes. *Methods Mol Med,* 25**,** 51-68.

AQIL, M., KAMRAN, M., AHAD, A. & IMAM, S. S. 2016. Development of clove oil based nanoemulsion of olmesartan for transdermal delivery: Box–Behnken design optimization and pharmacokinetic evaluation. *J Mol Liq,* 214**,** 238-248.

ARAÚJO, F. A., KELMANN, R. G., ARAÚJO, B. V., FINATTO, R. B., TEIXEIRA, H. F. & KOESTER, L. S. 2011. Development and characterization of parenteral nanoemulsions containing thalidomide. *Eur J Pharm Sci,* 42**,** 238-245.

ARGYO, C., WEISS, V., BRÄUCHLE, C. & BEIN, T. 2014. Multifunctional Mesoporous Silica Nanoparticles as a Universal Platform for Drug Delivery. *Chem Mater,* 26**,** 435-451.

AUCOUTURIER, J., DUPUIS, L., DEVILLE, S., ASCARATEIL, S. & GANNE, V. 2002. Montanide ISA 720 and 51: a new generation of water in oil emulsions as adjuvants for human vaccines. *Expert Rev Vaccines,* 1**,** 111-8.

AZARMI, S., ROA, W. H. & LOBENBERG, R. 2008. Targeted delivery of nanoparticles for the treatment of lung diseases. *Adv Drug Deliv Rev,* 60**,** 863-75.

AZEEM, A., RIZWAN, M., AHMAD, F. J., IQBAL, Z., KHAR, R. K., AQIL, M. & TALEGAONKAR, S. 2009. Nanoemulsion Components Screening and Selection: a Technical Note. *AAPS PharmSciTech,* 10**,** 69-76.

BADER, A. N., HOETZL, S., HOFMAN, E. G., VOORTMAN, J., VAN BERGEN EN HENEGOUWEN, P. M., VAN MEER, G. & GERRITSEN, H. C. 2011. Homo-FRET imaging as a tool to quantify protein and lipid clustering. *Chemphyschem,* 12**,** 475-83.

BALDRIDGE, J. R. & CRANE, R. T. 1999. Monophosphoryl lipid A (MPL) formulations for the next generation of vaccines. *Methods,* 19**,** 103-7.

BALDRIDGE, J. R. & WARD, J. R. 1997. Effective adjuvants for the induction of antigen-specific delayed-type hypersensitivity. *Vaccine,* 15**,** 395-401.

BALDUCCI, A., WEN, Y., ZHANG, Y., HELFER, B. M., HITCHENS, T. K., MENG, W. S., WESA, A. K. & JANJIC, J. M. 2013. A novel probe for the non-invasive detection of tumor-associated inflammation. *OncoImmunology,* 2**,** e23034.

BARENHOLZ, Y. 2012a. Doxil(R)--the first FDA-approved nano-drug: lessons learned. *J Control Release,* 160**,** 117-34.

BARENHOLZ, Y. 2012b. Doxil® — The first FDA-approved nano-drug: Lessons learned. *J Control Release,* 160**,** 117-134.

BARRY, B. W. 2004. Breaching the skin's barrier to drugs. *Nat Biotechnol,* 22**,** 165-7.

BEAUCHESNE, P. R., CHUNG, N. S. & WASAN, K. M. 2007. Cyclosporine A: a review of current oral and intravenous delivery systems. *Drug Dev Ind Pharm,* 33**,** 211-20.

BEIJA, M., SALVAYRE, R., LAUTH-DE VIGUERIE, N. & MARTY, J.-D. 2012. Colloidal systems for drug delivery: from design to therapy. *Trends Biotechnol,* 30**,** 485-496.

BENÍŠEK, Z., SÜLI, J., ELIÁŠ, D., LENHARDT, L. U. T., ONDREJKOVÁ, A., ONDREJKA, R., ŠVRČEK, Š. & BAJOVÁ, V. 2004. Experimental squalene adjuvant: II. Harmlessness and local reactogenity. *Vaccine,* 22**,** 3470-3474.

BIVAS-BENITA, M., OUDSHOORN, M., ROMEIJN, S., VAN MEIJGAARDEN, K., KOERTEN, H., VAN DER MEULEN, H., LAMBERT, G., OTTENHOFF, T., BENITA, S., JUNGINGER, H. & BORCHARD, G. 2004. Cationic submicron emulsions for pulmonary DNA immunization. *J Control Release,* 100**,** 145-55.

BLANCO, E., SHEN, H. & FERRARI, M. 2015. Principles of nanoparticle design for overcoming biological barriers to drug delivery. *Nat Biotechnol,* 33**,** 941.

BOBO, D., ROBINSON, K. J., ISLAM, J., THURECHT, K. J. & CORRIE, S. R. 2016. Nanoparticle-based medicines: a review of FDA-approved materials and clinical trials to date. *Pharm Res,* 33**,** 2373-2387.

BOCHE, M. & POKHARKAR, V. 2017. Quetiapine Nanoemulsion for Intranasal Drug Delivery: Evaluation of Brain-Targeting Efficiency. *AAPS PharmSciTech,* 18**,** 686-696.

BORHADE, V., PATHAK, S., SHARMA, S. & PATRAVALE, V. 2012. Clotrimazole nanoemulsion for malaria chemotherapy. Part I: Preformulation studies, formulation design and physicochemical evaluation. *Int J Pharm,* 431**,** 138-148.

BORTHAKUR, P., BORUAH, P. K., SHARMA, B. & DAS, M. R. 2016. 5 - Nanoemulsion: preparation and its application in food industry A2 - Grumezescu, Alexandru Mihai. *Emulsions.* Academic Press.

BOZZUTO, G. & MOLINARI, A. 2015. Liposomes as nanomedical devices. *Int J Nanomed,* 10**,** 975-999.

BRAJTBURG, J., POWDERLY, W. G., KOBAYASHI, G. S. & MEDOFF, G. 1990. Amphotericin B: current understanding of mechanisms of action. *Antimicrobe Agents Chemother,* 34**,** 183-188.

BROKX, R. D., BISLAND, S. K. & GARIEPY, J. 2002. Designing peptide-based scaffolds as drug delivery vehicles. *J Control Release,* 78**,** 115-23.

BULBAKE, U., DOPPALAPUDI, S., KOMMINENI, N. & KHAN, W. 2017. Liposomal Formulations in Clinical Use: An Updated Review. *Pharmaceutics,* 9.

CARON, W. P., LAY, J. C., FONG, A. M., LA-BECK, N. M., KUMAR, P., NEWMAN, S. E., ZHOU, H., MONACO, J. H., CLARKE-PEARSON, D. L., BREWSTER, W. R., VAN LE, L., BAE-JUMP, V. L., GEHRIG, P. A. & ZAMBONI, W. C. 2013. Translational studies of phenotypic probes for the mononuclear phagocyte system and liposomal pharmacology. *J Pharmacol Exp Ther,* 347**,** 599-606.

CHAN, J. M., VALENCIA, P. M., ZHANG, L., LANGER, R. & FAROKHZAD, O. C. 2010. Polymeric nanoparticles for drug delivery. *Methods Mol Biol,* 624**,** 163-75.

CHANANA, M., RIVERA GIL, P., CORREA-DUARTE, M. A., LIZ-MARZAN, L. M. & PARAK, W. J. 2013. Physicochemical properties of protein-coated gold nanoparticles in biological fluids and cells before and after proteolytic digestion. *Angew Chem Int Ed Engl,* 52**,** 4179-83.

CHEN, H., KIM, S., LI, L., WANG, S., PARK, K. & CHENG, J.-X. 2008. Release of hydrophobic molecules from polymer micelles into cell membranes revealed by Förster resonance energy transfer imaging. *P Natl Acad Sci USA,* 105**,** 6596-6601.

CHEN, X. & WONG, S. T. C. 2014. Chapter 1 - Cancer theranostics: an introduction. *In:* CHEN, X. & WONG, S. (eds.) *Cancer Theranostics.* Oxford: Academic Press.

CHENG, Y., XU, Z., MA, M. & XU, T. 2008a. Dendrimers as drug carriers: applications in different routes of drug administration. *J Pharm Sci,* 97**,** 123-143.

CHENG, Y., XU, Z., MA, M. & XU, T. 2008b. Dendrimers as Drug Carriers: Applications in Different Routes of Drug Administration. *Journal of Pharmaceutical Sciences,* 97**,** 123-143.

CHIDAMBARAN, V., COSTANDI, A. & D'MELLO, A. 2015. Propofol: a review of its role in pediatric anasthesia and sedation. *CNS drugs,* 29**,** 543-563.

CHO, K., WANG, X., NIE, S., CHEN, Z. G. & SHIN, D. M. 2008. Therapeutic nanoparticles for drug delivery in cancer. *Clin Cancer Res,* 14**,** 1310-6.

CHUAN, Y. P., ZENG, B. Y., O'SULLIVAN, B., THOMAS, R. & MIDDELBERG, A. P. 2012. Co-delivery of antigen and a lipophilic anti-inflammatory drug to cells via a tailorable nanocarrier emulsion. *J Colloid Interf Sci,* 368**,** 616-24.

CLEVIPREX. 2018. *Titratable Control of blood pressure reduction with CLEVIPREX® (clevidipine)* [Online]. Available: https://cleviprex.com/ [Accessed 09/03 2018].

COBO, I., LI, M., SUMERLIN, B. S. & PERRIER, S. 2014. Smart hybrid materials by conjugation of responsive polymers to biomacromolecules. *Nat Mater,* 14**,** 143.

COHEN, J. & DRUILHE, P. 2002. *Immunogenic compositions comprising liver stage malarial antigens*. EP1201250A1.

COMFORT, C., GARRASTAZU, G., POZZOLI, M. & SONVICO, F. 2015. Opportunities and challenges for the nasal administration of nanoemulsions. *Curr Top Med Chem,* 15**,** 356-68.

CONNOR, E. E., MWAMUKA, J., GOLE, A., MURPHY, C. J. & WYATT, M. D. 2005. Gold nanoparticles are taken up by human cells but do not cause acute cytotoxicity. *Small,* 1**,** 325-327.

COSCO, D., CELIA, C., CILURZO, F., TRAPASSO, E. & PAOLINO, D. 2008. Colloidal carriers for the enhanced delivery through the skin. *Expert Opin Drug Del,* 5**,** 737-755.

COURRIER, H., BUTZ, N. & VANDAMME, T. F. 2002. Pulmonary drug delivery systems: recent developments and prospects. *Crit Rev Ther Drug,* 19.

CREMER. March 2013. *MIGLYOL® 810, 812* [Online]. Cremer care. Available: http://s3.amazonaws.com/petercremerna/products/spec_sheets/159/339/301/original/MIGLYOL_810___812_TDS.pdf?1389204445 [Accessed 20 June 2018].

CRUCHO, C. I. C. & BARROS, M. T. 2017. Polymeric nanoparticles: a study on the preparation variables and characterization methods. *Mater Sci Eng,* 80**,** 771-784.

CUSSLER, E. L. 2009. *Diffusion: mass transfer in fluid systems*, Cambridge university press.

D'SOUZA, A. A. & SHEGOKAR, R. 2016. Polyethylene glycol (PEG): a versatile polymer for pharmaceutical applications. *Expert Opini Drug Del,* 13**,** 1257-1275.

DAHAN, A. & HOFFMAN, A. 2005. Evaluation of a chylomicron flow blocking approach to investigate the intestinal lymphatic transport of lipophilic drugs. *Eur J Pharm Sci,* 24**,** 381-8.

DAMODARAN, V. B., FEE, C. J., RUCKH, T. & POPAT, K. C. 2010. Conformational studies of covalently grafted poly (ethylene glycol) on modified solid matrices using X-ray photoelectron spectroscopy. *Langmuir,* 26**,** 7299-7306.

DANHIER, F., FERON, O. & PRÉAT, V. 2010. To exploit the tumor microenvironment: passive and active tumor targeting of nanocarriers for anti-cancer drug delivery. *J Control Release,* 148**,** 135-146.

DAS, S. C., HATTA, M., WILKER, P. R., MYC, A., HAMOUDA, T., NEUMANN, G., BAKER, J. R. & KAWAOKA, Y. 2012. Nanoemulsion W(80)5EC improves immune responses upon intranasal delivery of an inactivated pandemic H1N1 influenza vaccine. *Vaccine,* 30**,** 6871-6877.

DE JONG, W. H. & BORM, P. J. A. 2008. Drug delivery and nanoparticles: applications and hazards. *Int J Nanomed,* 3**,** 133-149.

DE VOLDER, M. F. L., TAWFICK, S. H., BAUGHMAN, R. H. & HART, A. J. 2013. Carbon nanotubes: present and future commercial applications. *Science,* 339**,** 535.

DELMAS, T., PIRAUX, H., COUFFIN, A. C., TEXIER, I., VINET, F., POULIN, P., CATES, M. E. & BIBETTE, J. 2011. How to prepare and stabilize very small nanoemulsions. *Langmuir,* 27**,** 1683-92.

DESAI, A., VYAS, T. & AMIJI, M. 2008. Cytotoxicity and apoptosis enhancement in brain tumor cells upon coadministration of paclitaxel and ceramide in nanoemulsion formulations. *J Pharm Sci,* 97**,** 2745-2756.

DEVALAPALLY, H., CHAKILAM, A. & AMIJI, M. M. 2007. Role of nanotechnology in pharmaceutical product development. *J Pharm Sci,* 96**,** 2547-65.

DEXTER, A. F., MALCOLM, A. S. & MIDDELBERG, A. P. J. 2006. Reversible active switching of the mechanical properties of a peptide film at a fluid–fluid interface. *Nat Mater,* 5**,** 502.

DICKINSON, E. 1986. Mixed proteinaceous emulsifiers: review of competitive protein adsorption and the relationship to food colloid stabilization. *Food Hydrocolloids,* 1**,** 3-23.

DICKINSON, E. 1994. Protein-Stabilized Emulsions. *Water in Foods.* Amsterdam: Pergamon.

DIMITRIJEV DWYER, M., BRECH, M., YU, L. & MIDDELBERG, A. P. J. 2014. Intensified expression and purification of a recombinant biosurfactant protein. *Chem Eng Sci,* 105**,** 12-21.

DIMITRIJEV-DWYER, M., HE, L., JAMES, M., NELSON, A., WANG, L. & MIDDELBERG, A. P. J. 2012. The effects of acid hydrolysis on protein biosurfactant molecular, interfacial, and foam properties: pH responsive protein hydrolysates. *Soft Matter,* 8**,** 5131-5139.

DOBROVOLSKAIA, M. A., PATRI, A. K., SIMAK, J., HALL, J. B., SEMBEROVA, J., DE PAOLI LACERDA, S. H. & MCNEIL, S. E. 2012. Nanoparticle size and surface charge determine effects of PAMAM dendrimers on human platelets in vitro. *Mol Pharm,* 9**,** 382-393.

DOWLING, A. Nanoscience and nanotechnologies. An international symposium on the nature, purposes, ethics and politics of evidence in a democracy, 2006. 61.

DWYER, M. D., HE, L., JAMES, M., NELSON, A. & MIDDELBERG, A. P. J. 2013. Insights into the role of protein molecule size and structure on interfacial properties using designed sequences. *J R Soc Interface,* 10.

EDELMAN, R. 1980. Vaccine adjuvants. *Review of Infectious Diseases,* 2**,** 370-383.

EVERS, P. 2017. Nanotechnology in medical applications: the global market. *BCC Research, USA*.

FAIRMAN, R., CHAO, H.-G., MUELLER, L., LAVOIE, T. B., SHEN, L., NOVOTNY, J. & MATSUEDA, G. R. 1995. Characterization of a new four-chain coiled-coil: Influence of chain length on stability. *Protein Sci,* 4**,** 1457-1469.

FAROKHZAD, O. C. & LANGER, R. 2009. Impact of nanotechnology on drug delivery. *ACS Nano,* 3**,** 16-20.

FASOLO, D., BASSANI, V. L. & TEIXEIRA, H. F. 2009. Development of topical nanoemulsions containing quercetin and 3-O-methylquercetin. *Pharmazie,* 64**,** 726-730.

FEE, C. J. & VAN ALSTINE, J. M. 2006. PEG-proteins: reaction engineering and separation issues. *Chem Eng Sci,* 61**,** 924-939.

FORSSEN, E. A. 1997. The design and development of DaunoXome® for solid tumor targeting in vivo. *Adv Drug Deliver Rev,* 24**,** 133-150.

FOX, C. B. 2009. Squalene emulsions for parenteral vaccine and drug delivery. *Molecules,* 14**,** 3286-312.

FOX, C. B., ANDERSON, R. C., DUTILL, T. S., GOTO, Y., REED, S. G. & VEDVICK, T. S. 2008. Monitoring the effects of component structure and source on formulation stability and adjuvant activity of oil-in-water emulsions. *Colloid Surface B* 65**,** 98-105.

FRYD, M. M. & MASON, T. G. 2012. Advanced nanoemulsions. *Annu Rev Phys Chem,* 63**,** 493-518.

GALHO, A. R., CORDEIRO, M. F., RIBEIRO, S. A., MARQUES, M. S., ANTUNES, M. F., LUZ, D. C., HADRICH, G., MUCCILLO-BAISCH, A. L., BARROS, D. M., LIMA, J. V., DORA, C. L. & HORN, A. P. 2016. Protective role of free and quercetin-loaded nanoemulsion against damage induced by intracerebral haemorrhage in rats. *Nanotechnology,* 27**,** 175101.

GANTA, S., SHARMA, P., PAXTON, J. W., BAGULEY, B. C. & GARG, S. 2010. Pharmacokinetics and pharmacodynamics of chlorambucil delivered in long-circulating nanoemulsion. *J Drug Target,* 18**,** 125-33.

GANTA, S., SINGH, A., KULKARNI, P., KEELER, A. W., PIROYAN, A., SAWANT, R. R., PATEL, N. R., DAVIS, B., FERRIS, C. & O'NEAL, S. 2015. EGFR targeted theranostic nanoemulsion for image-guided ovarian cancer therapy. *Pharm Res***,** 1-11.

GANTA, S., SINGH, A., PATEL, N. R., CACACCIO, J., RAWAL, Y. H., DAVIS, B. J., AMIJI, M. M. & COLEMAN, T. P. 2014a. Development of EGFR-targeted nanoemulsion for imaging and novel platinum therapy of ovarian cancer. *Pharm Res***,** 1-13.

GANTA, S., SINGH, A., RAWAL, Y., CACACCIO, J., PATEL, N. R., KULKARNI, P., FERRIS, C. F., AMIJI, M. M. & COLEMAN, T. P. 2016. Formulation development of a novel targeted theranostic nanoemulsion of docetaxel to overcome multidrug resistance in ovarian cancer. *Drug Deliv,* 23**,** 968-980.

GANTA, S., TALEKAR, M., SINGH, A., COLEMAN, T. & AMIJI, M. 2014b. Nanoemulsions in translational research—opportunities and challenges in targeted cancer Therapy. *AAPS PharmSciTech,* 15**,** 694-708.

GARÇON, N. & DI PASQUALE, A. 2017. From discovery to licensure, the adjuvant system story. *Hum Vaccines Immunother,* 13**,** 19-33.

GARÇON, N., VAUGHN, D. W. & DIDIERLAURENT, A. M. 2012. Development and evaluation of AS03, an adjuvant system containing α-tocopherol and squalene in an oil-in-water emulsion. *Expert Rev vaccines,* 11**,** 349-366.

GASPAR, M. M., BAKOWSKY, U. & EHRHARDT, C. 2008. Inhaled liposomes–current strategies and future challenges. *J Biomed Nanotechnol,* 4**,** 245-257.

GEORGIEV, G. A., SARKER, D. K., AL-HANBALI, O., GEORGIEV, G. D. & LALCHEV, Z. 2007. Effects of poly (ethylene glycol) chains conformational transition on the properties of mixed DMPC/DMPE-PEG thin liquid films and monolayers. *Colloid Surface B,* 59**,** 184-93.

GERARD, J., LLOYD, R., BARSBY, T., HADEN, P., KELLY, M. T. & ANDERSEN, R. J. 1997. Massetolides A-H, antimycobacterial cyclic depsipeptides produced by two pseudomonads isolated from marine habitats. *J Nat Prod,* 60**,** 223-9.

GIANELLA, A., MIESZAWSKA, A. J., HOEBEN, F. J. M., JANSSEN, H. M., JARZYNA, P. A., CORMODE, D. P., COSTA, K. D., RAO, S., FAROKHZAD, O. C., LANGER, R., FAYAD, Z. A. & MULDER, W. J. M. 2013. Synthesis and in vitro evaluation of a multifunctional and surface-switchable nanoemulsion platform. *Chem Commun,* 49**,** 9392-9394.

GILLET, J.-P. & GOTTESMAN, M. M. 2010. Mechanisms of multidrug resistance in cancer. *In:* ZHOU, J. (ed.) *Multi-Drug Resistance in Cancer.* Totowa, NJ: Humana Press.

GINER-CASARES, J. J., HENRIKSEN-LACEY, M., CORONADO-PUCHAU, M. & LIZ-MARZÁN, L. M. 2016. Inorganic nanoparticles for biomedicine: where materials scientists meet medical research. *Mater Today,* 19**,** 19-28.

GOMEZ, J. A., CRIADO, M. T. & FERREIROS, C. M. 1998. Bactericidal activity of antibodies elicited against the Neisseria meningitidis 37-kDa ferric binding protein (FbpA) with different adjuvants. *FEMS Immunol Med Microbiol,* 20**,** 79-86.

GRADISHAR, W. J., TJULANDIN, S., DAVIDSON, N., SHAW, H., DESAI, N., BHAR, P., HAWKINS, M. & O'SHAUGHNESSY, J. 2005. Phase III trial of nanoparticle albumin-bound paclitaxel compared with polyethylated castor oil-based paclitaxel in women with breast cancer. *J Clin Oncol,* 23**,** 7794-803.

GREF, R., LUCK, M., QUELLEC, P., MARCHAND, M., DELLACHERIE, E., HARNISCH, S., BLUNK, T. & MULLER, R. H. 2000. 'Stealth' corona-core nanoparticles surface modified by polyethylene glycol (PEG): influences of the corona (PEG chain length and surface density) and of the core composition on phagocytic uptake and plasma protein adsorption. *Colloid Surface B* 18**,** 301-313.

GRONEBERG, D. A., WITT, C., WAGNER, U., CHUNG, K. F. & FISCHER, A. 2003. Fundamentals of pulmonary drug delivery. *Resp Med,* 97**,** 382-387.

GUDIÑA, E. J., RANGARAJAN, V., SEN, R. & RODRIGUES, L. R. 2013. Potential therapeutic applications of biosurfactants. *Trends Pharmacol Sci,* 34**,** 667-675.

GUPTA, A., ERAL, H. B., HATTON, T. A. & DOYLE, P. S. 2016. Nanoemulsions: formation, properties and applications. *Soft Matter,* 12**,** 2826-41.

GUSTAFSON, H. H., HOLT-CASPER, D., GRAINGER, D. W. & GHANDEHARI, H. 2015. Nanoparticle uptake: the phagocyte problem. *Nano Today*.

HAENSLER, J., PROBECK, P., SU, J., PIRAS, F., DALENCON, F., COTTE, J. F., CHAMBON, V., IQBAL, S. M., HAWKINS, L. & BURDIN, N. 2015. Design and preclinical characterization of a novel vaccine adjuvant formulation consisting of a synthetic TLR4 agonist in a thermoreversible squalene emulsion. *Int J Pharm,* 486**,** 99-111.

HAGIGIT, T., ABDULRAZIK, M., VALAMANESH, F., BEHAR-COHEN, F. & BENITA, S. 2012. Ocular antisense oligonucleotide delivery by cationic nanoemulsion for improved treatment

of ocular neovascularization: An in-vivo study in rats and mice. *J Control Release,* 160**,** 225-231.

HAK, S., HELGESEN, E., HEKTOEN, H. H., HUUSE, E. M., JARZYNA, P. A., MULDER, W. J., HARALDSETH, O. & DAVIES CDE, L. 2012. The effect of nanoparticle polyethylene glycol surface density on ligand-directed tumor targeting studied in vivo by dual modality imaging. *ACS Nano,* 6**,** 5648-58.

HÅKANSSON, A. & RAYNER, M. 2018. Chapter 5 - General principles of nanoemulsion formation by high-energy mechanical methods A2 - Jafari, Seid Mahdi. *In:* MCCLEMENTS, D. J. (ed.) *Nanoemulsions.* Academic Press.

HARADA, T. & YOKOMIZO, K. 2000. Demulsification of oil-in-water emulsion under freezing conditions: effect of crystal structure modifier. *J Am Oil Chem Soc,* 77**,** 859-864.

HARRIS, J. M. & CHESS, R. B. 2003. Effect of pegylation on pharmaceuticals. *Nat Rev Drug Discov,* 2**,** 214.

HAUSER-KAWAGUCHI, A. M. & LUYT, L. G. 2015. Nanomedicine—nanoparticles in cancer imaging and therapy. *Genomic Instability and Cancer Metastasis.* Springer.

HELMLINGER, J., SENGSTOCK, C., GRO, MAYER, C., SCHILDHAUER, T. A., KOLLER, M. & EPPLE, M. 2016. Silver nanoparticles with different size and shape: equal cytotoxicity, but different antibacterial effects. *RSC Adv,* 6**,** 18490-18501.

HERMAN, S., HOOFTMAN, G. & SCHACHT, E. 1995. Poly(ethylene glycol) with reactive endgroups: I. modification of proteins. *J Bioact Compat Pol,* 10**,** 145-187.

HILLEMAN, M. R. 1966. Critical appraisal of emulsified oil adjuvants applied to viral vaccines. *Prog Med Virol,* 8**,** 131-82.

HIPPALGAONKAR, K., MAJUMDAR, S. & KANSARA, V. 2010. Injectable lipid emulsions—advancements, opportunities and challenges. *AAPS PharmSciTech,* 11**,** 1526-1540.

HÖRMANN, K. & ZIMMER, A. 2016. Drug delivery and drug targeting with parenteral lipid nanoemulsions — A review. *J Control Release,* 223**,** 85-98.

HOSNY, K. M. & BANJAR, Z. M. 2013. The formulation of a nasal nanoemulsion zaleplon in situ gel for the treatment of insomnia. *Expert Opin Drug Deliv,* 10**,** 1033-41.

HU, Z., TAWA, R., KONISHI, T., SHIBATA, N. & TAKADA, K. 2001. A novel emulsifier, labrasol, enhances gastrointestinal absorption of gentamicin. *Life Sci,* 69**,** 2899-910.

IKEDA, Y. & NAGASAKI, Y. 2012. PEGylation technology in nanomedicine. *Adv Polym Sci.* Springer.

INSIGHT, A. 2017. *Paclitaxel tocopheryl-based emulsion - Sorrento Therapeutics* [Online]. Springer. Available: http://adisinsight.springer.com/drugs/800013518 [Accessed 09/03 2018].

ISLAM, N. & GLADKI, E. 2008. Dry powder inhalers (DPIs)--a review of device reliability and innovation. *Int J Pharm,* 360**,** 1-11.

JAIN, R. & PATRAVALE, V. B. 2009. Development and evaluation of nitrendipine nanoemulsion for intranasal delivery. *J Biomed Nanotechnol,* 5**,** 62-8.

JAISWAL, M., DUDHE, R. & SHARMA, P. 2014. Nanoemulsion: an advanced mode of drug delivery system. *3 Biotech***,** 1-5.

JARES-ERIJMAN, E. A. & JOVIN, T. M. 2003. FRET imaging. *Nat Biotechnol,* 21**,** 1387.

JEEVANANDAM, J., CHAN, Y. S. & DANQUAH, M. K. 2016. Nano-formulations of drugs: recent developments, impact and challenges. *Biochimie,* 128-129**,** 99-112.

JOKERST, J. V., LOBOVKINA, T., ZARE, R. N. & GAMBHIR, S. S. 2011. Nanoparticle PEGylation for imaging and therapy. *Nanomedicine (London, England),* 6**,** 715-728.

JONES, M.-C. & LEROUX, J.-C. 1999. Polymeric micelles – a new generation of colloidal drug carriers. *Eur J Pharm Biopharm,* 48**,** 101-111.

JULIANO, R. 1988. Factors affecting the clearance kinetics and tissue distribution of liposomes, microspheres and emulsions. *Adv Drug Deliv Rev,* 2**,** 31-54.

KABALNOV, A. 2001. Ostwald ripening and related phenomena. *J Disper Sci Technol,* 22**,** 1-12.

KAKWERE, H., CHUN, C. K., JOLLIFFE, K. A., PAYNE, R. J. & PERRIER, S. 2010. Polymer-peptide chimeras for the multivalent display of immunogenic peptides. *Chem Commun,* 46**,** 2188-90.

KALIA, J. & RAINES, R. T. 2010. Advances in bioconjugation. *Curr org chem,* 14**,** 138-147.

KAUR, P., GARG, T., RATH, G., MURTHY, R. S. R. & GOYAL, A. K. 2016. Surfactant-based drug delivery systems for treating drug-resistant lung cancer. *Drug Deliv,* 23**,** 717-728.

KAUSHIK, A. K., JAYANT, R. D. & NAIR, M. 2017. *Advances in personalized nanotherapeutics*, Springer.

KAWAKAMI, K., YOSHIKAWA, T., HAYASHI, T., NISHIHARA, Y. & MASUDA, K. 2002. Microemulsion formulation for enhanced absorption of poorly soluble drugs. II. In vivo study. *J Control Release,* 81**,** 75-82.

KELMANN, R. G., COLOMBO, M., DE ARAUJO LOPES, S. C., NUNES, R. J., PISTORE, M., DALL AGNOL, D., RIGOTTO, C., SILVA, I. T., ROMAN, S. S., TEIXEIRA, H. F., OLIVEIRA SIMOES, C. M. & KOESTER, L. S. 2016. Pentyl gallate nanoemulsions as potential topical treatment of herpes labialis. *J Pharm Sci,* 105**,** 2194-203.

KELMANN, R. G., KUMINEK, G., TEIXEIRA, H. F. & KOESTER, L. S. 2007. Carbamazepine parenteral nanoemulsions prepared by spontaneous emulsification process. *Int J Pharm,* 342**,** 231-239.

KENTISH, S., WOOSTER, T., ASHOKKUMAR, M., BALACHANDRAN, S., MAWSON, R. & SIMONS, L. 2008. The use of ultrasonics for nanoemulsion preparation. *Innov Food Sci Emerg,* 9**,** 170-175.

KHANDAVILLI, S. & PANCHAGNULA, R. 2007. nanoemulsions as versatile formulations for paclitaxel delivery: peroral and dermal delivery studies in rats. *J Invest Dermatol,* 127**,** 154-162.

KHANI, S., KEYHANFAR, F. & AMANI, A. 2016. Design and evaluation of oral nanoemulsion drug delivery system of mebudipine. *Drug Deliv,* 23**,** 2035-2043.

KIM, B. Y., RUTKA, J. T. & CHAN, W. C. 2010. Nanomedicine. *New Engl J Med,* 363**,** 2434-2443.

KIM, I.-Y., JOACHIM, E., CHOI, H. & KIM, K. 2015. Toxicity of silica nanoparticles depends on size, dose, and cell type. *NBM,* 11**,** 1407-1416.

KISLUKHIN, A. A., XU, H., ADAMS, S. R., NARSINH, K. H., TSIEN, R. Y. & AHRENS, E. T. 2016. Paramagnetic fluorinated nanoemulsions for sensitive cellular fluorine-19 magnetic resonance imaging. *Nat Mater,* 15**,** 662-668.

KLUCKER, M. F., DALENCON, F., PROBECK, P. & HAENSLER, J. 2012. AF03, an alternative squalene emulsion-based vaccine adjuvant prepared by a phase inversion temperature method. *J Pharm Sci,* 101**,** 4490-500.

KLUCKER, M. F., HAENSLER, J., PROBECK-QUELLEEC, P. & CHAUX, P. 2007. *Thermoreversible oil-In-water emulsion*. EP1976560A2.

KNOP, K., HOOGENBOOM, R., FISCHER, D. & SCHUBERT, U. S. 2010. Poly(ethylene glycol) in drug delivery: pros and cons as well as potential alternatives. *Angew Chem Int Ed Engl,* 49**,** 6288-308.

KOLB, H. C., FINN, M. & SHARPLESS, K. B. 2001. Click chemistry: diverse chemical function from a few good reactions. *Angew Chem Int Ed Engl,* 40**,** 2004-2021.

KOMAIKO, J. S. & MCCLEMENTS, D. J. 2016. Formation of food-grade nanoemulsions using low-energy preparation methods: a review of available methods. *Compr Rev Food Sci F,* 15**,** 331-352.

KONG, F. & SINGH, R. P. 2008. Disintegration of solid foods in human stomach. *J Food Sci,* 73**,** R67-80.

KOO, O. M., RUBINSTEIN, I. & ONYUKSEL, H. 2005. Role of nanotechnology in targeted drug delivery and imaging: a concise review. *NBM,* 1**,** 193-212.

KOTTA, S., KHAN, A. W., PRAMOD, K., ANSARI, S. H., SHARMA, R. K. & ALI, J. 2012. Exploring oral nanoemulsions for bioavailability enhancement of poorly water-soluble drugs. *Expert Opin Drug Deliv,* 9**,** 585-98.

KRAFFT, M. P. & RIESS, J. G. 2007. Perfluorocarbons: Life sciences and biomedical uses Dedicated to the memory of Professor Guy Ourisson, a true RENAISSANCE man. *J Polym Sci Pol Chem,* 45**,** 1185-1198.

KRALOVA, I. & SJÖBLOM, J. 2009. Surfactants used in food industry: a review. *J Disper Sci Technol,* 30**,** 1363-1383.

KRUGER, P., EHRLEIN, B., ZIER, M. & GREGULETZ, R. 2014. *Inspiratory flow resistance of marketed dry powder inhalers (DPI)*.

KUE, C. S., KAMKAEW, A., BURGESS, K., KIEW, L. V., CHUNG, L. Y. & LEE, H. B. 2016. Small molecules for active targeting in cancer. *Med Res Rev,* 36**,** 494-575.

KUMAR, A. & JAIN, S. K. 2017. Preliminary studies for the development of intranasal nanoemulsion containing CNS agent: emphasizing the utilization of cut and weigh method. *Artif Cell Nanomed B,* 45**,** 515-521.

KUMAR BISHWAJIT, S. & MD. LUTFUL, A. 2014. Nanotechnology in cancer drug delivery and selective targeting. *ISRN Nanotechnology*.

KUMAR, M., MISRA, A., MISHRA, A. K., MISHRA, P. & PATHAK, K. 2008. Mucoadhesive nanoemulsion-based intranasal drug delivery system of olanzapine for brain targeting. *J Drug Target,* 16**,** 806-814.

KUO, F., SUBRAMANIAN, B., KOTYLA, T., WILSON, T. A., YOGANATHAN, S. & NICOLOSI, R. J. 2008. Nanoemulsions of an anti-oxidant synergy formulation containing gamma tocopherol have enhanced bioavailability and anti-inflammatory properties. *Int J Pharm,* 363**,** 206-213.

LAMMERS, T., KIESSLING, F., ASHFORD, M., HENNINK, W., CROMMELIN, D. & STORM, G. 2016. Cancer nanomedicine: is targeting our target? *Nat Rev Mater,* 1**,** 16069.

LANE, L. A., QIAN, X., SMITH, A. M. & NIE, S. 2015. Physical chemistry of nanomedicine: understanding the complex behaviors of nanoparticles in vivo. *Annu Rev Phys Chem,* 66**,** 521-547.

LANZA, G. M., WINTER, P. M., CARUTHERS, S. D., HUGHES, M. S., HU, G., SCHMIEDER, A. H. & WICKLINE, S. A. 2010. Theragnostics for tumor and plaque angiogenesis with perfluorocarbon nanoemulsions. *Angiogenesis,* 13**,** 189-202.

LAURENT, S., FORGE, D., PORT, M., ROCH, A., ROBIC, C., VANDER ELST, L. & MULLER, R. N. 2008. Magnetic iron oxide nanoparticles: synthesis, stabilization, vectorization, physicochemical characterizations, and biological applications. *Chem Rev,* 108**,** 2064-2110.

LEDERER, S. E. & PARASCANDOLA, J. 1998. Screening syphilis: Dr. Ehrlich's magic bullet meets the public health service. *J Hist Med Allied Sci,* 53**,** 345-70.

LEESMAN, G. D. 2003. *Adjuvant composition and methods for its use*. US09307321.

LELEUX, J. & ROY, K. 2013. Micro and nanoparticle-based delivery systems for vaccine immunotherapy: an immunological and materials perspective. *Adv Healthc Mater,* 2**,** 72-94.

LI, H., LE BRUN, A. P., AGYEI, D., SHEN, W., MIDDELBERG, A. P. & HE, L. 2016. Stabilizing and destabilizing protein surfactant-based foams in the presence of a chemical surfactant: effect of adsorption kinetics. *J Colloid Interf Sci,* 462**,** 56-63.

LI, Y., SONG, Y., ZHAO, L., GAIDOSH, G., LATIES, A. M. & WEN, R. 2008. Direct labeling and visualization of blood vessels with lipophilic carbocyanine dye DiI. *Nat Protoc,* 3**,** 1703-1708.

LIDGATE, D. M. & BYARS, N. E. 1995. Development of an emulsion-based muramyl dipeptide adjuvant formulation for vaccines. *In:* POWELL, M. F. & NEWMAN, M. J. (eds.) *Vaccine design: The subunit and adjuvant approach.* Boston, MA: Springer US.

LIFSHITZ, I. M. & SLYOZOV, V. V. 1961. The kinetics of precipitation from supersaturated solid solutions. *J Phys Chem Solids,* 19**,** 35-50.

LIM, C., KIM, D.-W., SIM, T., HOANG, N. H., LEE, J. W., LEE, E. S., YOUN, Y. S. & OH, K. T. 2016. Preparation and characterization of a lutein loading nanoemulsion system for ophthalmic eye drops. *J Drug Deliv Sci Tec,* 36**,** 168-174.

LOFTSSON, T. & BREWSTER, M. E. 2010. Pharmaceutical applications of cyclodextrins: basic science and product development. *J Pharm Pharmacol,* 62**,** 1607-21.

LOPES, J. R., SANTOS, G., BARATA, P., OLIVEIRA, R. & LOPES, C. M. 2013. Physical and chemical stimuli-responsive drug delivery systems: targeted delivery and main routes of administration. *Curr Pharm Des,* 19**,** 7169-84.

LOVELYN, C. & ATTAMA, A. A. 2011. Current state of nanoemulsions in drug delivery. *JBNB,* Vol.02No.05**,** 14.

LU, Y., QI, J. & WU, W. 2012. Absorption, disposition and pharmacokinetics of nanoemulsions. *Curr Drug Metab,* 13**,** 396-417.

LU, Z.-R., SHIAH, J.-G., SAKUMA, S., KOPEČKOVÁ, P. & KOPEČEK, J. 2002. Design of novel bioconjugates for targeted drug delivery. *J Control Release,* 78**,** 165-173.

MAA, Y. F. & HSU, C. C. 1999. Performance of sonication and microfluidization for liquid-liquid emulsification. *Pharm Dev Technol,* 4**,** 233-40.

MAEDA, H., WU, J., SAWA, T., MATSUMURA, Y. & HORI, K. 2000. Tumor vascular permeability and the EPR effect in macromolecular therapeutics: a review. *J Control Release,* 65**,** 271-84.

MAGFORCE. 2018. *How does nanotherm® therapy work?* [Online]. Available: http://www.magforce.de/en/produkte/nanotherm-therapie.html [Accessed].

MAHAJAN, H. S., MAHAJAN, M. S., NERKAR, P. P. & AGRAWAL, A. 2014. Nanoemulsion-based intranasal drug delivery system of saquinavir mesylate for brain targeting. *Drug Deliv,* 21**,** 148-54.

MAHMOUDI, M., SANT, S., WANG, B., LAURENT, S. & SEN, T. 2011. Superparamagnetic iron oxide nanoparticles (SPIONs): development, surface modification and applications in chemotherapy. *Adv Drug Deliv Rev,* 63**,** 24-46.

MALAM, Y., LOIZIDOU, M. & SEIFALIAN, A. M. 2009. Liposomes and nanoparticles: nanosized vehicles for drug delivery in cancer. *Trends Pharmacol Sci,* 30**,** 592-599.

MALCOLM, A. S., DEXTER, A. F., KATAKDHOND, J. A., KARAKASHEV, S. I., NGUYEN, A. V. & MIDDELBERG, A. P. 2009. Tuneable control of interfacial rheology and emulsion coalescence. *ChemPhysChem,* 10**,** 778-781.

MALCOLM, A. S., DEXTER, A. F. & MIDDELBERG, A. P. J. 2006. Foaming properties of a peptide designed to form stimuli-responsive interfacial films. *Soft Matter,* 2**,** 1057-1066.

MANSOOR, M. A. & SANDIP, B. T. 2006. Nanoemulsion formulations for tumor-targeted delivery. *Nanotechnology for cancer therapy.* CRC Press.

MARCHANT, R. & BANAT, I. M. 2012. Microbial biosurfactants: challenges and opportunities for future exploitation. *Trends Biotechnol,* 30**,** 558-565.

MARIN, S., VLASCEANU, G. M., TIPLEA, R. E., BUCUR, I. R., LEMNARU, M., MARIN, M. M. & GRUMEZESCU, A. M. 2015. Applications and toxicity of silver nanoparticles: a recent review. *Curr Top Med Chem,* 15**,** 1596-604.

MARQUES, M. R., LOEBENBERG, R. & ALMUKAINZI, M. 2011. Simulated biological fluids with possible application in dissolution testing. *Dissolut Technol,* 18**,** 15-28.

MARTIN, A. R. & FINLAY, W. H. 2015. Nebulizers for drug delivery to the lungs. *Expert Opin Drug Deliv,* 12**,** 889-900.

MASON, T. 1999. New fundamental concepts in emulsion rheology. *Curr Opin Colloid In,* 4**,** 231-238.

MASON, T. G., WILKING, J., MELESON, K., CHANG, C. & GRAVES, S. 2006. Nanoemulsions: formation, structure, and physical properties. *J Phys-Condens Mat,* 18**,** R635.

MATEO, C., LOMBARDERO, J., MORENO, E., MORALES, A., BOMBINO, G., COLOMA, J., WIMS, L., MORRISON, S. L. & PÉREZ, R. 2000. Removal of amphipathic epitopes from genetically engineered antibodies: production of modified immunoglobulins with reduced immunogenicity. *Hybridoma,* 19**,** 463-471.

MATHIAS, N. & SRIDHARAN, S. 2017. Alternate routes of administration. *In:* BHATTACHAR, S. N., MORRISON, J. S., MUDRA, D. R. & BENDER, D. M. (eds.) *Translating molecules*

into medicines: cross-functional integration at the drug discovery-development interface. Cham: Springer International Publishing.

MCCARTHY, J. R. 2009. The future of theranostic nanoagents. *Nanomedicine,* 4**,** 693-695.

MCCLEMENTS, D. J. 2004. Protein-stabilized emulsions. *Curr Opin Colloid In,* 9**,** 305-313.

MCCLEMENTS, D. J. 2011. Edible nanoemulsions: fabrication, properties, and functional performance. *Soft Matter,* 7**,** 2297-2316.

MCCLEMENTS, D. J. 2015. Nanoscale nutrient delivery systems for food applications: improving bioactive dispersibility, stability, and bioavailability. *J Food Sci,* 80**,** N1602-N1611.

MCCLEMENTS, D. J. & GUMUS, C. E. 2016. Natural emulsifiers — biosurfactants, phospholipids, biopolymers, and colloidal particles: molecular and physicochemical basis of functional performance. *Adv Colloid Interfac,* 234**,** 3-26.

MCCLEMENTS, D. J. & JAFARI, S. M. 2018. Chapter 1 - General aspects of nanoemulsions and their formulation. *Nanoemulsions.* Academic Press.

MCCLEMENTS, D. J. & RAO, J. 2011. Food-grade nanoemulsions: formulation, fabrication, properties, performance, biological fate, and potential toxicity. *Crit Rev Food Sci Nutr,* 51**,** 285-330.

MENG, F., ENGBERS, G. H. M. & FEIJEN, J. 2004. Polyethylene glycol–grafted polystyrene particles. *J Biomed Mater Res A,* 70A**,** 49-58.

MENG, L., XIA, X., YANG, Y., YE, J., DONG, W., MA, P., JIN, Y. & LIU, Y. 2016. Co-encapsulation of paclitaxel and baicalein in nanoemulsions to overcome multidrug resistance via oxidative stress augmentation and P-glycoprotein inhibition. *Int J Pharm* 513**,** 8-16.

MEWIS, J. & WAGNER, N. J. 2012. *Colloidal suspension rheology*, Cambridge University Press.

MIDDELBERG, A. P. J. & DIMITRIJEV-DWYER, M. 2011. A designed biosurfactant protein for switchable foam control. *ChemPhysChem,* 12**,** 1426-1429.

MIGOTTO, A., CARVALHO, V. F. M., SALATA, G. C., DA SILVA, F. W. M., YAN, C. Y. I., ISHIDA, K., COSTA-LOTUFO, L. V., STEINER, A. A. & LOPES, L. B. 2018. Multifunctional nanoemulsions for intraductal delivery as a new platform for local treatment of breast cancer. *Drug Deliv,* 25**,** 654-667.

MILANE, L., DUAN, Z. & AMIJI, M. 2010. Development of EGFR-targeted polymer blend nanocarriers for combination paclitaxel/lonidamine delivery to treat multi-drug resistance in human breast and ovarian tumor cells. *Mol Pharm,* 8**,** 185-203.

MIN, Y., CASTER, J. M., EBLAN, M. J. & WANG, A. Z. 2015. Clinical translation of nanomedicine. *Chem Rev,* 115**,** 11147-11190.

MONFARDINI, C. & VERONESE, F. M. 1998. Stabilization of substances in circulation. *Bioconjugate Chem,* 9**,** 418-50.

MOORE, T. L., RODRIGUEZ-LORENZO, L., HIRSCH, V., BALOG, S., URBAN, D., JUD, C., ROTHEN-RUTISHAUSER, B., LATTUADA, M. & PETRI-FINK, A. 2015. Nanoparticle colloidal stability in cell culture media and impact on cellular interactions. *Chem Soc Rev,* 44**,** 6287-6305.

MORROW, D., MCCARRON, P., WOOLFSON, A. & DONNELLY, R. 2007. Innovative strategies for enhancing topical and transdermal drug delivery. *Open Drug Deliv J,* 1**,** 36-59.

MOSCA, F., TRITTO, E., MUZZI, A., MONACI, E., BAGNOLI, F., IAVARONE, C., O'HAGAN, D., RAPPUOLI, R. & DE GREGORIO, E. 2008. Molecular and cellular signatures of human vaccine adjuvants. *P Natl Acad Sci USA,* 105**,** 10501-10506.

MOU, D., CHEN, H., DU, D., MAO, C., WAN, J., XU, H. & YANG, X. 2008. Hydrogel-thickened nanoemulsion system for topical delivery of lipophilic drugs. *Int J Pharm,* 353**,** 270-276.

MOVASSAGHIAN, S., MERKEL, O. M. & TORCHILIN, V. P. 2015. Applications of polymer micelles for imaging and drug delivery. *Wires Nanomed Nanobio,* 7**,** 691-707.

MULIK, R. S., MÖNKKÖNEN, J., JUVONEN, R. O., MAHADIK, K. R. & PARADKAR, A. R. 2010. Transferrin mediated solid lipid nanoparticles containing curcumin: enhanced in vitro anticancer activity by induction of apoptosis. *Int J pharm,* 398**,** 190-203.

MÜLLER, R., LASCHOBER, C., SZYMANSKI, W. W. & ALLMAIER, G. 2007. Determination of molecular weight, particle size, and density of high number generation PAMAM dendrimers using MALDI−TOF−MS and nES−GEMMA. *Macromolecules,* 40**,** 5599-5605.

MURA, S., NICOLAS, J. & COUVREUR, P. 2013. Stimuli-responsive nanocarriers for drug delivery. *Nat Mater,* 12**,** 991.

MURUGADOSS, S., LISON, D., GODDERIS, L., VAN DEN BRULE, S., MAST, J., BRASSINNE, F., SEBAIHI, N. & HOET, P. H. 2017. Toxicology of silica nanoparticles: an update. *Arch Toxicol,* 91**,** 2967-3010.

MUSA, S. H., BASRI, M., MASOUMI, H. R. F., KARJIBAN, R. A., MALEK, E. A., BASRI, H. & SHAMSUDDIN, A. F. 2013. Formulation optimization of palm kernel oil esters nanoemulsion-loaded with chloramphenicol suitable for meningitis treatment. *Colloid Surface B,* 112**,** 113-119.

NAIR, D. P., PODGÓRSKI, M., CHATANI, S., GONG, T., XI, W., FENOLI, C. R. & BOWMAN, C. N. 2014. The thiol-michael addition click reaction: a powerful and widely used tool in materials chemistry. *Chem Mater,* 26**,** 724-744.

NASR, M., NAWAZ, S. & ELHISSI, A. 2012. Amphotericin B lipid nanoemulsion aerosols for targeting peripheral respiratory airways via nebulization. *Int J Pharm,* 436**,** 611-6.

NELSON, A. 2006. Co-refinement of multiple-contrast neutron/X-ray reflectivity data using MOTOFIT. *J Appl Crystallogr,* 39**,** 273-276.

NESAMONY, J., SHAH, I. S., KALRA, A. & JUNG, R. 2014. Nebulized oil-in-water nanoemulsion mists for pulmonary delivery: development, physico-chemical characterization and in vitro evaluation. *Drug Dev Ind Pharm,* 40**,** 1253-1263.

NEWMAN, R. H. & ZHANG, J. 2008. Visualization of phosphatase activity in living cells with a FRET-based calcineurin activity sensor. *Mol BioSyst,* 4**,** 496-501.

NICOLAOS, G., CRAUSTE-MANCIET, S., FARINOTTI, R. & BROSSARD, D. 2003. Improvement of cefpodoxime proxetil oral absorption in rats by an oil-in-water submicron emulsion. *Int J Pharm,* 263**,** 165-171.

NORTHFELT, D. W., DEZUBE, B. J., THOMMES, J. A., MILLER, B. J., FISCHL, M. A., FRIEDMAN-KIEN, A., KAPLAN, L. D., DU MOND, C., MAMELOK, R. D. & HENRY, D. H. 1998. Pegylated-liposomal doxorubicin versus doxorubicin, bleomycin, and vincristine in the treatment of AIDS-related Kaposi's sarcoma: results of a randomized phase III clinical trial. *J Clin Oncol,* 16**,** 2445-51.

O'BRIEN, M. E., WIGLER, N., INBAR, M., ROSSO, R., GRISCHKE, E., SANTORO, A., CATANE, R., KIEBACK, D. G., TOMCZAK, P., ACKLAND, S. P., ORLANDI, F., MELLARS, L., ALLAND, L. & TENDLER, C. 2004. Reduced cardiotoxicity and comparable efficacy in a phase III trial of pegylated liposomal doxorubicin HCl (CAELYX/Doxil) versus conventional doxorubicin for first-line treatment of metastatic breast cancer. *Ann Oncol,* 15**,** 440-9.

O'KONEK, J. J., MAKIDON, P. E., LANDERS, J. J., CAO, Z., MALINCZAK, C. A., PANNU, J., SUN, J., BITKO, V., CIOTTI, S., HAMOUDA, T., WOJCINSKI, Z. W., LUKACS, N. W., FATTOM, A. & BAKER, J. R., JR. 2015. Intranasal nanoemulsion-based inactivated respiratory syncytial virus vaccines protect against viral challenge in cotton rats. *Hum Vaccin Immunother,* 11**,** 2904-12.

O'SHAUGHNESSY, J. A. 2003. Pegylated liposomal doxorubicin in the treatment of breast cancer. *Clin breast cancer,* 4**,** 318-328.

O'HAGAN, D. T. & PODDA, A. 2008. MF59: a safe and potent oil in water emulsion adjuvant for influenza vaccines, which induces enhanced protection against virus challenge. *In:* RAPPUOLI, R. & DEL GIUDICE, G. (eds.) *Influenza vaccines for the future.* Basel: Birkhäuser Basel.

OHGUCHI, Y., KAWANO, K., HATTORI, Y. & MAITANI, Y. 2008. Selective delivery of folate–PEG-linked, nanoemulsion-loaded aclacinomycin A to KB nasopharyngeal cells and xenograft: effect of chain length and amount of folate–PEG linker. *J Drug Target,* 16**,** 660-667.

OJEA-JIMENEZ, I., COMENGE, J., GARCIA-FERNANDEZ, L., MEGSON, Z. A., CASALS, E. & PUNTES, V. F. 2013. Engineered inorganic nanoparticles for drug delivery applications. *Curr Drug Metab,* 14**,** 518-30.

ONOUE, S., SATO, H., OGAWA, K., KOJO, Y., AOKI, Y., KAWABATA, Y., WADA, K., MIZUMOTO, T. & YAMADA, S. 2012. Inhalable dry-emulsion formulation of cyclosporine A with improved anti-inflammatory effects in experimental asthma/COPD-model rats. *Eur J Pharm Biopharm,* 80**,** 54-60.

OTT, G., BARCHFELD, G. L., CHERNOFF, D., RADHAKRISHNAN, R., VAN HOOGEVEST, P. & VAN NEST, G. 1995. MF59. Design and evaluation of a safe and potent adjuvant for human vaccines. *Pharm Biotechnol,* 6**,** 277-96.

OTT, G. & VAN NEST, G. 2007. *Development of vaccine adjuvants: a historical perspective*, John Wiley & Sons: Hoboken, NJ, USA.

OTTO, A. & DU PLESSIS, J. 2015. The effects of emulsifiers and emulsion formulation types on dermal and transdermal drug delivery. *In:* DRAGICEVIC, N. & MAIBACH, H. I. (eds.) *Percutaneous penetration enhancers chemical methods in penetration enhancement: drug manipulation strategies and vehicle effects.* Berlin, Heidelberg: Springer Berlin Heidelberg.

OWENS, D. E. & PEPPAS, N. A. 2006. Opsonization, biodistribution, and pharmacokinetics of polymeric nanoparticles. *Int J Pharm,* 307**,** 93-102.

PACWA-PŁOCINICZAK, M., PŁAZA, G. A., PIOTROWSKA-SEGET, Z. & CAMEOTRA, S. S. 2011. Environmental applications of biosurfactants: recent advances. *Int J Mol Sci,* 12**,** 633-654.

PANDEY, Y. R., KUMAR, S., GUPTA, B. K., ALI, J. & BABOOTA, S. 2015. Intranasal delivery of paroxetine nanoemulsion via the olfactory region for the management of depression: formulation, behavioural and biochemical estimation. *Nanotechnology,* 27**,** 025102.

PARDESHI, C. V. & BELGAMWAR, V. S. 2013. Direct nose to brain drug delivery via integrated nerve pathways bypassing the blood-brain barrier: an excellent platform for brain targeting. *Expert Opin Drug Deliv,* 10**,** 957-72.

PARKER, D. 1990. Tumour targeting with radiolabelled macrocycle-antibody conjugates. *Chem Soc Rev,* 19**,** 271-291.

PASCHE, S., VOROS, J., GRIESSER, H. J., SPENCER, N. D. & TEXTOR, M. 2005. Effects of ionic strength and surface charge on protein adsorption at PEGylated surfaces. *J Phys Chem B,* 109**,** 17545-52.

PASUT, G. & VERONESE, F. M. 2007. Polymer–drug conjugation, recent achievements and general strategies. *Prog Polym Sci,* 32**,** 933-961.

PATEL, N., NAKRANI, H., RAVAL, M. & SHETH, N. 2016. Development of loteprednol etabonate-loaded cationic nanoemulsified in-situ ophthalmic gel for sustained delivery and enhanced ocular bioavailability. *Drug Deliv,* 23**,** 3712-3723.

PATEL, S. K., BEAINO, W., ANDERSON, C. J. & JANJIC, J. M. 2015. Theranostic nanoemulsions for macrophage COX-2 inhibition in a murine inflammation model. *Clin Immunol,* 160**,** 59-70.

PATTON, J. S. & BYRON, P. R. 2007. Inhaling medicines: delivering drugs to the body through the lungs. *Nat Rev Drug Discov,* 6**,** 67-74.

PAUDEL, K. S., MILEWSKI, M., SWADLEY, C. L., BROGDEN, N. K., GHOSH, P. & STINCHCOMB, A. L. 2010. Challenges and opportunities in dermal/transdermal delivery. *Ther deliv,* 1**,** 109-131.

PEER, D. 2014. Precision medicine–delivering the goods? *Cancer lett*.

PEER, D., KARP, J. M., HONG, S., FAROKHZAD, O. C., MARGALIT, R. & LANGER, R. 2007. Nanocarriers as an emerging platform for cancer therapy. *Nat Nanotechnol,* 2**,** 751.

PELLEGRINI, M., NICOLAY, U., LINDERT, K., GROTH, N. & DELLA CIOPPA, G. 2009. MF59-adjuvanted versus non-adjuvanted influenza vaccines: integrated analysis from a large safety database. *Vaccine,* 27**,** 6959-65.

PERFUMO, A., RANCICH, I. & BANAT, I. M. 2010. Possibilities and challenges for biosurfactants use in petroleum industry. *Adv Exp Med Biol,* 672**,** 135-45.

PHAM, J., NAYEL, A., HOANG, C. & ELBAYOUMI, T. 2016. Enhanced effectiveness of tocotrienol-based nano-emulsified system for topical delivery against skin carcinomas. *Drug Deliv,* 23**,** 1514-24.

PRÉVOT, G., KAUSS, T., LORENZATO, C., GAUBERT, A., LARIVIÈRE, M., BAILLET, J., LAROCHE-TRAINEAU, J., JACOBIN-VALAT, M. J., ADUMEAU, L. & MORNET, S. 2017. Iron oxide core oil-in-water nanoemulsion as tracer for atherosclerosis MPI and MRI imaging. *Int J Pharm,* 532**,** 669-676.

QI, J., ZHUANG, J., LU, Y., DONG, X., ZHAO, W. & WU, W. 2017. In vivo fate of lipid-based nanoparticles. *Drug Discov Today,* 22**,** 166-172.

QUINTANILLA-CARVAJAL, M. X., CAMACHO-DÍAZ, B. H., MERAZ-TORRES, L. S., CHANONA-PÉREZ, J. J., ALAMILLA-BELTRÁN, L., JIMENÉZ-APARICIO, A. & GUTIÉRREZ-LÓPEZ, G. F. 2010. Nanoencapsulation: a new trend in food engineering processing. *Food Eng Rev,* 2**,** 39-50.

RAGELLE, H., CRAUSTE-MANCIET, S., SEGUIN, J. & BROSSARD, D. 2012. Nanoemulsion formulation of fisetin improves bioavailability and antitumour activity in mice. *Int J Pharm,* 427**,** 452-459.

RAGELLE, H., DANHIER, F., PRÉAT, V., LANGER, R. & ANDERSON, D. G. 2017. Nanoparticle-based drug delivery systems: a commercial and regulatory outlook as the field matures. *Expert Opin Drug Deliv,* 14**,** 851-864.

RAHN-CHIQUE, K., PUERTAS, A. M., ROMERO-CANO, M. S., ROJAS, C. & URBINA-VILLALBA, G. 2012. Nanoemulsion stability: experimental evaluation of the flocculation rate from turbidity measurements. *Adv Colloid Interfac Sci,* 178**,** 1-20.

RAPHAEL, A. P., PRIMIERO, C. A., ANSALDO, A. B., KEATES, H. L., SOYER, H. P. & PROW, T. W. 2013. Elongate microparticles for enhanced drug delivery to ex vivo and in vivo pig skin. *J Control Release,* 172**,** 96-104.

RAPHAEL, A. P., PRIMIERO, C. A., LIN, L. L., SMITH, R. F., DYER, P., SOYER, H. P. & PROW, T. W. 2014. High aspect ratio elongated microparticles for enhanced topical drug delivery in human volunteers. *Adv Healthc Mater,* 3**,** 860-866.

REED, S. G., BERTHOLET, S., COLER, R. N. & FRIEDE, M. 2009. New horizons in adjuvants for vaccine development. *Trends immunol,* 30**,** 23-32.

RHEE, Y.-S., CHOI, J.-G., PARK, E.-S. & CHI, S.-C. 2001. Transdermal delivery of ketoprofen using microemulsions. *Int J Pharm,* 228**,** 161-170.

RINGSDORF, H. 1975. Structure and properties of pharmacologically active polymers. *J Polym Sci Pol Sym,* 51**,** 135-153.

ROBERTS, M. J., BENTLEY, M. D. & HARRIS, J. M. 2002. Chemistry for peptide and protein PEGylation. *Adv Drug Deliv Rev,* 54**,** 459-476.

RODRIGUES, L., BANAT, I. M., TEIXEIRA, J. & OLIVEIRA, R. 2006. Biosurfactants: potential applications in medicine. *J Antimicrob Chemoth,* 57**,** 609-618.

ROESTENBERG, M., REMARQUE, E., DE JONGE, E., HERMSEN, R., BLYTHMAN, H., LEROY, O., IMOUKHUEDE, E., JEPSEN, S., OFORI-ANYINAM, O., FABER, B., KOCKEN, C. H. M., ARNOLD, M., WALRAVEN, V., TEELEN, K., ROEFFEN, W., DE MAST, Q., BALLOU, W. R., COHEN, J., DUBOIS, M. C., ASCARATEIL, S., VAN DER VEN, A., THOMAS, A. & SAUERWEIN, R. 2008. Safety and immunogenicity of a recombinant plasmodium falciparum AMA1 malaria vaccine adjuvanted with Alhydrogel™, Montanide ISA 720 or AS02. *PLOS ONE,* 3**,** e3960.

ROSENBLUM, L. T., KOSAKA, N., MITSUNAGA, M., CHOYKE, P. L. & KOBAYASHI, H. 2010. In vivo molecular imaging using nanomaterials: general in vivo characteristics of nano-sized reagents and applications for cancer diagnosis. *Mol Membr Biol,* 27**,** 274-85.

ROSENTHAL, E., POIZOT-MARTIN, I., SAINT-MARC, T., SPANO, J.-P., CACOUB, P. & GROUP, D. S. 2002. Phase IV study of liposomal daunorubicin (DaunoXome) in AIDS-related Kaposi sarcoma. *Am J Clin Oncol,* 25**,** 57-59.

ROTENBERG, M., RUBIN, M., BOR, A., MEYUHAS, D., TALMON, Y. & LICHTENBERG, D. 1991. Physico-chemical characterization of Intralipid emulsions. *Biochim Biophys Acta,* 1086**,** 265-72.

RUBINSTEIN, A., PATHAK, Y. V., KLEINSTERN, J., RECHES, A. & BENITA, S. 1991. In vitro release and intestinal absorption of physostigmine salicylate from submicron emulsions. *J Pharm Sci,* 80**,** 643-7.

RUP, B. & O'HARA, D. 2007. Critical ligand binding reagent preparation/selection: when specificity depends on reagents. *AAPS J,* 9**,** E148-E155.

SAFRA, T., MUGGIA, F., JEFFERS, S., TSAO-WEI, D., GROSHEN, S., LYASS, O., HENDERSON, R., BERRY, G. & GABIZON, A. 2000. Pegylated liposomal doxorubicin (doxil): reduced clinical cardiotoxicity in patients reaching or exceeding cumulative doses of 500 mg/m2. *Ann Oncol,* 11**,** 1029-1033.

SAINSBURY, F., ZENG, B. & MIDDELBERG, A. P. 2014. Towards designer nanoemulsions for precision delivery of therapeutics. *Curr Opin Chem Eng,* 4**,** 11-17.

SALIM, N., AHMAD, N., MUSA, S. H., HASHIM, R., TADROS, T. F. & BASRI, M. 2016. Nanoemulsion as a topical delivery system of antipsoriatic drugs. *RSC Adv,* 6**,** 6234-6250.

SALK, J. E., LAURENT, A. M. & BAILEY, M. L. 1951. Direction of Research on Vaccination against Influenza—New Studies with Immunologic Adjuvants*. *American Journal of Public Health and the Nations Health,* 41**,** 669-677.

SALMASO, S., BERSANI, S., SCOMPARIN, A., MASTROTTO, F., SCHERPFER, R., TONON, G. & CALICETI, P. 2009. Tailored PEG for rh-G-CSF analogue site-specific conjugation. *Bioconjugate Chem,* 20**,** 1179-1185.

SASTRY, S. V., NYSHADHAM, J. R. & FIX, J. A. 2000. Recent technological advances in oral drug delivery - a review. *Pharm Sci Technol To,* 3**,** 138-145.

SATO, H. 2002. Enzymatic procedure for site-specific pegylation of proteins. *Adv Drug Deliv Rev,* 54**,** 487-504.

SAVI, L. A., LEAL, P. C., VIEIRA, T. O., ROSSO, R., NUNES, R. J., YUNES, R. A., CRECZYNSKI-PASA, T. B., BARARDI, C. R. & SIMOES, C. M. 2005. Evaluation of anti-herpetic and antioxidant activities, and cytotoxic and genotoxic effects of synthetic alkyl-esters of gallic acid. *Arzneimittelforschung,* 55**,** 66-75.

SCHALLER, A., CONNORS, N. K., DWYER, M. D., OELMEIER, S. A., HUBBUCH, J. & MIDDELBERG, A. P. J. 2015. Computational study of elements of stability of a four-helix bundle protein biosurfactant. *J Comput Aid Mol Des,* 29**,** 47-58.

SCHEINBERG, D. A., VILLA, C. H., ESCORCIA, F. E. & MCDEVITT, M. R. 2010. Conscripts of the infinite armada: systemic cancer therapy using nanomaterials. *Nat Rev Clin Oncol,* 7**,** 266-276.

SCHLESSINGER, J., AXELROD, D., KOPPEL, D., WEBB, W. & ELSON, E. 1977. Lateral transport of a lipid probe and labeled proteins on a cell membrane. *Science,* 195**,** 307-309.

SCHÖTTLER, S., BECKER, G., WINZEN, S., STEINBACH, T., MOHR, K., LANDFESTER, K., MAILÄNDER, V. & WURM, F. R. 2016. Protein adsorption is required for stealth effect of poly(ethylene glycol)- and poly(phosphoester)-coated nanocarriers. *Nat Nanotechnol,* 11**,** 372-377.

SCHWARZ, T. F., HORACEK, T., KNUF, M., DAMMAN, H.-G., ROMAN, F., DRAMÉ, M., GILLARD, P. & JILG, W. 2009. Single dose vaccination with AS03-adjuvanted H5N1 vaccines in a randomized trial induces strong and broad immune responsiveness to booster vaccination in adults. *Vaccine,* 27**,** 6284-6290.

SELLERS, R. S., ANTMAN, M., PHILLIPS, J., KHAN, K. N. & FURST, S. M. 2005. Effects of miglyol 812 on rats after 4 weeks of gavage as compared with methylcellulose/tween 80. *Drug Chem Toxicol,* 28**,** 423-32.

SHI, J., KANTOFF, P. W., WOOSTER, R. & FAROKHZAD, O. C. 2016. Cancer nanomedicine: progress, challenges and opportunities. *Nat Rev Cancer,* 17**,** 20.

SHINODA, K. & SAITO, H. 1968. The effect of temperature on the phase equilibria and the types of dispersions of the ternary system composed of water, cyclohexane, and nonionic surfactant. *J Colloid Interf Sci,* 26**,** 70-74.

SHUKLA, P., DWIVEDI, P., GUPTA, P. K. & MISHRA, P. R. 2014. Optimization of novel tocopheryl acetate nanoemulsions for parenteral delivery of curcumin for therapeutic intervention of sepsis. *Expert Opin Drug Deliv,* 11**,** 1697-1712.

SIKWAL, D. R., KALHAPURE, R. S. & GOVENDER, T. 2017. An emerging class of amphiphilic dendrimers for pharmaceutical and biomedical applications: Janus amphiphilic dendrimers. *European Journal of Pharmaceutical Sciences,* 97**,** 113-134.

SILVA, H. D., CERQUEIRA, M. Â. & VICENTE, A. A. 2012. Nanoemulsions for food applications: development and characterization. *Food Bioprocess Tech,* 5**,** 854-867.

SILVERMAN, J. A. & DEITCHER, S. R. 2013. Marqibo(®) (vincristine sulfate liposome injection) improves the pharmacokinetics and pharmacodynamics of vincristine. *Cancer Chemoth Pharm,* 71**,** 555-564.

SIMION, V., CONSTANTINESCU, C. A., STAN, D., DELEANU, M., TUCUREANU, M. M., BUTOI, E., MANDUTEANU, I., SIMIONESCU, M. & CALIN, M. 2016. P-selectin targeted

dexamethasone-loaded lipid nanoemulsions: a novel therapy to reduce vascular inflammation. *Mediat Inflamm,* 2016**,** 15.

SIMON, J. A. 2006. Estradiol in micellar nanoparticles: the efficacy and safety of a novel transdermal drug-delivery technology in the management of moderate to severe vasomotor symptoms. *Menopause,* 13**,** 222-31.

SINGH, K. K. & VINGKAR, S. K. 2008. Formulation, antimalarial activity and biodistribution of oral lipid nanoemulsion of primaquine. *Int J Pharm,* 347**,** 136-143.

SINGH, Y., MEHER, J. G., RAVAL, K., KHAN, F. A., CHAURASIA, M., JAIN, N. K. & CHOURASIA, M. K. 2017. Nanoemulsion: concepts, development and applications in drug delivery. *J Control Release,* 252**,** 28-49.

SJOLANDER, S., HANSEN, J. E., LOVGREN-BENGTSSON, K., AKERBLOM, L. & MOREIN, B. 1996. Induction of homologous virus neutralizing antibodies in guinea-pigs immunized with two human immunodeficiency virus type 1 glycoprotein gp120-iscom preparations. A comparison with other adjuvant systems. *Vaccine,* 14**,** 344-52.

SMITH, S., LORENZ, D., PEACE, J., MCLEOD, K., CROCKETT, R. S. & VOGEL, R. 2010. Difluprednate ophthalmic emulsion 0.05% (Durezol) administered two times daily for managing ocular inflammation and pain following cataract surgery. *Clin Ophthalmol,* 4**,** 983-91.

SOENEN, S. J., PARAK, W. J., REJMAN, J. & MANSHIAN, B. 2015. (Intra)cellular stability of inorganic nanoparticles: effects on cytotoxicity, particle functionality, and biomedical applications. *Chem Rev,* 115**,** 2109-35.

SOLANS, C., IZQUIERDO, P., NOLLA, J., AZEMAR, N. & GARCIA-CELMA, M. J. 2005. Nano-emulsions. *Curr Opin Colloid In,* 10**,** 102-110.

SOLANS, C. & SOLÉ, I. 2012. Nano-emulsions: formation by low-energy methods. *Curr Opin Colloid In,* 17**,** 246-254.

SONNEVILLE-AUBRUN, O., SIMONNET, J.-T. & L'ALLORET, F. 2004. Nanoemulsions: a new vehicle for skincare products. *Adv Colloid Interfac,* 108**,** 145-149.

SOSMAN, J. A. & SONDAK, V. K. 2003. Melacine®: an allogeneic melanoma tumor cell lysate vaccine. *Expert Rev Vaccines,* 2**,** 353-368.

SOUBANI, A. O. & CHANDRASEKAR, P. H. 2002. THe clinical spectrum of pulmonary aspergillosis*. *Chest,* 121**,** 1988-1999.

STEPHANOPOULOS, N. & FRANCIS, M. B. 2011. Choosing an effective protein bioconjugation strategy. *Nat Chem Biol,* 7**,** 876.

STONE, N. R. H., BICANIC, T., SALIM, R. & HOPE, W. 2016. Liposomal Amphotericin B (AmBisome®): A review of the pharmacokinetics, pharmacodynamics, clinical experience and future directions. *Drugs,* 76**,** 485-500.

STRICKLEY, R. G. 2004. Solubilizing excipients in oral and injectable formulations. *Pharm Res,* 21**,** 201-230.

STRUCK, D. & PAGANO, R. 1980. Insertion of fluorescent phospholipids into the plasma membrane of a mammalian cell. *J Biol Chem,* 255**,** 5404-5410.

SUBRAMANIAN, N. & GHOSAL, S. K. 2004. Enhancement of gastrointestinal absorption of poorly water soluble drugs via lipid based systems. *Indian J Exp Biol,* 42**,** 1056-65.

SULI, J., BENISEK, Z., ELIAS, D., SVRCEK, S., ONDREJKOVA, A., ONDREJKA, R. & BAJOVA, V. 2004. Experimental squalene adjuvant. I. Preparation and testing of its effectiveness. *Vaccine,* 22**,** 3464-9.

SUMER, B. & GAO, J. 2008. Theranostic nanomedicine for cancer. *Nanomedicine (Lond),* 3**,** 137-40.

SUN, C., DING, Y., ZHOU, L., SHI, D., SUN, L., WEBSTER, T. J. & SHEN, Y. 2017. Noninvasive nanoparticle strategies for brain tumor targeting. *Nanomed-Nanotechnol,* 13**,** 2605-2621.

SUN, H., LIU, K., LIU, W., WANG, W., GUO, C., TANG, B., GU, J., ZHANG, J., LI, H., MAO, X., ZOU, Q. & ZENG, H. 2012. Development and characterization of a novel nanoemulsion drug-delivery system for potential application in oral delivery of protein drugs. *Int J Nanomedicine,* 7**,** 5529-43.

SWENSON, C., PERKINS, W., ROBERTS, P. & JANOFF, A. 2001. Liposome technology and the development of Myocet™(liposomal doxorubicin citrate). *The Breast,* 10**,** 1-7.

SZAKACS, G., PATERSON, J. K., LUDWIG, J. A., BOOTH-GENTHE, C. & GOTTESMAN, M. M. 2006. Targeting multidrug resistance in cancer. *Nat Rev Drug Discov,* 5**,** 219-34.

TADROS, T., IZQUIERDO, P., ESQUENA, J. & SOLANS, C. 2004. Formation and stability of nano-emulsions. *Adv Colloid Interfac,* 108–109**,** 303-318.

TALEGAONKAR, S. & NEGI, L. M. 2015. Nanoemulsion in drug targeting. *Targeted Drug Delivery: Concepts and Design.* Springer.

TALEKAR, M., GANTA, S., SINGH, A., AMIJI, M., KENDALL, J., DENNY, W. A. & GARG, S. 2012. Phosphatidylinositol 3-kinase inhibitor (PIK75) containing surface functionalized nanoemulsion for enhanced drug delivery, cytotoxicity and pro-apoptotic activity in ovarian cancer cells. *Pharm Res,* 29**,** 2874-86.

TANG, S. Y., SIVAKUMAR, M., NG, A. M.-H. & SHRIDHARAN, P. 2012. Anti-inflammatory and analgesic activity of novel oral aspirin-loaded nanoemulsion and nano multiple emulsion formulations generated using ultrasound cavitation. *Int J Pharm,* 430**,** 299-306.

TAYEB, H. H., PIANTAVIGNA, S., HOWARD, C. B., NOUWENS, A., MAHLER, S. M., MIDDELBERG, A. J., HE, L., HOLT, S. & SAINSBURY, F. 2017. Insights into the interfacial structure-function of poly(ethylene glycol)-decorated peptide-stabilised nanoscale emulsions. *Soft Matter***,** 7953-7961.

TCHOLAKOVA, S., DENKOV, N. D., IVANOV, I. B. & CAMPBELL, B. 2006. Coalescence stability of emulsions containing globular milk proteins. *Adv Colloid Interfac,* 123-126**,** 259-293.

TIRNAKSIZ, F., AKKUS, S., CELEBI, N. & FANUN, M. 2010. Nanoemulsions as drug delivery systems. *Colloids Drug Deliv***,** 221-44.

TIWARI, S., TAN, Y.-M. & AMIJI, M. 2006. Preparation and in vitro characterization of multifunctional nanoemulsions for simultaneous MR imaging and targeted drug delivery. *J Biomed Nanotechnol,* 2**,** 217-224.

TOMEE, J. F. & VAN DER WERF, T. S. 2001. Pulmonary aspergillosis. *Neth J Med,* 59**,** 244-58.

TORCHILIN, V. P. 2005. Recent advances with liposomes as pharmaceutical carriers. *Nat Rev Drug Discov,* 4**,** 145-60.

USÓN, N., GARCIA, M. J. & SOLANS, C. 2004. Formation of water-in-oil (W/O) nano-emulsions in a water/mixed non-ionic surfactant/oil systems prepared by a low-energy emulsification method. *Colloid Surface A,* 250**,** 415-421.

VAN BOEKEL, M. A. J. S. & WALSTRA, P. 1981. Stability of oil-in-water emulsions with crystals in the disperse phase. *Colloid Surface,* 3**,** 109-118.

VANAPALLI, S. A., PALANUWECH, J. & COUPLAND, J. N. 2002. Stability of emulsions to dispersed phase crystallization: effect of oil type, dispersed phase volume fraction, and cooling rate. *Colloid Surface A,* 204**,** 227-237.

VARVARESOU, A. & IAKOVOU, K. 2015. Biosurfactants in cosmetics and biopharmaceuticals. *Lett Appl Microbiol,* 61**,** 214-23.

VECINO, X., CRUZ, J. M., MOLDES, A. B. & RODRIGUES, L. R. 2017. Biosurfactants in cosmetic formulations: trends and challenges. *Crit Rev Biotechnol,* 37**,** 911-923.

VENKATESHWARLU, I., PRABHAKAR, K., ALI, M. & KISHAN, V. 2010. Development and in vitro cytotoxic evaluation of parenteral docetaxel lipid nanoemulsions for application in cancer treatment. *PDA J Pharm Sci Tech,* 64**,** 233-241.

VERONESE, F. M. & MORPURGO, M. 1999. Bioconjugation in pharmaceutical chemistry. *Il Farmaco,* 54**,** 497-516.

VIRCHOW, J. C. 2004. Guidelines versus clinical practice--which therapy and which device? *Respir Med,* 98 Suppl B**,** S28-34.

VOLKOV, Y. 2015. Quantum dots in nanomedicine: recent trends, advances and unresolved issues. *Biochem Bioph Res Co,* 468**,** 419-427.

VONARBOURG, A., PASSIRANI, C., SAULNIER, P. & BENOIT, J.-P. 2006. Parameters influencing the stealthiness of colloidal drug delivery systems. *Biomaterials,* 27**,** 4356-4373.

WANG, M. & THANOU, M. 2010. Targeting nanoparticles to cancer. *Pharm Res,* 62**,** 90-99.

WANG, X., JIANG, Y., WANG, Y.-W., HUANG, M.-T., HO, C.-T. & HUANG, Q. 2008. Enhancing anti-inflammation activity of curcumin through O/W nanoemulsions. *Food Chem,* 108**,** 419-424.

WARENIUS, H. M. 2009. Technological challenges of theranostics in oncology. *Expert Opin Med Diagn,* 3**,** 381-393.

WEBSTER, T. J. 2006. Nanomedicine: what's in a definition? *Int J Nanomed,* 1**,** 115-116.

WEI, L., LU, J., XU, H., PATEL, A., CHEN, Z.-S. & CHEN, G. 2015. Silver nanoparticles: synthesis, properties, and therapeutic applications. *Drug Discov Today,* 20**,** 595-601.

WESTER, H. J. & SCHOTTELIUS, M. 2007. Fluorine-18 labeling of peptides and proteins. *In:* SCHUBIGER, P. A., LEHMANN, L. & FRIEBE, M. (eds.) *PET Chemistry: the Driving force in molecular imaging.* Berlin, Heidelberg: Springer Berlin Heidelberg.

WIBOWO, D., ZHAO, C.-X. & MIDDELBERG, A. P. J. 2015. Interfacial biomimetic synthesis of silica nanocapsules using a recombinant catalytic modular protein. *Langmuir,* 31**,** 1999-2007.

WILHELM, S., TAVARES, A. J., DAI, Q., OHTA, S., AUDET, J., DVORAK, H. F. & CHAN, W. C. W. 2016. Analysis of nanoparticle delivery to tumours. *Nat Rev Mater,* 1**,** 16014.

WILLIAMS, A. C. & BARRY, B. W. 2004. Penetration enhancers. *Adv Drug Deliv Rev,* 56**,** 603-618.

WONG, C.-H. & WHITESIDES, G. M. 1994. *Enzymes in synthetic organic chemistry*, Academic Press.

WU, X., CHEN, J., WU, M. & ZHAO, J. X. 2015. Aptamers: active targeting ligands for cancer diagnosis and therapy. *Theranostics,* 5**,** 322-344.

XIN, Y., YIN, M., ZHAO, L., MENG, F. & LUO, L. 2017. Recent progress on nanoparticle-based drug delivery systems for cancer therapy. *Cancer Biol Med,* 14**,** 228-241.

XU, Q., ENSIGN, L. M., BOYLAN, N. J., SCHÖN, A., GONG, X., YANG, J.-C., LAMB, N. W., CAI, S., YU, T., FREIRE, E. & HANES, J. 2015. Impact of surface polyethylene glycol (PEG) density on biodegradable nanoparticle transport in mucus ex vivo and distribution in vivo. *ACS Nano,* 9**,** 9217-9227.

XU, Z., ZHANG, Z., CHEN, Y., CHEN, L., LIN, L. & LI, Y. 2010. The characteristics and performance of a multifunctional nanoassembly system for the co-delivery of docetaxel and iSur-pDNA in a mouse hepatocellular carcinoma model. *Biomaterials,* 31**,** 916-22.

YANG, X., WANG, D., MA, Y., ZHAO, Q., FALLON, J. K., LIU, D., XU, X. E., WANG, Y., HE, Z. & LIU, F. 2014. Theranostic nanoemulsions: codelivery of hydrophobic drug and hydrophilic imaging probe for cancer therapy and imaging. *Nanomedicine***,** 1-13.

YEH, Y.-C., CRERAN, B. & ROTELLO, V. M. 2012. Gold nanoparticles: preparation, properties, and applications in bionanotechnology. *Nanoscale,* 4**,** 1871-1880.

YOKOYAMA, M. 2014. Polymeric micelles as drug carriers: their lights and shadows. *J Drug Target,* 22**,** 576-583.

YOUNG, N. A., BRUSS, M. S., GARDNER, M., WILLIS, W. L., MO, X., VALIENTE, G. R., CAO, Y., LIU, Z., JARJOUR, W. N. & WU, L.-C. 2014. Oral administration of nano-emulsion curcumin in mice suppresses inflammatory-induced NFκB signaling and macrophage migration. *PLOS ONE,* 9**,** e111559.

ZALIPSKY, S. 1995. Functionalized poly (ethylene glycols) for preparation of biologically relevant conjugates. *Bioconjugate Chem,* 6**,** 150-165.

ZENG, B., CHUAN, Y., O'SULLIVAN, B., CAMINSCHI, I., LAHOUD, M., THOMAS, R. & MIDDELBERG, A. 2013. Receptor‐specific delivery of protein antigen to dendritic cells by a nanoemulsion formed using top‐down non‐covalent click self‐assembly. *Small,* 9**,** 3736-3742.

ZHANG, L., GU, F. X., CHAN, J. M., WANG, A. Z., LANGER, R. S. & FAROKHZAD, O. C. 2008. Nanoparticles in medicine: therapeutic applications and developments. *Clin Pharmacol Ther,* 83**,** 761-9.

ZHANG, Y. F., WANG, J. C., BIAN, D. Y., ZHANG, X. & ZHANG, Q. 2010. Targeted delivery of RGD-modified liposomes encapsulating both combretastatin A-4 and doxorubicin for tumor therapy: in vitro and in vivo studies. *Eur J Pharm Biopharm,* 74**,** 467-73.

ZHENG, C. Y., MA, G. & SU, Z. 2007. Native PAGE eliminates the problem of PEG‐SDS interaction in SDS‐PAGE and provides an alternative to HPLC in characterization of protein PEGylation. *Electrophoresis,* 28**,** 2801-2807.

7 Appendix A

Animal Ethics Approval Certificate:

The targeting and biodistribution studies (Chapter 3) were performed in compliance with the Australian National Health and Medical Research Council guidelines for the care and use of laboratory animals, and with the approval of the EnGeneIC Animal Ethics Committee under ethics application number: AIBN/400/13/ARC/NHMRC (certificate attached in the following page).

THE UNIVERSITY OF QUEENSLAND
AUSTRALIA

UQ Research and Innovation
Director, Research Management Office
Nicole Thompson

Animal Ethics Approval Certificate

23-Sep-2015

Please check all details below and inform the Animal Welfare Unit within 10 working days if anything is incorrect.

Activity Details

Chief Investigator: Dr Barbara Rolfe, Australian Institute for Bioengineering and Nanotechnology

Title: Imaging and drug delivery to cancer tissue using polymers

AEC Approval Number: AIBN/400/13/ARC/NHMRC

Previous AEC Number:

Approval Duration: 13-Dec-2013 to 13-Dec-2015

Funding Body: ARC, NHMRC

Group: Anatomical Biosciences

Other Staff/Students: Kristofer Thurecht, Simon Puttick, Nathan Boase, Nick Fletcher, Zachary Houston, Anna Gemmell

Location(s): St Lucia Bldg 57 - Centre of Advanced Imaging

Summary

Subspecies	Strain	Class	Gender	Source	Approved	Remaining
Mice - genetically modified	BALB/c Nude	Adults	Female	Commercial breeding colony	64	21
Mice - genetically modified	BALB/c-Foxn1nu/nu	Adults	Mix	Commercial breeding colony	144	96
Mice - genetically modified	C.B-17/IcrHanHsdArc Prkdc scid	Adults	Mix	Commercial breeding colony	72	72
Mice - non genetically modified	BALB/c Inbred	Adults	Female	Commercial breeding colony	148	143
Mice - non genetically modified	C57BL/6	Adults	Mix	Commercial breeding colony	20	20

Permits

Provisos

Approval Details

Description	Amount	Balance
Mice - genetically modified (BALB/c Nude, Female, Adults, Commercial breeding colony)		
11 Dec 2013 Initial approval	64	64
31 Dec 2013 Use in 2013 (from 2014 MAR)	0	64
31 Dec 2014 Use in 2014 (from 2015 MAR)	-43	21
Mice - genetically modified (BALB/c-Foxn1nu/nu , Mix, Adults, Commercial breeding colony)		
11 Dec 2013 Initial approval	48	48

31 Dec 2013	Use in 2013 (from 2014 MAR)	0	48
31 Dec 2014	Use in 2014 (from 2015 MAR)	-48	0
20 Jan 2015	Mod #4	60	60
9 Sep 2015	Mod #5	36	96
Mice - genetically modified (C.B-17/IcrHanHsdArcPrkdc scid, Mix, Adults, Commercial breeding colony)			
31 Dec 2014	Use in 2014 (from 2015 MAR)	0	0
20 Jan 2015	Mod #4	36	36
9 Sep 2015	Mod #5	36	72
Mice - non genetically modified (BALB/c Inbred, Female, Adults, Commercial breeding colony)			
11 Dec 2013	Initial approval	112	112
31 Dec 2013	Use in 2013 (from 2014 MAR)	0	112
6 May 2014	Modification #2	36	148
31 Dec 2014	Use in 2014 (from 2015 MAR)	-5	143
Mice - non genetically modified (C57BL/6, Mix, Adults, Commercial breeding colony)			
9 Sep 2015	Mod #5	20	20

Please note the animal numbers supplied on this certificate are the total allocated for the approval duration

Please use this Approval Number:

1. When ordering animals from Animal Breeding Houses
2. For labelling of all animal cages or holding areas. In addition please include on the label, Chief Investigator's name and contact phone number.
3. When you need to communicate with this office about the project.

It is a condition of this approval that all project animal details be made available to Animal House OIC. (UAEC Ruling 14/12/2001)

The Chief Investigator takes responsibility for ensuring all legislative, regulatory and compliance objectives are satisfied for this project.

This certificate supercedes all preceeding certificates for this project (i.e. those certificates dated before 23-Sep-2015)

Animal Welfare Unit
UQ Research and Innovation
The University of Queensland

Cumbrae-Stewart Building
Research Road
Brisbane Qld 4072 Australia

+61 7 336 52925 (Enquiries)
+61 7 334 68710 (Enquiries)
+61 7 336 52713 (Coordinator)

animalwelfare@research.uq.edu.au
uq.edu.au/research